

THESIS

OXIDATIVE STABILITY AND IGNITION QUALITY OF ALGAE DERIVED
METHYL ESTERS CONTAINING VARYING LEVELS OF METHYL
EICOSAPENTAENOATE AND METHYL DOCOSAHEXAENOATE

Submitted by

Harrison Bucy

Department of Mechanical Engineering

In partial fulfillment of the requirements

For the Degree of Master of Science

Colorado State University

Fort Collins, Colorado

Spring 2011

Master's Committee:

Advisor: Anthony J. Marchese

Bryan D. Willson

T. Gordon Smith

ABSTRACT

OXIDATIVE STABILITY AND IGNITION QUALITY OF ALGAE DERIVED METHYL ESTERS CONTAINING VARYING LEVELS OF METHYL EICOSAPENTAENOATE AND METHYL DOCOSAHEXAENOATE

Microalgae is currently receiving strong consideration as a potential biofuel feedstock to help meet the advanced biofuels mandate of the 2007 Energy Independence and Security Act because of its theoretically high yield (gallons/acre/year) in comparison to current terrestrial feedstocks. Additionally, microalgae also do not compete with food and can be cultivated with wastewater on non-arable land. Microalgae lipids can be converted into a variety of biofuels including fatty acid methyl esters (e.g. FAME biodiesel), renewable diesel, renewable gasoline, or jet fuel. For microalgae derived FAME, the fuel properties will be directly related to the fatty acid composition of the lipids produced by the given microalgae strain. Several microalgae species under consideration for wide scale cultivation, such as *Nannochloropsis*, produce lipids with fatty acid compositions containing substantially higher quantities of long chain-polyunsaturated fatty acids (LC-PUFA) in comparison to terrestrial feedstocks. It is expected that increased levels of LC-PUFA will be problematic in terms of meeting all of the current ASTM specifications for biodiesel. For example, it is known that oxidative stability and cetane number decrease with increasing levels of LC-PUFA. However, these same LC-PUFA fatty acids, such as eicosapentaenoic acid (EPA: C20:5) and docosahexaenoic acid (DHA: C22:6) are known to have high nutritional value thereby making separation of these compounds economically

attractive. Given the uncertainty in the future value of these LC-PUFA compounds and the economic viability of the separation process, the goal of this study was to examine the oxidative stability and ignition quality of algae-based FAME with varying levels of EPA and DHA removal. Oxidative stability tests were conducted at a temperature of 110 °C and airflow of 10 L/h using a Metrohm 743 Rancimat with automatic induction period determination following the EN 14112 Method from the ASTM D6751 and EN 14214 Standards, which call for induction periods of at least three hours and six hours, respectively. Derived Cetane Number testing was conducted using a Waukesha FIT following the ASTM D7170 Method. Tests were conducted with synthetic algal oil blends manufactured from various sources to match the fatty acid compositions of several algae strains subjected to varying removal amounts of roughly 0 – 100 percent LC-PUFA. In addition, tests were also conducted with real algal methyl esters produced from multiple sources. The bis-allylic position equivalent (BAPE) was calculated for each fuel sample to quantify the level of unsaturation. The induction period was then plotted as a function of BAPE, which showed that the oxidative stability varied exponentially with the amount of LC-PUFA. The results suggest that removal of 45 – 65 percent of the LC-PUFA from Nannochloropsis-based algal methyl esters would be sufficient for meeting existing ASTM specifications for oxidative stability and 75 – 85 percent removal would be needed to meet the EN specification. The oxidative stability additive *tert*-butylhydroquinone (TBHQ) was found to increase Nannochloropsis-based algal methyl esters' oxidative stability to ASTM and EN specifications at only 0.03 percent and 0.06 percent additions by mass, respectively, when no LC-PUFA was removed. The ignition quality tests showed that the Derived Cetane Number varied linearly with BAPE and the algae formulations were found to pass the ASTM cetane specification of 47 only if all the LC-PUFA were removed.

Acknowledgements

Many people contributed to this project during all the stages of planning and implementation and without them, this project would have been much more difficult. First and foremost, great thanks to Dr. Anthony Marchese for the research plan and guidance. His support and encouragement helped me overcome many obstacles and further grow as a student, researcher, and engineer. Many people at the EECL were very helpful and encouraging; their knowledge and technical expertise were greatly appreciated. Tim Vaughn provided guidance during installation of the FIT. David Martinez and Esteban Hincapie worked to setup additional fuel characterization equipment, so that I could finish my testing. Marc Baumgardner assisted greatly during the FIT injector maintenance. A special thanks to Hayden Schappell from Broomfield High School for volunteering at the EECL and conducting the density, viscosity, and speed of sound measurements. Roshan Joseph coordinated lab space and arranged for Greg Wardle of Solix Biofuels to profile the algae samples. This work was supported by a grant from the Department of Energy to the National Alliance for Advanced Biofuels and Bioproducts.

Table of Contents

1	Introduction.....	1
1.1	Motivation for Research	1
1.1.1	Global Climate Change.....	1
1.1.2	Peak Oil.....	3
1.2	Liquid Biofuels	4
1.3	The Algae Solution	7
1.4	Algae Biodiesel.....	13
1.4.1	Long-Chain Polyunsaturated Fatty Acids	16
1.5	Problematic Fuel Issues	18
1.5.1	Oxidative Stability	19
1.5.2	Cetane Number	25
1.5.3	Cold Temperature Properties	26
1.6	Fuel Improvement Solutions.....	27
1.6.1	LC-PUFA Removal	27
1.6.2	Additives	28
1.7	Thesis Overview	29
2	Experimental Equipment	31
2.1	Metrohm 743 Rancimat Description.....	31
2.2	Waukesha FIT Description	36
2.3	Anton Paar Stabinger SVM 3000 Description.....	39
2.4	Anton Paar DSA 5000 M Description	41

3	Fuel Production and Analysis	44
3.1	Model Algal Methyl Ester Compounds	45
3.2	Model Algal Methyl Ester Fuel Formulation.....	48
4	Experimental Procedure.....	57
4.1	Oxidative Stability	57
4.2	Derived Cetane Number	59
4.3	Density, Speed of Sound, and Viscosity	60
5	Results and Discussion	62
5.1	Oxidative Stability	62
5.1.1	Effect of Oxidative Stability Additives.....	78
5.2	Derived Cetane Number	87
5.3	Density, Viscosity, Speed of Sound.....	94
6	Conclusions.....	99
6.1	Recommendations for Future Work.....	100
7	References.....	102

LIST OF FIGURES

Figure 1.1. U.S. annual biodiesel production. Adapted from (National Biodiesel Board 2009).	11
Figure 1.2. Transesterification of triglyceride with methanol. Adapted from (Van Gerpen, et al. 2006).....	16
Figure 1.3. Schematic of BAPE and APE sites.....	22
Figure 1.4. Mechanism for peroxy radical formation on a methylene group. Adapted from (Arisoy 2008).....	23
Figure 1.5. Induction period as a function of BAPE for (Sanford, et al. 2009).	24
Figure 1.6. Induction period as a function of BAPE + APE for (Sanford, et al. 2009).	24
Figure 2.1. Metrohm 743 Rancimat pictured at EECL.	32
Figure 2.2. Example Rancimat curve determine induction period.....	34
Figure 2.3. Rancimat schematic.....	34
Figure 2.4. Biodiesel sample before (left) and after (right) Rancimat test.....	35
Figure 2.5. Measuring vessel before (left) and after (right) Rancimat test.	36
Figure 2.6. FIT pictured at EECL.	37
Figure 2.7. FIT fuel injection system.....	38
Figure 2.8. SVM 3000 pictured at the EECL.....	40
Figure 2.9. DSA 5000 M pictured at the EECL.....	42
Figure 3.1. Bench-scale reactor at EECL. Left image: initial methoxide-oil reaction. Right image: glycerol-FAME separation.....	47
Figure 3.2. Ingredient and algae FAMES. Left to right: methyl laurate, corn, canola, soy, fish, Inventure, Catilin.	48
Figure 3.3. Nannochloropsis Oculata Growth Formulation BAPE, APE, and BAPE + APE comparison.....	54

Figure 3.4. Nannochloropsis Sp - Formulation BAPE, APE, and BAPE + APE comparison.....	54
Figure 3.5. Isochrysis Galbana - Formulation BAPE, APE, and BAPE + APE comparison.....	55
Figure 3.6. Nannochloropsis Oculata - Formulation and actual BAPE, APE, and BAPE + APE comparison.....	55
Figure 3.7. Nannochloropsis Sp - Formulation and actual BAPE, APE, and BAPE + APE comparison.....	56
Figure 3.8. Isochrysis Galbana - Formulation and actual BAPE, APE, and BAPE + APE comparison.....	56
Figure 5.1. Induction period as a function of BAPE for the methyl laurate-fish methyl ester blends.....	63
Figure 5.2. Induction period as a function of BAPE + APE for the methyl laurate-fish methyl ester blends.....	64
Figure 5.3. Induction period as a function of BAPE for all tested methyl esters.....	65
Figure 5.4. Induction period as a function of BAPE + APE for all tested methyl esters.....	66
Figure 5.5. Induction period as a function of BAPE for the Nanno Oculata Growth formulations.....	67
Figure 5.6. Induction period as a function of modeled percent EPA and DHA removed for the Nanno Oculata Growth formulations.....	68
Figure 5.7. Induction period as a function of percent EPA and DHA formulated for the Nanno Oculata Growth formulations.....	69
Figure 5.8. Induction period as a function of BAPE for Nanno Sp formulations.....	70
Figure 5.9. Induction period as a function of modeled percent EPA and DHA removed for Nanno Sp formulations.....	71
Figure 5.10. Induction period as a function of percent EPA and DHA formulated for Nanno Sp formulations.....	72
Figure 5.11. Induction period as a function of BAPE for Iso Galbana formulations.....	73
Figure 5.12. Induction period as a function of modeled percent EPA and DHA removed for Iso Galbana formulations.....	74
Figure 5.13. Induction period as a function of percent EPA and DHA formulated for Iso Galbana formulations.....	75
Figure 5.14. Induction period as a function of BAPE including algae methyl esters.....	77
Figure 5.15. Induction period as a function of BAPE for Nanno Sp formulations with additive.....	83

Figure 5.16. Induction Period as a function of modeled percent EPA and DHA removed for Nanno Sp formulations with additive.	83
Figure 5.17. Induction period as a function of additive percentage for Nanno Sp formulation of 104.54 percent EPA and DHA removal.	84
Figure 5.18. Induction period as a function of additive percentage for Nanno Sp formulation of 71.01 percent EPA and DHA removal.	85
Figure 5.19. Induction period as a function of additive percentage for Nanno Sp formulation of 44.32 percent EPA and DHA removal.	85
Figure 5.20. Induction period as a function of additive percentage for Nanno Sp formulation of 28.69 percent EPA and DHA removal.	86
Figure 5.21. Ignition delay as a function of BAPE for algae methyl ester formulations.	89
Figure 5.22. Ignition delay as a function of modeled percent EPA and DHA removed from the algae methyl ester formulations.	89
Figure 5.23. Ignition delay as a function of percent EPA and DHA formulated for algae methyl ester formulations.	90
Figure 5.24. Derived cetane number as a function of BAPE for algae methyl ester formulations.	92
Figure 5.25. Derived cetane number as a function of modeled percent EPA and DHA removed from the algae methyl ester formulations.	92
Figure 5.26. Derived cetane number as a function of percent EPA and DHA formulated for algae methyl ester formulations.	93
Figure 5.27. Dynamic viscosity for tested methyl esters.	95
Figure 5.28. Kinematic viscosity for tested methyl esters.	95
Figure 5.29. Density for tested methyl esters.	96
Figure 5.30. Speed of sound for tested methyl esters.	97
Figure 5.31. Bulk modulus as a function of BAPE.	97

LIST OF TABLES

Table 1.1. EISA 2007 Renewable Fuel Standard. Adapted from (Congress 2007).....	5
Table 1.2. U. S. Production of Biofuels from various feedstocks. Adapted from (Congress 2007).	6
Table 1.3. Comparison of some sources of biodiesel. Adapted from (Chisti 2007).....	10
Table 1.4. Comparison of fatty acid profiles for seven biodiesel sources based on fatty acid composition by percent weight ^a , fatty acids denoted by Carbon #: Double Bond #.....	17
Table 1.5. Common fatty acids found in vegetable and algae oils, along with their carbon number: double bond number description and structure. Adapted from (Fisher 2009).....	18
Table 2.1. Metrohm 743 Rancimat oxidative stability testing specifications.....	31
Table 2.2. Several of the Waukesha FIT DCN testing specifications.....	37
Table 2.3. Summary of test parameters, instruments used, and methods followed.	43
Table 3.1. Aglae FAME samples' fatty acid profiles. *Algal oil converted to FAME for gas chromatography – mass spectrometry analysis.....	45
Table 3.2. Modeled algae fatty acid profiles. 1 (Roncarati, et al. 2004) , 2 (Benamotz, Tornabene and Thomas 1985) , 3 (Hu, et al. 2008)	49
Table 3.3. Ingredient fatty acid profiles. 1 (Berthiaume and Tremblay, Study of Rancimat Test Method in Measuring the Oxidation Stability of Biodiesel Ester and Blends November 2006), 2 (Knothe 2002), 3 (Proctor & Gamble), 4 (Fisher 2009)	50
Table 3.4. Test fuel formulations.....	51
Table 3.5. BAPE and APE comparisons with actual removal rates.....	53
Table 4.1. Oxidative stability test matrix.....	57
Table 4.2. Oxidative stability with additive test matrix.....	58
Table 4.3. Ignition quality test matrix.....	59
Table 4.4. Density, speed of sound, and viscosity test matrix.	60
Table 5.1. Methyl laurate - fish methyl ester oxidatve stability results.	63

Table 5.2. Nanno Oculata Growth formulation oxidative stability results.	67
Table 5.3. Nanno Sp formulation oxidative stability results.....	70
Table 5.4. Iso Galbana formulaton oxidative stability results.	73
Table 5.5. Algae oxidative stability results.....	76
Table 5.6. Additional oxidative stability results.	77
Table 5.7. Flaxseed methyl ester comparison with DHA additive. * Data from (Sanford, et al. 2009).	78
Table 5.8. Nanno Sp formulations oxidative stability results with no additive.	79
Table 5.9. Nanno Sp formulations oxdiative stability results with 0.1 percent additive.	80
Table 5.10. Nanno Sp formulations oxidative stability results with 0.15 percent additive.	81
Table 5.11. Nanno Sp formulations oxidative stability results with 0.2 percent additive.	81
Table 5.12. Nanno Sp formulations oxidative stability results with 0.33 percent additive.	82
Table 5.13. Ignition delay results for algae methyl ester formulations. (* Invalid results)	88
Table 5.14. Derived cetane number results for algae methyl ester formulations.....	91
Table 5.15. Density, viscosity, and speed of sound results for tested methyl esters and oil.....	94

LIST OF ABBREVIATIONS

ASP	-	Aquatic Species Program
B100	-	100% Biodiesel fuel
B20	-	20% Biodiesel and 80% Petroleum diesel blend by volume
BAPE	-	Bis-allylic Position Equivalents
APE	-	Allylic Position Equivalents
LC-PUFA	-	Long Chain – Polyunsaturated Fatty Acid
CFR	-	Cooperative Fuels Research
CH₂	-	Methylene
CN	-	Cetane Number
CO₂	-	Carbon Dioxide
DCN	-	Derived Cetane Number
DHA	-	Docosahexaenoic acid
DOE	-	Department of Energy
EECL	-	Engine and Energy Conversion Lab
EIA	-	U.S. Energy Information Administration
EISA	-	The Energy Independence and Security Act
EPA	-	Eicosapentaenoic acid
FAME	-	Fatty Acid Methyl Ester
FIT	-	Fuels Ignition Tester
FT-ICR	-	Fourier Transform Ion Cyclotron Resonance

IPCC	-	Intergovernmental Panel on Climate Change
IQT	-	Ignition Quality Tester
IV	-	Iodine Value
MCH	-	Methylcyclohexane
NAABB	-	National Alliance for Advanced Biofuels and Bioproducts Consortium
NREL	-	National Renewable Energy Laboratory
PUFA	-	Polyunsaturated Fatty Acid
TBHQ	-	<i>tert</i> -Butylhydroquinone

1 INTRODUCTION

1.1 Motivation for Research

Global climate change and fossil fuel depletion are among the most critical issues facing human civilization. The development and use of renewable energy sources has the potential to address both issues. Biofuels have been gaining increasing interest in the past decade as a substitute for petroleum in the transportation sector to mitigate the effects of greenhouse carbon dioxide (CO₂) emissions on climate change and offset the depletion of fossil fuels. However, if biofuels are to obtain a substantial penetration into the transportation sector, their production must be highly scalable and result in minimal environmental impact. Moreover, the physical and chemical properties of biofuels must be consistent with the properties of petroleum based transportation fuels. Microalgae derived biofuels have potential as scalable, environmentally benign fossil fuel replacements. Microalgae derived lipids and biomass can be converted into alcohols, methyl esters and alkanes for direct use in spark ignited gasoline engines, compression ignition (i.e. diesel) engines and aircraft engines. This thesis focuses on the physical and chemical properties of microalgae derived fatty acid methyl esters (i.e. FAME).

1.1.1 Global Climate Change

Warming of the climate system is unmistakable and is evident from observations of increased global average air and ocean temperatures, widespread decrease of permanent snow and

ice, and rising global average sea level (IPCC 2007). The Earth has always experienced a changing climate, but anthropogenic activity has significantly threatened the world during the last century (Chapman 2007). The Intergovernmental Panel on Climate Change's (IPCC) Fourth Assessment in 2007 determined that the increase in global average temperatures observed since the mid-20th century is very likely due to increased anthropogenic greenhouse gas concentrations. These global greenhouse gas emissions have grown since pre-industrial times with a substantial increase of 70 percent between 1970 and 2004 (IPCC 2007). Carbon dioxide (CO₂) is the most important anthropogenic greenhouse gas and its emissions have grown by 80 percent between 1970 and 2004 (IPCC 2007). The IPCC has also stated that global increases in CO₂ concentrations are predominantly due to the combustion of fossil fuels. Land-use change was also identified as another significant contributor. If renewable energies were used, the process of liberating naturally sequestered carbon into the atmosphere from the combustion of fossil fuels could be slowed.

Transportation is one of the few industrial sectors where CO₂ emissions are still rising, accounting for 26 percent of the global total emissions (Chapman 2007). Road transportation accounts for 81 percent of the total energy use in the transport sector and hence road transport is the largest producer of greenhouse gases (Chapman 2007). Personal vehicles are not the only culprit in greenhouse gas emissions. Road freight accounts for 43 percent, of all road transportation emissions (Chapman 2007). Today, vehicles emit less CO₂ than earlier models, but this reduction is being offset by the burgeoning growth in the number of on-road vehicles in countries like India and China (Chapman 2007). The United States (U.S.) Energy Information Administration (EIA) also expects new fuel efficiency standards to be outpaced by increases in population and gross domestic product (GDP) in the U.S. (U.S. Energy Information Administration 2010).

1.1.2 Peak Oil

Even if fossil fuel burning was not warming the planet, fossil fuels are still a finite source. With record oil field discoveries in the Gulf of Mexico and gasoline prices cheaper than bottled water, many find it hard to believe that global crude production will someday end (Appenzeller 2004). However, current estimates predict that the world oil supply could be depleted within the next fifty years, with some models predicting a much sooner date (Appenzeller 2004). In fact, the U.S. and Canada have already reached peak production in 1972 and production in Russia has fallen by 45 percent since 1987 (Chapman 2007).

Major new discoveries are becoming rarer and the production costs of each barrel of oil increase as the remote and hostile areas of the planet are tapped for resources. Today's new technology is discovering an increasing number of oil fields, but due to their insignificant size, they tend to deplete quickly after entering into production (Tsokounogiou, Ayerides and Tritopoulou 2008). With new discoveries falling short and demand continuously increasing, two to three barrels of oil are consumed for every new barrel discovered (Tsokounogiou, Ayerides and Tritopoulou 2008). The increase in demand is global with oil currently rising at more than two percent per year (Chapman 2007). The EIA forecasts that worldwide demand for oil will increase 60 percent by 2020.

This increase in demand and decrease in availability can be quite volatile to economies, such as the U.S., that depend largely on freight. Crude oil is the fossil fuel of choice for vehicular transportation and 97 percent of transportation and freight is powered by engines that burn this finite oil supply (Chapman 2007). From an economic perspective, the exact date at which the oil supply is completely depleted is not the critical date. Rather, the critical date is the date at which global production begins to taper off. The date at which global oil production begins to decline is referred to as "peak oil". Beyond the point of peak oil, prices will rise unless demand declines equally. The demand is not expected to decline and the EIA is predicting a rise in U. S.

consumption of liquid fuels, both fossil fuels and biofuels, from a demand of 20 million barrels per day in 2008 to 22 million barrels per day in 2035, which the EIA is expecting to be met primarily by diesel fuel and biofuels (U.S. Energy Information Administration 2010).

Since petroleum's end is looming and transportation continues to grow, energy alternatives such as biofuels, hydrogen, electric motors, and hybrids need to be considered. Biofuels provide one of the best solutions because they can be adapted for use with existing technologies. Liquid fuels are also critical to the U.S. military fleet, especially aviation, because to their high energy density compared to batteries.

1.2 Liquid Biofuels

Biofuels are a renewable solution to replace petroleum derived liquid fuels in the transportation sector. Two of the major renewable liquid fuels currently used in the United States are ethanol and biodiesel from vegetable crops (Durrett, Benning and Ohlrogge 2008). Often, the vegetables used for renewable feedstocks occur abundantly in the country of production. For example, in the U.S. ethanol is produced primarily from corn, whereas in Brazil ethanol is produced primarily from sugarcane. Similarly, in the U.S. biodiesel is produced primarily from soybeans, whereas many European countries produce biodiesel from rapeseed (Knothe, Dunn and Bagby 1997), (Grundwald March 27, 2008). Countries in tropical climates favor coconut oil or palm oil for biodiesel production.

The use of vegetable oils as an energy source is not a new concept and has been around for over 100 years. Rudolph Diesel reportedly unveiled his namesake engine running on peanut oil at the 1900 World's Fair in Paris (Knothe 2010), but because of the low cost of petroleum based fuels, vegetable oil derived fuels in diesel engines were quickly replaced by petroleum derived diesel fuel (Meher, Sagar and Naik 2006).

However interest in liquid biofuels has recently been renewed because of concerns about meeting air quality standards and national energy security (EPA 2002). There has been a major push by the U.S. government for renewable fuels to secure energy independence because feedstocks can be grown domestically. The Energy Independence and Security Act (EISA) of 2007 raised the renewable fuel standard by mandating the production of 36 billion gallons of renewable fuel per year by 2022 (Congress 2007). The EISA Act is incrementally increasing the renewable fuel production requirement each year until 2022. Starting in 2015, the EISA Act also places a cap of 15 billion gallons of corn starch ethanol per year, thereby requiring 21 billion gallons of advanced biofuels. The entire EISA Act renewable fuel standard requirements are shown in Table 1.1.

Table 1.1. EISA 2007 Renewable Fuel Standard. Adapted from (Congress 2007).

Year	Advanced Biofuel Production (billion gallons)	Corn Starch-Derived Ethanol Production (billion gallons)	Total Production (billion gallons)
2006	0.00	4.0	4.00
2007	0.00	4.7	4.70
2008	0.00	9.0	9.00
2009	0.60	10.5	11.10
2010	0.95	12.0	12.95
2011	1.35	12.6	13.95
2012	2.00	13.2	15.20
2013	2.75	13.8	16.55
2014	3.75	14.4	18.15
2015	5.50	15.0	20.50
2016	7.25	15.0	22.25
2017	9.00	15.0	24.00
2018	11.00	15.0	26.00
2019	13.00	15.0	28.00
2020	15.00	15.0	30.00
2021	18.00	15.0	33.00
2022	21.00	15.0	36.00

Advanced biofuels generally refer to cellulosic ethanol, but the EISA advanced biofuels renewable fuels standard may be met by any non-corn starch-derived biofuel (Congress 2007). One method of meeting the advanced biofuels standard domestically is to increase biodiesel and or renewable diesel production, since the United States is limited in its cellulosic ethanol production (Table 1.2). Since the data in Table 1.2 was compiled for the EISA of 2007 the production of biodiesel and corn ethanol has increased dramatically.

Table 1.2. U. S. Production of Biofuels from various feedstocks. Adapted from (Congress 2007).

Fuel	Feedstock	U. S. Production in 2006
Ethanol	Corn	4.9 billion gallons
	Sorghum	less than 100 million gallons
	Cane Sugar	No production (656 million gallons imported from Brazil and Caribbean countries)
	Cellulose	No production (one demonstration plant in Canada)
Biodiesel	Soybean Oil	approximately 200 million gallons
	Other Vegetable Oils	less than 10 million gallons
	Recycled Grease	less than 10 million gallons
	Cellulose	No production
Methanol	Cellulose	No production
Butanol	Cellulose, other biomass	No production

One major obstacle preventing widespread use of biofuels is the high cost of production relative to petroleum (Graboski and McCormick 1998). Common feedstocks such as corn, soybean, and rapeseed are generally more expensive than petroleum unless subsidized in some form (Knothe 2010). Additional feedstocks such as animal fats, used cooking oils, and yard waste (e.g. tree clippings) have more favorable economics, but their availability has limited impact on total biofuel production (Knothe 2010). Apart from supply and production economics, food versus fuel issues have gained attention in recent years. Grains (e.g. corn) make up approximately 80 percent of the world’s food supply and as more of this foodstock is used as

feedstock for biofuel production, global food security becomes increasingly threatened (Carolan 2009).

Due to the need for a liquid biofuel, and the various problems and issues with current liquid biofuels, new feedstocks must be explored. One such feedstock that is currently being cultivated domestically is microalgae.

1.3 The Algae Solution

The algae of interest are phototropic organisms that grow using CO₂ as their carbon source (Ratledge and Cohen 2008). Solazyme, though, has successfully cultivated heterotrophic algae for biofuels by feeding it sugar, but the scale and sustainability of this process is uncertain (Feroohar 2010). Sunlight and atmospheric CO₂ of course are both abundant and free.

Microalgae have long been known to be rich in lipids. Depending on the species they produce many different kinds of lipids (oils): triglycerides, diglycerides, phospholipids, glycolipids, and hydrocarbons (Greenwell, et al. 2010). The triglycerides are of interest for direct conversion into biodiesel via the transesterification process or conversion into renewable diesel or synthetic paraffinic aviation kerosene via hydrotreating.

The accumulation of oils is not a normal feature of most microbial cells, but is confined to a relatively small number of oleaginous species of yeasts, fungi, and algae (Ratledge and Cohen 2008). Oil accumulation is a result of unbalanced metabolism. When all the proper nutrients are present in the growth medium the synthesis of new cells will proceed with minimal levels of lipid accumulation. It is only when the cells become depleted (or are deliberately deprived) of key nutrients that they start to accumulate storage lipids (Ratledge and Cohen 2008).

Cells can be purposely grown to produce lipids through nutrient control. For example, the cells are grown to maximum density (stationary phase) and then lipid production is induced through nitrogen starvation (Wang, et al. 2009).

Algae have many cultivation and growth benefits. They are the fastest growing photosynthesizing organisms completing an entire growth cycle every few days (Demirbas 2007). Algae are also the most efficient biological producer of oil on the planet (Gouveia and Oliveira 2009). Algae can grow practically in every place where there is enough sunshine. They require less land and can grow in non-potable water, and they do not displace food crops. The main potential advantages of algae as feedstocks for biofuels are summarized by their ability to:

- (i) Synthesize and accumulate large quantities of lipids at 20-50 percent by weight;
- (ii) Rapidly grow doubling 1-3 times per day;
- (iii) Produce more oil yield per area than the yield of the best oilseed crops;
- (iv) Thrive in saline, brackish, and coastal seawater or wastewater;
- (v) Grow in an aquatic medium, though require less water than terrestrial crops;
- (vi) Tolerate non-arable lands (e.g. desert, arid- and semi-arid lands);
- (vii) Utilize growth nutrients such as nitrogen and phosphorus from a variety of wastewater sources (e.g. agricultural run-off, concentrated animal feed operations, and industrial and municipal wastewaters);
- (viii) Sequester carbon dioxide from flue gases emitted from fossil fuel-fired power plants and other sources;
- (ix) Produce value-added co-products or by-products (e.g. biopolymers, proteins, polysaccharides, pigments, animal feed, and fertilizer);
- (x) Produce residual algal biomass after oil extraction for feed or fertilizer, or fermented to produce ethanol or methane;

(Rodolfi, et al. 2009) and (Hu, et al. 2008)

While the general idea of using algae for energy production has been around for over 50 years, the concept of using lipids derived from algal cells to produce liquid fuels has arisen more

recently. Historically, algae were first seen as a promising source of protein and were harvested for food. Large scale open pond cultivation of algae for food was first conceived by German scientists during World War II (Hu, et al. 2008). It was not until after the war that the U.S. first began large scale algae cultivation at the Stanford Research Institute from 1948-1950 and algae methane production research began shortly thereafter (Hu, et al. 2008).

However, while terrestrial crop production and harvesting have many centuries of development history, the algal biofuels industry is still in its very early stages of technology development and commercially viable production has yet to be demonstrated at scale. Today, the production of algal oil is primarily confined to high-value specialty oils with nutritional value, rather than commodity oils for biofuel (Hu, et al. 2008).

Much of the pioneering research on microalgal biofuel production was performed by the National Renewable Energy Laboratory (NREL) through the Department of Energy's (DOE) Aquatic Species Program (ASP) from 1978 to the 1996 (Sheehan, Dunahey, et al. 1998). The DOE's ASP represents the most comprehensive effort to date in the algal biofuels arena. This 18 year program was supported by more than \$25 million of government funding and yielded numerous advances in algal strain isolation and characterization, physiology, biochemistry, genetic engineering, process development, and algal culture piloting. However, the program was ended when petroleum fuels still proved more economically and widely available (Sheehan, Dunahey, et al. 1998). Fortunately, the U.S. government has recently recommitted to algal biofuels through a variety of programs including the \$50 million DOE National Alliance for Advanced Biofuels and Bioproducts Consortium (NAABB), which supported the work presented in this thesis.

Algae are a far more suitable biofuel feedstock compared to terrestrial crops due to their superior growth rates and oil production capabilities. Microalgae commonly double their biomass within 24 hours and biomass doubling times during exponential growth are commonly as short as 3.5 hours (Chisti 2007). Their oil content can exceed 80 percent by weight of dry

biomass, but oil levels of 20-50 percent are more common (Chisti 2007). According to some estimates, the yield (per acre) of oil from algae is over 200 times the yield from customary biofuel plants (Demirbas 2007). Table 1.3 shows a comparison of common biofuel feedstock crops and their production per year.

Table 1.3. Comparison of some sources of biodiesel. Adapted from (Chisti 2007).

Crop	Oil Yield (L/ha)	Land Area Need (Mha)^a	Percent of Existing US Crop Area^a
Corn	172	1540	846
Soybean	446	594	326
Canola	1190	223	122
Jatropha	1892	140	77
Coconut	2689	99	54
Oil Palm	5950	45	24
Microalgae ^b	136,900	2	1.1
Microalgae ^c	58,700	4.5	2.5

a - for meeting 50% of all transport fuel needs of the United States

b - 70% oil (by wt) in biomass

c - 30% oil (by wt) in biomass

As shown in Table 1.3, it is conceivable that less than 3 percent of the total existing U.S. crop area would be sufficient for producing algal biomass to satisfy 50 percent of all the transport fuel needs for the U.S. Conversely, there is clearly not enough arable land available to produce this same amount of biofuels from corn or soybeans. In the short term, an influx of algae oil could also help the U.S. reach its biodiesel (i.e. FAME) production capacity. The production of biodiesel in the U.S. in 2008 was roughly 700 million gallons (Figure 1.1), which was well below the production capacity of 2.7 billion gallons available (National Biodiesel Board 2009).

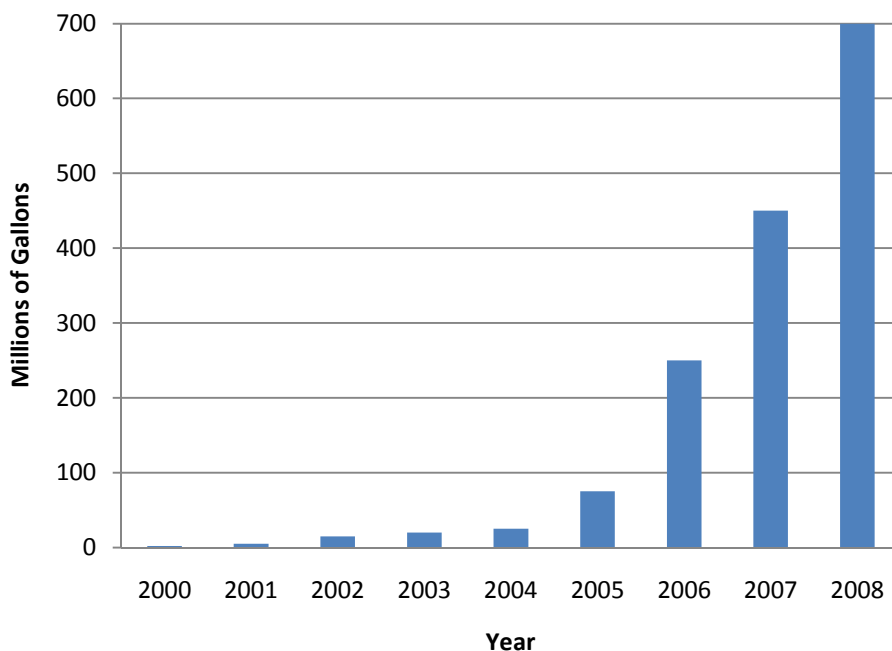


Figure 1.1. U.S. annual biodiesel production. Adapted from (National Biodiesel Board 2009).

More recently, Weyer and coworkers (2010) performed a more detailed study to estimate the maximum algal oil productivity (L/ha/yr) possible given the theoretical photosynthetic efficiency of algae. Based on this approach, the theoretical maximum oil production from algae at 50 percent cell oil content was calculated to be 354,000 L/ha/yr (38,000 gal/acre/yr) at the equator with an uncertainty of roughly ten percent. An achievable best case scenario was calculated to range from 40,700-53,200 L/ha/yr (4,350 to 5,700 gal/acre/yr), which is slightly less than Christi's algal oil prediction shown in Table 1.3 (Weyer, et al. 2010).

Another study (Hu, et al. 2008) determined a theoretical algae production of greater than 30,000 L/ha/yr. Although there is still slight disagreement in the literature, all of the calculated theoretical maximum yields are two orders of magnitude greater than that achievable by the current primary U.S. biofuel feedstocks (corn and soybeans). Therefore, even if algal biofuel productivity were to approach even a reasonable fraction of the calculated theoretical maximum, algae biofuels have high potential for increased productivity in comparison to current biofuels.

The ability of algae to fix CO₂ also creates interesting opportunities for greenhouse gas reduction. Terrestrial crops also fix atmospheric CO₂ during their development, but since algae cultivation does not require arable land, algae plants can be coupled with coal-fired power plants (Gouveia and Oliveira 2009) (Zeiler, et al. 1995) (Sawayama, et al. 1995). The two main CO₂ mitigation strategies normally used in power plants are chemical reaction-based or biological mitigation. Chemical reaction-based solutions are energy-consuming and costly, and they create disposal issues for the captured CO₂ and used absorbents (Mata, Martins and Caetano 2010). Microalgae can biologically fix CO₂ in flue gases in two possible ways: CO₂ separated from the flue gas or directly in the flue gas (Maeda, et al. 1995). If algae utilize power plant CO₂, the emissions are not permanently sequestered due to the later fuel combustion, but more energy is produced per unit of CO₂ released.

Water requirement is another potential benefit of algae cultivation in comparison to terrestrial biofuel feedstocks. Many algae species do not need freshwater or potable water. Not only can algae grow in non-potable water, but it can be used to treat wastewater. Algae cultivated in wastewater uses inorganic chemicals such as phosphates and nitrates as nutrients, reduces the amount of toxic metals, and saves water usage (Mata, Martins and Caetano 2010) (Sawayama, et al. 1995). Algae farms could also be paired with waste streams from intensive animal farming operations (Greenwell, et al. 2010).

Algae biomass can also be useful after oil extraction, further adding to cultivation benefits. After oil extraction the resulting algae biomass can be processed into ethanol using fermentation or methane via anaerobic digestion, sold as livestock feed, used as organic fertilizer, or simply burned for energy cogeneration (electricity and heat) (Mata, Martins and Caetano 2010) (Ratlidge and Cohen 2008).

1.4 Algae Biodiesel

Microalgae can provide several different types of renewable biofuels. These include methane produced by anaerobic digestion of the algal biomass, bio-oil derived from microalgal oil, and photobiologically produced biohydrogen (Chisti 2007). The bio-oil can be used to produce biodiesel, renewable diesel, renewable gasoline or synthetic paraffinic aviation kerosene. The latter three fuels would be composed of mixtures of straight and branched alkanes with composition tailored to produce the required properties for the specific application. Conversely, algae derived biodiesel (i.e. alkyl esters produced directly from algae triglycerides via transesterification reaction with an alcohol) will have properties that are directly related to the fatty acid composition of the algal triglycerides.

This thesis focuses on fuel properties of algae derived biodiesel. The ASTM D 6751 Standard Specification for Biodiesel Fuel Blend Stock (B100) for Middle Distillate Fuels defines biodiesel as a fuel comprised of mono-alkyl esters of long chain fatty acids derived from vegetable oils or animal fats.

Ethanol and biodiesel are the two major renewable liquid fuels currently used in the U.S., but biodiesel has several advantages over ethanol as a liquid fuel. First, biodiesel has a 25 percent higher energy content per volume, which translates directly into greater fuel economy. Secondly, ethanol can lead to corrosion of pipelines and therefore must be stored separately from gasoline and mixed before use. Third, a fermentation step is required for the conversion of carbohydrate to ethanol, which is then followed by substantial energy inputs to distill ethanol from water (Durrett, Benning and Ohlrogge 2008).

Biodiesel on the other hand is not corrosive. It is completely miscible with petroleum diesel fuel (referred to as D-1 for Number 1 and D-2 for Number 2 diesel fuels) and is usually used as a blend (Graboski and McCormick 1998). One of the most common blends of biodiesel in the U.S. is 20 volume-percent biodiesel and 80 volume-percent conventional diesel designated

B20 (EPA 2002). A B100 diesel fuel indicates 100 percent biodiesel. An important compositional difference between petroleum diesel and biodiesel is oxygen content. Biodiesel contains 10 – 12 weight-percent oxygen, which lowers the energy density, but it also lowers particulate emissions (Graboski and McCormick 1998) and the reduction in particulate emissions is also imparted to biodiesel-diesel fuel blends (McCormick, Graboski, et al. 2001). Biodiesel can also be run either pure or in blends with diesel fuel in an unmodified diesel engine (Van Gerpen, et al. 2006).

The fuel lubricity in diesel engines is important because many fuel pumps are lubricated by the diesel fuel itself and fuel pumps have been known to fail since the arrival of low-sulfur diesel and, more recently, ultra-low sulfur diesel regulations (Graboski and McCormick 1998). But the mixing of petroleum diesel with biodiesel improves lubricity of the fuel because biodiesel has superior natural lubricating properties compared to petroleum diesel (Knothe 2010).

The use of biodiesel also decreased U.S. dependence on imported petroleum. Although the percentage of the U.S. fuel supply displaced by biodiesel is small, an additional source of fuel has a surprising impact on stabilizing fuel prices since petroleum markets are sensitive to small fluctuations in supply (Van Gerpen, et al. 2006). Even though more gasoline is used than diesel, on-road diesel demand is increasing at almost four percent per year whereas gasoline is only increasing at one and a half percent per year in the U.S. (Canes 2007). Also, since most on-road freight transportation relies on diesel fuel, the demand for diesel fuel is highly sensitive to economic growth. If the U.S. GDP continues to rise, so will the demand for diesel (Canes 2007).

If algae-derived biodiesel is to capture a substantial percentage of the diesel fuel market, it must qualify as “fit for purpose” as a drop in substitute for existing compression ignition engine technologies. To ensure that algal biodiesel is compliant, it must meet the ASTM Biodiesel Standard D6751 in the U.S. and the EN 14214 in the European Union (EU) for B100 use in diesel engines.

The process of chemically altering renewable oil to biodiesel is called transesterification. Feedstock oils are typically transesterified to reduce viscosity and improve engine longevity. Straight vegetable oil (SVO) can be safely burned for short periods of time in a diesel engine, but extended run periods can result in engine problems. The high viscosity of SVO reduces fuel atomization and increases fuel spray penetration, which is thought to lead to severe engine deposits, piston ring sticking, injector coking, and thickening of the lubricating oil (Monyem, Van Gerpen and Canakci 2001). Other disadvantages to the use of high viscosity (about 11-17 times higher than diesel fuel) SVO are the lower volatilities that cause the formation of deposits in engines due to incomplete combustion and incorrect vaporization characteristics (Meher, Sagar and Naik 2006).

However, these effects can be reduced or eliminated through transesterification of the vegetable oil (or animal fat). Transesterification is the process of reacting a triglyceride molecule with an excess of alcohol in the presence of a catalyst (e.g. KOH, NaOH) to produce glycerol and mono-alkyl fatty acid esters. If the triglycerides were derived from vegetable oil or animal fat the mixture of mono-alkyl esters are what is defined as biodiesel (Van Gerpen, et al. 2006). The catalyst must be used for the reaction to occur in a reasonable amount of time.

Biodiesel is typically transesterified using methanol and, therefore the fatty acid alkyl esters that are produced are fatty acid methyl esters (FAME). FAME are the most prevalent esters because of the price and availability of methanol compared to other alcohols (Knothe, Dunn and Bagby 1997). The transesterification reaction occurs within approximately one hour at slightly above room temperature with an excess of 90 – 97 percent methanol (Graboski and McCormick 1998). The chemical reaction with methanol is shown schematically in Figure 1.2. R1, R2, and R3 represent the hydrocarbon chains of the fatty alkyl groups of the triglyceride.

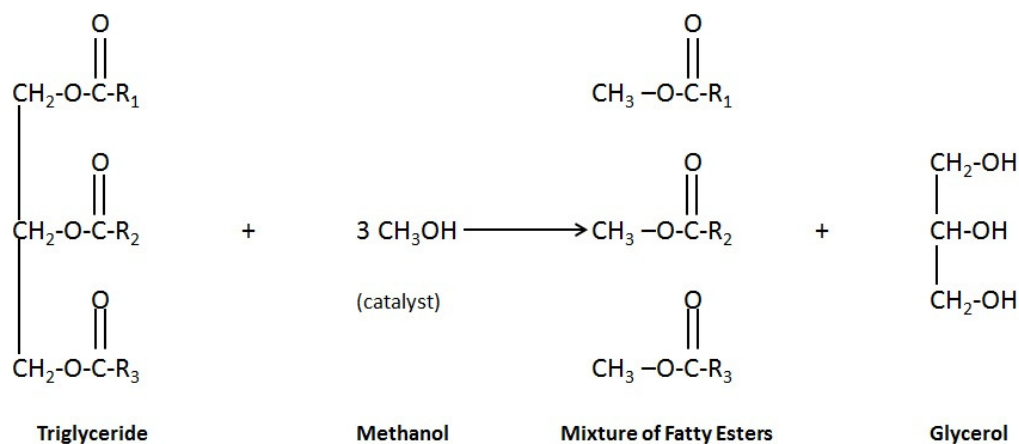


Figure 1.2. Transesterification of triglyceride with methanol. Adapted from (Van Gerpen, et al. 2006)

Transesterification reduces the viscosity of the FAME compared to the parent oil, but the fatty acid composition is not altered from the feedstock (Ramos, et al. 2009). This is important since the chain length and number of double bonds determine the characteristics of some critical parameters of biodiesel such as oxidative stability, cetane number, and cold flow properties.

1.4.1 Long-Chain Polyunsaturated Fatty Acids

A distinguishing difference between algal FAME and most common vegetable FAME is that some algal lipids contain a substantial amount of polyunsaturated fatty acids (PUFA: four or more double bonds). The long chain-polyunsaturated fatty acids (LC-PUFA) with a carbon chain length greater than 18 (C18) cannot be synthesized in significant amounts by naturally occurring higher plants, but algae have been known to accumulate large quantities of LC-PUFA (Hu, et al. 2008). For example, eicosapentaenoic acid (EPA, C20:5), a 20 carbon chain with five double bonds, and docosahexaenoic acid (DHA, C22:6), a 22 carbon chain with six double bonds, occur commonly in algal oils (Chisti 2007). Table 1.4 shows a comparison of fatty acid composition

between several common biodiesel feedstocks and algal lipids. The algal lipids clearly have greater quantities of unsaturated compounds compared to typical feedstocks.

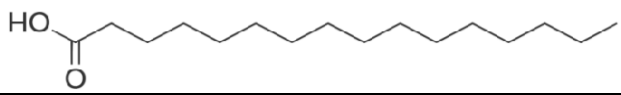
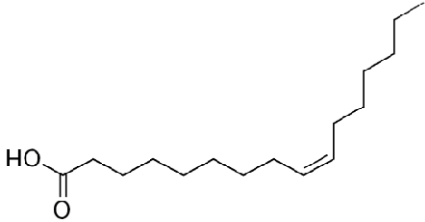
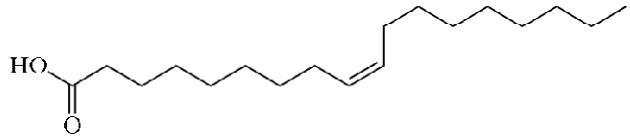
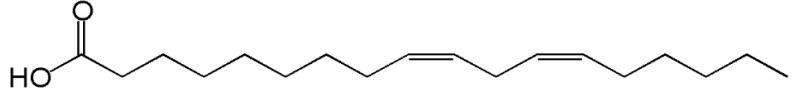
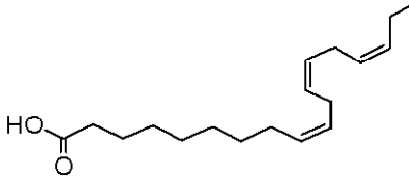
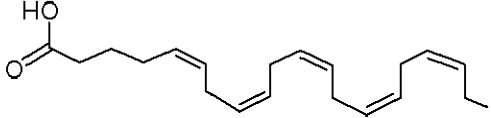
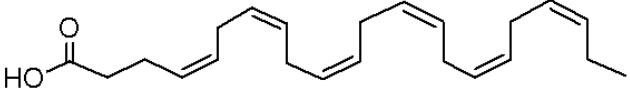
Table 1.4. Comparison of fatty acid profiles for seven biodiesel sources based on fatty acid composition by percent weight^a, fatty acids denoted by Carbon #: Double Bond #.

Feedstock	8:0	10:0	12:0	14:0	16:0	16:1	18:0	18:1	18:2	18:3	20:4	20:5	22:6
Soy					11		4	24	53	8			
Canola					4		2	61	19	10			
Coconut	9	6	49	17	8		2	5	2				
Palm				1	42		5	41	10				
Jatropha					11		17	13	47				
Nanno. Oculata				2	15	16	2	10	4	3	6	21	3
Isochrysis Galbana				23	14	3	1	14	5	7		5	14

^a The fatty acid profiles shown were compiled from several sources: (Berthiaume and Tremblay 2006) (Moser 2008) (Tiwari, Kumar and Raheman 2007) (Yuan, Hansen and Zhang 2009) (Roncarati, et al. 2004) (Hu, et al. 2008)

Table 1.5 shows a the chemical structure of some of the common fatty acids found in vegetable and algae oils. From the graphic it is clear that double bonds play a major role making EPA's and DHA's structure highly unsaturated.

Table 1.5. Common fatty acids found in vegetable and algae oils, along with their carbon number: double bond number description and structure. Adapted from (Fisher 2009).

Name	Chain Length: Double Bonds	Structure
Palmitic Acid	16:0	
Palmitoleic Acid	16:1	
Stearic Acid	18:0	
Oleic Acid	18:1	
Linoleic Acid	18:2	
Linolenic Acid	18:3	
EPA	20:5	
DHA	22:6	

1.5 Problematic Fuel Issues

It is well understood that the fatty acid composition of FAME has a major effect on fuel properties. While saturation and fatty acid profile do not appear to affect the production of

biodiesel by the transesterification process, they do affect the fuel properties of the final product. The most important characteristics affected by the level of unsaturation are oxidative stability, ignition quality (i.e. cetane number), and cold flow properties (Hu, et al. 2008), (Greenwell, et al. 2010), (Ramos, et al. 2009).

For example, saturated oils produce a biodiesel with superior oxidative stability and a higher cetane number, but they are more likely to gel at ambient temperatures with their rather poor low-temperature properties (Hu, et al. 2008). Conversely, biodiesel produced from feedstocks like algal lipids that are high in PUFA are particularly susceptible to oxidation resulting in deterioration during storage but they have good cold-flow properties (Hu, et al. 2008) (Greenwell, et al. 2010).

1.5.1 Oxidative Stability

Oxidative stability is an important issue for biodiesel due to its natural biodegradability. Oxidation of the liquid fuel may occur not only during storage, but also during production and use (Knothe and Dunn 2003). The issue is that even low concentrations of polyunsaturated fatty esters have a disproportionately large effect on oxidative stability (Durrett, Benning and Ohlrogge 2008).

Oxidative stability is an industrial concern because byproducts formed during decomposition contribute to deposit formations in tanks, fuel systems, and filters (Graboski and McCormick 1998). Biodiesel oxidation products can result from the initial accumulation of hydroperoxides, which eventually polymerize and form the insoluble sediments that are capable of plugging filters, fouling injectors, and interfering with engine performance (Durrett, Benning and Ohlrogge 2008) (Karavalakis, Karonis and Stournas 2009). The polymerization reaction can also lead to an increase in viscosity (Knothe 2007). Furthermore, very high levels of oxidation in biodiesel can cause separation of two phases causing fuel pump and injector operation problems

(McCormick, Ratcliff, et al. 2007). Thus, companies that transport and store biodiesel are very concerned about oxidative stability. Factors promoting oxidation are the presence of air, light, elevated temperatures, and the presence of extraneous materials (Knothe 2010).

The oxidative stability of biodiesel can be further affected during production. It has been noted that minor natural antioxidants are removed during distillation purification, and biodiesel produced by distillation typically contains little or no natural antioxidants (Graboski and McCormick 1998) (McCormick, Ratcliff, et al. 2007).

Oxidative stability is determined in biodiesel using the EN 14112 method, which measures an induction period for oxidation when the fuel is subjected to an elevated temperature. The period of slow oxidation that precedes rapid oxidation is the induction period (Van Gerpen, et al. 1997). Both the EU and the U.S. have standards for a minimum induction period; the U.S. requires a minimum of three hours (ASTM D6751) and the EU requires a minimum of six hours (EN 14214). McCormick and coworkers have determined that if the induction time is near or below the three hour limit, B100 will most likely go out of specification within four months (McCormick and Westbrook 2010). It was also determined that the three hour induction time limit appears to be adequate to prevent oxidative degradation for B5 blends in storage for up to 12 months and B20 blends for up to four months (McCormick and Westbrook 2010).

The EU biodiesel standard also contains specifications in regards to saturation content such as the iodine value (IV), but this specification has some drawbacks (Knothe 2010). The IV is a structure-related index in fatty acid chemistry that relates to the total number of double bonds in a fat or oil. A major drawback of the IV is that it does not distinguish between the structural differences in fatty compounds such as the position of the double bonds and so it treats all double bonds as equally reactive (Knothe and Dunn 2003). A new saturation index was developed by Knothe after the IV was determined to be insufficient in providing technical details in biodiesel standards. These indices are the bis-allylic position equivalents (BAPE) and the allylic position

equivalents (APE) and are reported to correlate more accurately with oxidative stability (Knothe 2002); Waynick 2005).

Since the introduction of the BAPE and APE, many researchers have also concluded that oxidative stability does not correlate with the total number of double bonds, but with the total number of bis-allylic sites [(Berthiaume and Tremblay 2006) (Jain and Sharma 2010) (Waynick 2005) (Karavalakis, Karonis and Stournas 2009) (Arisoy 2008) (McCormick, Ratcliff, et al. 2007) (McCormick and Westbrook 2010) (Knothe and Dunn 2003) (Pahgova, Jorikova and Cvengros 2008) (Sarin, et al. 2009)].

The allylic and bis-allylic sites are important because they are the location most susceptible to the attack from oxygen in air. The allylic site is a methylene group (CH₂) adjacent to a double bond and the bis-allylic site is a methylene group adjacent to two double bonds (Knothe 2002). The equations to calculate BAPE and APE developed by Knothe are:

$$\text{Equation 1.1: } APE = ap_a \times A_{Ca} + ap_b \times A_{Cb} + ap_c \times A_{Cc} + \dots$$

$$\text{Equation 1.2: } BAPE = bp_a \times A_{Ca} + bp_b \times A_{Cb} + bp_c \times A_{Cc} + \dots$$

where ap_x is the number of allylic positions in a specific fatty acid, bp_x is the number of bis-allylic positions in a specific acid, and A_{Cx} is the amount (mass-percent) of each fatty acid in the mixture. A visual representation of an allylic site and a bis-allylic site, shown in Figure 1.3 on the end of a fatty acid chain, clearly shows that there are always two allylic sites whenever there are one or more double bonds and one less bis-allylic site than double bonds present. This bond structure where two single bonds are between the double bonds occurs naturally.

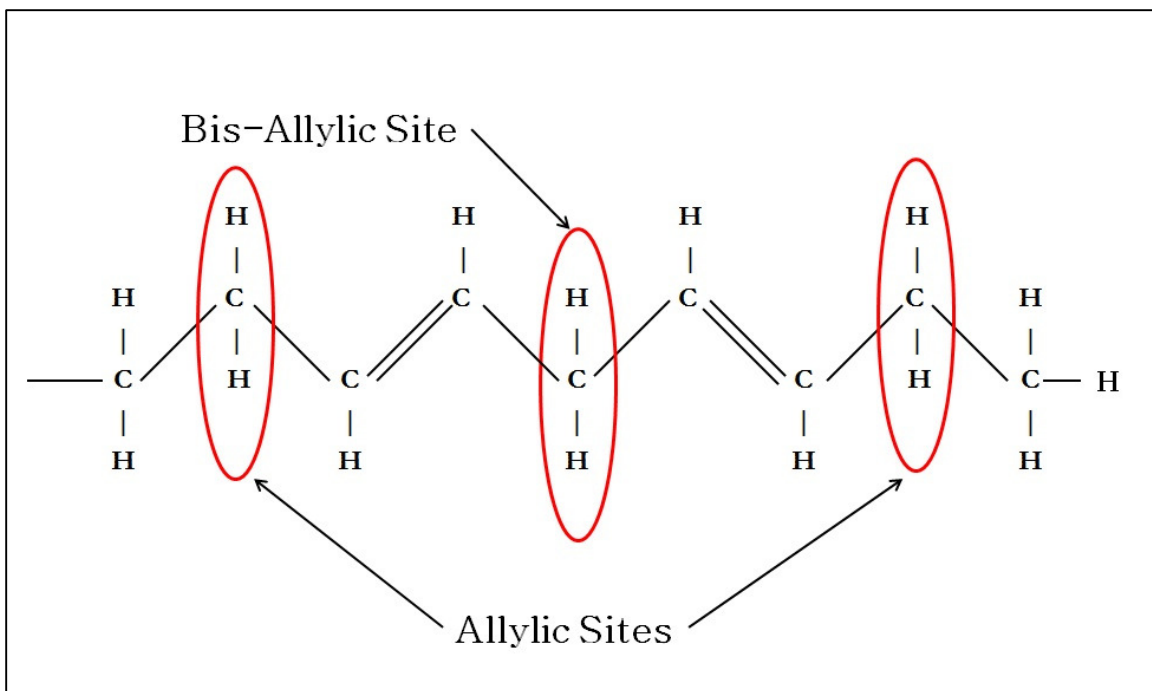


Figure 1.3. Schematic of BAPE and APE sites.

These sites react with oxygen via the autoxidation mechanism with the classical radical chain reaction steps of initiation, propagation, and termination (McCormick, Ratcliff, et al. 2007) (Frankel 1998). The susceptibility to autoxidation in unsaturated oils is dependent on the availability of allylic hydrogen for reaction with peroxy radicals. The initiation step is the formation of a free radical that can react directly with oxygen to form a peroxide or hydroperoxide. This peroxy radical formation mechanism on a methylene group is shown in Figure 1.4. The most reactive position for initial radical formation is the bis-allylic position, and the allylic position is much less reactive, thus autoxidation of unsaturated fatty compounds proceed at different rates depending on the number and position of double bonds (McCormick, Ratcliff, et al. 2007), (Knothe 2010) This is why small amounts of more highly unsaturated fatty compounds containing bis-allylic carbons have been observed to have a disproportionately strong effect on oxidative stability (Knothe and Dunn 2003).

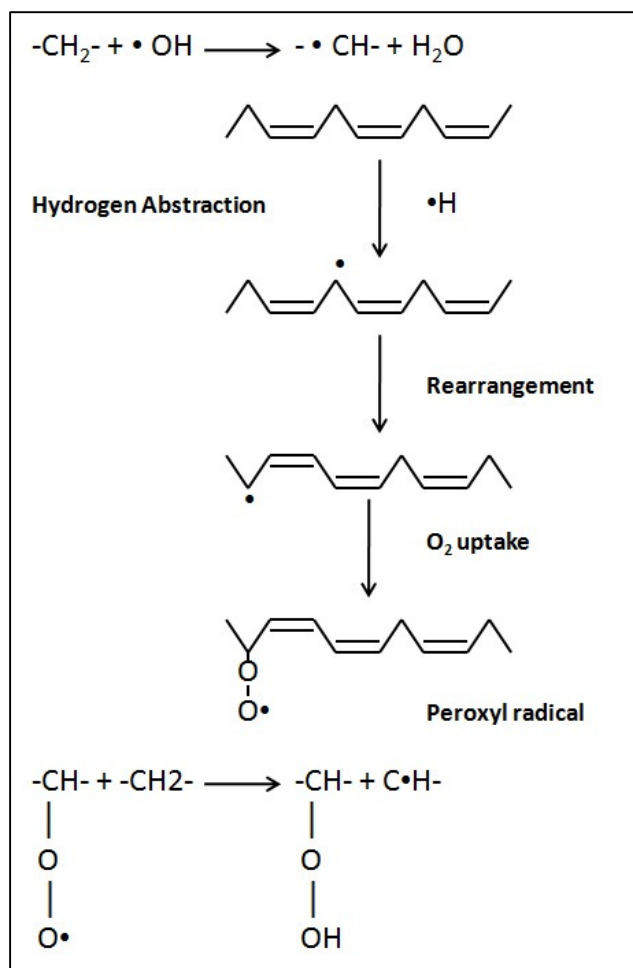


Figure 1.4. Mechanism for peroxy radical formation on a methylene group. Adapted from (Arisoy 2008).

To explore the validity of BAPE and APE correlations with oxidative stability, the BAPE and APE were calculated for methyl esters reported from a study by the Renewable Energy Group (Sanford, et al. 2009). In that study, the oxidative stability induction period was found to vary exponentially with the BAPE with an R-squared value of only 0.53 (Figure 1.5) because of several outlying data points. A correlation of BAPE + APE, or the overall double bond position and structure, to induction period was also explored (Figure 1.6), but there appeared to be no correlation. The induction period, as will be described later, is the length of time required for oxidation products to be created during testing.

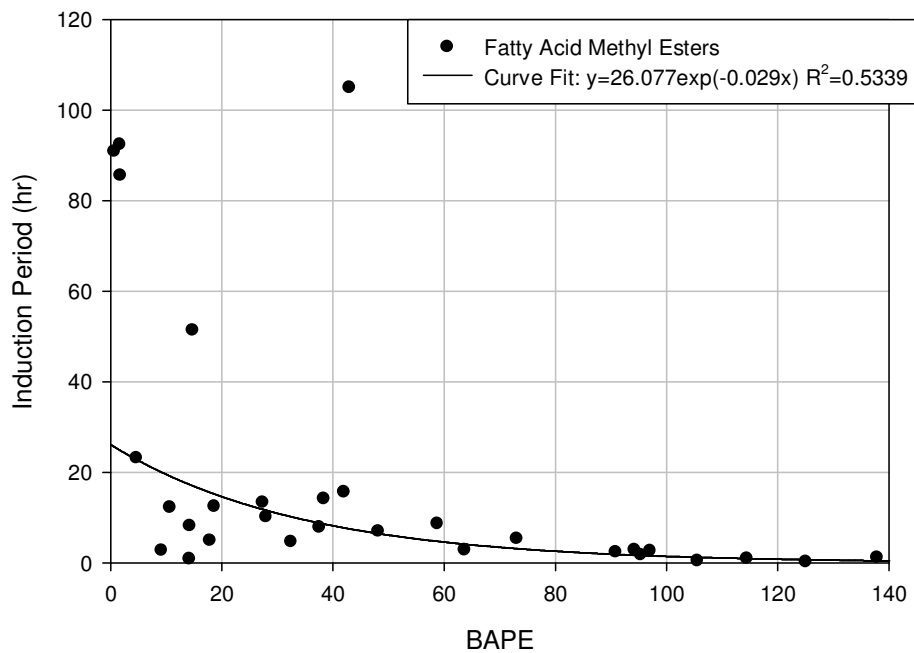


Figure 1.5. Induction period as a function of BAPE for (Sanford, et al. 2009).

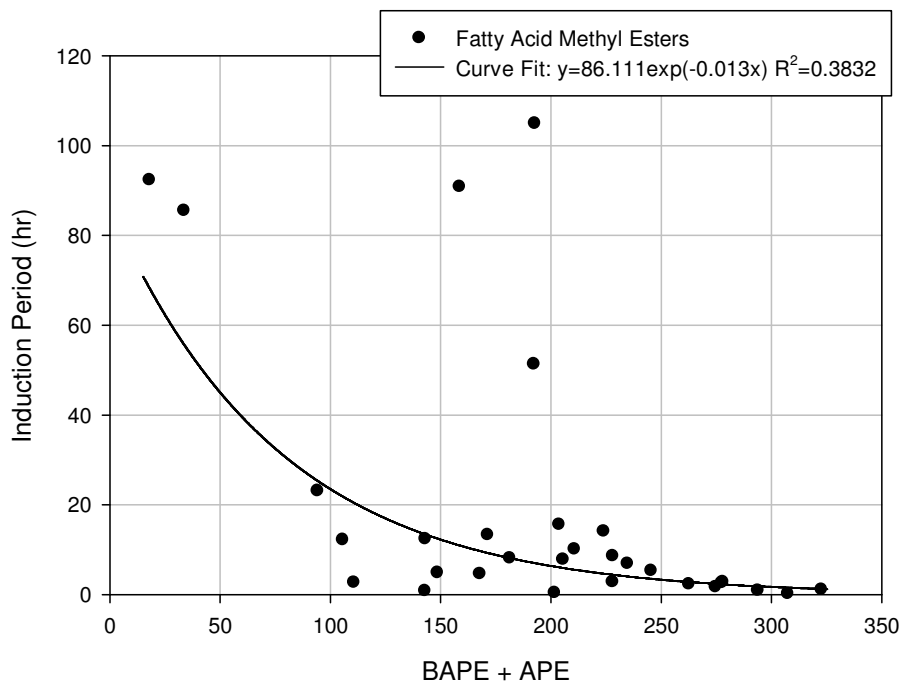


Figure 1.6. Induction period as a function of BAPE + APE for (Sanford, et al. 2009).

1.5.2 Cetane Number

The fatty acid composition of the feedstock used for biodiesel production also affects the ignition quality of the fuel as measured by its Cetane Number (CN). The carbon chain length and the number of double bonds in the fatty acid chain both affect the ignition quality. The Cetane Number (CN) is a dimensionless parameter related to the ignition delay period that the fuel experiences upon injection into the cylinder of a diesel engine. The higher the CN, the shorter the ignition delay period, and the lower the CN, the longer the ignition delay period. A CN scale using hydrocarbons has been established in which n-hexadecane ($C_{16}H_{34}$) is the high CN (CN=100) reference compound with a very short ignition delay period and 2,2,4,4,6,8,8-heptamethylnonane (HMN; also $C_{16}H_{34}$) is the low CN (CN=15) reference with a long, poor quality ignition. The ASTM D6751 standard for biodiesel requires a minimum CN of 47 and the EN 14214 requires a minimum CN of 51. The ignition quality of diesel fuel is commonly measured using a Cooperative Fuels Research (CFR) engine, but recently newly developed instruments such as the Ignition Quality Tester (IQT) and Fuels Ignition Tester (FIT) have been accepted as alternative standards for measuring ignition quality as described in ASTM D6890 and ASTM D7170 for the IQT and FIT, respectively. These instruments measure a Derived Cetane Number (DCN), which has been shown to correlate directly with CN as measured using a CFR engine as specified in ASTM D613.

The CN of a diesel fuel must be within acceptable limits for proper operation of a compression ignition engine. If the CN of the fuel is too high, combustion can occur before the fuel and air are properly mixed resulting in incomplete combustion and smoke; Conversely, low CN leads to misfiring, higher combustion air temperatures, slower engine warm-up, and incomplete combustion (Knothe, Dunn and Bagby 1997). Moderately high CN (≈ 50) are desired for proper operation of a compression ignition engine and also help to ensure good cold start properties (Ramos, et al. 2009).

It is well known that biodiesel CN increases with the length of the fatty acid chain and with saturation of the alkyl chain (Ramos, et al. 2009) (Knothe 2010) (Knothe, Matheaus and Ryan 2003) (Knothe, Dunn and Bagby 1997). As discussed above, some of the algae species that are currently being considered for large scale production of biofuels produce a substantial percentage of LC-PUFA lipids such as EPA (C20:5) and DHA (C22:6). Although the chain lengths of these fatty acids are higher than those found in typical terrestrial feedstocks (which might imply higher CN), the results presented herein show that the high degree of unsaturation of these fatty acids has a stronger effect on the ignition quality, thereby resulting in decreased CN. Indeed, for the feedstocks considered in the present work, the CN was found to vary linearly with BAPE.

1.5.3 Cold Temperature Properties

The cold temperature properties of biodiesel are likewise affected by the fatty acid composition of the feedstocks. However, the degree of saturation has an opposite effect on the cold temperature properties in comparison to its effect on oxidative stability and CN. Biodiesel with high amounts of saturated methyl esters has poor low-temperature properties whereas biodiesel with high amounts of unsaturated methyl esters has superior low-temperature properties (Knothe, Dunn and Bagby 1997). Poor cold temperature properties can lead to fuel gelling or crystallizing in cold weather, which can lead to poor fuel atomization or fuel system clogging. Based on the fatty acid composition of lipids produced by some of the species under consideration for wide scale cultivation, it is expected that methyl esters produced from these lipids will have acceptable cold temperature properties.

1.6 Fuel Improvement Solutions

There are several scenarios that might be employed in the future to improve the fuel properties of algae FAME. The fatty acid composition of the algal lipids could be altered, fuel property improving additives could be used, or a combination of the two. It has been shown that genetic alteration of algae is possible (Dunahay, et al. 1996), but this would add to production costs. Plus, there have already been vast numbers of discovered algae species, and there is an almost unlimited potential to discover new species, any of which could already have ideal oil cultivation genetics (Sheehan, Dunahey, et al. 1998). But given the antagonistic saturation characteristics between oxidative stability and cetane number and cold flow properties, there might not be a fatty acid profile that would optimize all three parameters (Durrett, Benning and Ohlrogge 2008).

1.6.1 LC-PUFA Removal

Another solution to improve the fuel quality of algae FAME would be to remove the troublesome LC-PUFA to produce a product with a fatty acid composition similar to that of commonly used feedstocks such as soy or rapeseed. This process would improve the oxidative stability and the cetane number. Another advantage to removal of LC-PUFA from algae is that many LC-PUFA, such as EPA and DHA, can be sold as a valuable co-product in areas such as cosmetics, pharmaceuticals, nutrition, food additives, and aquaculture (Mata, Martins and Caetano 2010).

The LC-PUFA (e.g. EPA and DHA) are considered pharmacologically important for dietetics and therapeutics. They have been used for treatments of chronic inflammation such as rheumatism, skin diseases, and inflammation of the gastrointestinal tract. Also, they are believed to have a positive effect on cardio-circulatory diseases, coronary heart diseases, atherosclerosis, hypertension, cholesterol, and cancer treatment (Mata, Martins and Caetano 2010). In fact, EPA

specifically has been the subject of intense study because dietary supplements appear to protect against coronary thrombosis and have some beneficial effects in the treatment of hypertriglyceridemia, hypertension, and certain inflammatory diseases (Williard, et al. 1998).

There are already several successful companies that specialize in the production of LC-PUFA from algal lipids for nutritional additives. For example, Martek Biosciences Corporation (Columbia, MD) sells oil rich in DHA extracted from algae to companies that package it in vitamins and in a number of food items, such as milk, cooking oils, and infant formulas (Martek Biosciences Corporation 2009).

Because of the high value of EPA and DHA, combined with the fact that some algae species that accumulate EPA and/or DHA in substantial quantities (i.e. *Nannochloropsis*) also have high productivity in terms of growth rate and total lipid accumulation, it is expected that conditions will be economically favorable for the removal of some percentage of EPA and DHA from algal lipids prior to conversion of the remaining lipids into biofuels. Such an approach would improve the quality of the fuel feedstock and decrease the consumer costs for the high nutritional products. The DOE is also suggesting this approach of pursuing high value co-products to offset production costs in the short term (U.S. Department of Energy 2010). It should be noted, however, that if algal biofuels obtain annual production rates on the order of the EISA Advanced Biofuels standards (≈ 10 billion gal/year) then the EPA and DHA would likely no longer have a high economic value.

1.6.2 Additives

The use of additives have been widely employed during biodiesel production and may be a solution to enhance algae biodiesel fuel properties. One study with Karavalakis and coworkers determined that the use of synthetic phenolic antioxidant additives at a concentration of 1000 mg/kg improved oxidative stability for each additive tested. The additives in question, listed in

order of effectiveness in B100, were propyl gallate (PG), pyrogallol (PA), tert-butyl hydroquinone (TBHQ), butylated hydroxytoluene (BHT), and butylated hydroxyanisole (BHA). The phenolic antioxidants generally improve stability by providing protons that inhibit the formation of free radicals or interrupt the propagation of free radicals through their active hydroxyl group (Karavalakis and Stournas 2010).

1.7 Thesis Overview

This thesis presents the results of several fuel property tests that were performed to determine the amount of the LC-PUFA removal of EPA and DHA that would need to be removed from algal lipids such that the methyl esters produced from the remaining lipids would meet oxidative stability and cetane number specifications for B100 biodiesel. Three algae species known to accumulate substantial quantities of EPA and/or DHA were considered as model compounds for this study. Chapter 2 describes the instrumentation used to perform this study. The instrumentation used is designed specifically to accurately measure key biodiesel properties.

The fuel formulation procedure and fatty acid composition for each of the fuels tested are provided in Chapter 3. Methyl esters with fatty acid composition similar to that of the three algae species under consideration were formulated using several different methyl esters that were transesterified in-house. The algae based methyl ester model compounds were synthesized by matching the degree of saturation using both a BAPE and APE comparison to the actual algal lipid profiles. Transesterified pharmaceutical grade fish oil was used along with soy, canola, and corn methyl esters and a pure saturated methyl ester from Proctor & Gamble. Additional algae based methyl ester model compounds were then synthesized to represent varying amounts of EPA and DHA removal. In addition to the algae based methyl ester model compounds, tests were also performed with actual algal methyl esters, which were produced from algal lipids obtained from multiple sources.

In Chapter 4, the test procedures are described. The test conditions and quality control measures are described for each instrument. The set of fuels tested for each instrument are also described.

Chapter 5 presents the results for each fuel property test. All of the algae based methyl ester model compounds failed the oxidative stability tests, as expected. But the oxidative stability was found to improve with the removal of EPA/DHA and two of the three model compounds were found to pass the ASTM biodiesel oxidative stability standards by removing 45 to 65 percent of the LC-PUFA. The third species did not pass specifications with 100 percent EPA and DHA removal. Additives were found to greatly improve the oxidative stability of the algae FAME. With the addition of additives, the algae FAME were able to pass oxidative stability specification without the removal of EPA and DHA. The cetane number testing also revealed a correlation between EPA and DHA removal and improved cetane number. The results showed that 100 percent of the EPA and DHA would need to be removed for the algae FAME to meet ASTM CN specifications for two of the three model compounds. The third model compound did not meet ASTM CN standards with 100 percent EPA/DHA removal.

The speed of sound, density, and viscosity of the model algae FAME formulations were also measured. The speed of sound and density increased with increasing levels of saturation of the methyl ester formulations. The viscosity measurements did not appear to show much of a correlation with fatty acid composition but all of the methyl esters fell within ASTM specifications.

In Chapter 6, conclusions from this work are summarized and future measurements of key biodiesel properties are described to further explore the capabilities of algae biodiesel.

2 EXPERIMENTAL EQUIPMENT

All of the experimental work for this project was conducted at Engines and Energy Conversion Laboratory (EECL) at Colorado State University. The EECL was founded in 1992 for engines research but has been recently equipped for advanced biofuels characterization through the National Alliance for Advanced Biofuels and Bioproducts (NAABB).

2.1 Metrohm 743 Rancimat Description

The oxidative stability tests were conducted using a Metrohm 743 Rancimat instrument. The 743 Rancimat is an approved instrument for measurement of B100 induction period as specified by the ASTM D6751 and EN 14214 Standards. Both standards refer to the EN 14112 method to determine the oxidative stability induction period with the 743 Rancimat. Metrohm has developed the Rancimat as an automatic variant to the extremely complex Active Oxygen Method for determining the induction period of fats and oils. The Rancimat test parameters and specifications are shown in Table 2.1.

Table 2.1. Metrohm 743 Rancimat oxidative stability testing specifications.

Instrument	Method Followed	Standard	Specification	Test Parameters		
Metrohm 743Rancimat	EN 14112	D6751	3 hours minimum	10 L/h air flow	110°C	3 gram sample
		EN 14214	6 hours minimum			

The 743 Rancimat is controlled by a personal-computer (PC) through an RS-232 interface and the 743 Rancimat control and evaluation computer program. Up to four instruments can be connected to one PC allowing 32 samples to be analyzed, but only one 743 Rancimat was used for this research. Each determination is automatically saved in the Rancimat program along with the method used and determination data.

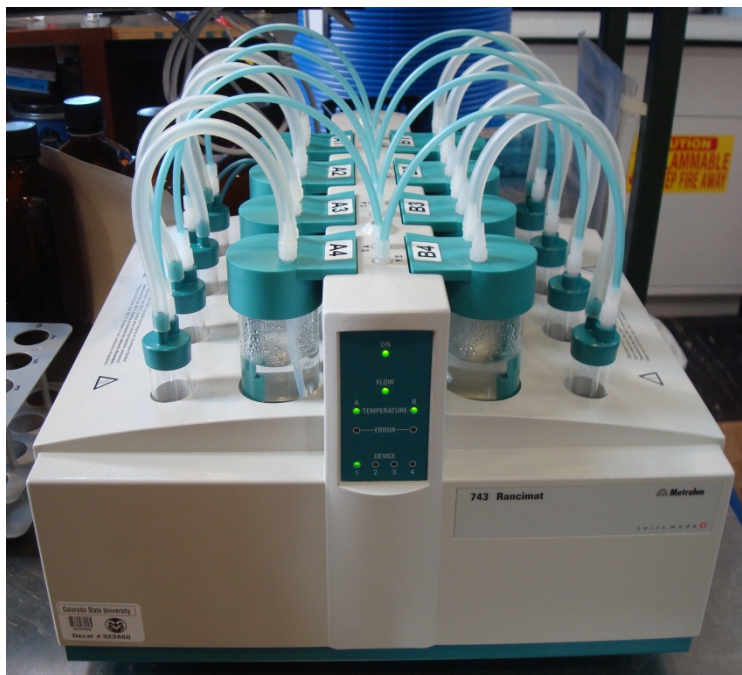


Figure 2.1. Metrohm 743 Rancimat pictured at EECL.

The 743 Rancimat contains two separate heating blocks, each with four measuring positions (channels). Each block is heated individually allowing tests at two different temperatures. For the experiments reported herein, both heating blocks were maintained at 110°C per the EN 14112 method resulting in eight simultaneous standard tests.

The Rancimat computer program uses an algorithm to determine the induction period automatically from a measured Rancimat curve. The Rancimat curve is the measured electrical conductivity in micro-siemens per centimeter of the solution as a function of time in hours. The stability time (or time duration to reach a specified conductivity change) is determined using the

Rancimat program. The Rancimat curve can also be evaluated manually using the tangential method to evaluate extreme cases.

The Rancimat method uses an accelerated autoxidation process that normally occurs slowly at ambient temperatures to study the decay of vegetable and animal oils. The Rancimat method allows the sample to be exposed to an air flow at a constant temperature ranging between 50 and 220°C, but standard tests were conducted at ten liters per hour and 110°C per the EN 14112 method.

The Rancimat internal pump supplies the air flow through fluorinated ethylene propylene (FEP) tubing by first passing the ambient air through absorbent molecular sieves. A glass reaction vessel, which holds a 3 gram fuel sample, sits in the heating block and the air is bubbled through the sample via a glass tube attached to the FEP tubing. The volatile compounds that are released from the liquid sample then flow up through a silicone tube to the measuring vessel. The air is bubbled through a distilled water solution via a polytetrafluoroethylene (PTFE) tube attached to the silicone tubing. Finally, an electrode in measuring vessel cell measured the electrical conductivity of the solution, which is recorded as a function of time by the Rancimat program. This process is shown in Figure 2.3. When the airflow carries highly volatile secondary oxidation products (mainly formic acid) to the measuring vessel where they are absorbed in the distilled water, the conductivity of the solution rapidly increases. The time period from the beginning of the test to the rapid increase in thermal conductivity of the solution is defined as the induction period. A typical Rancimat curve, which is a plot of conductivity vs. time, is shown in Figure 2.2.

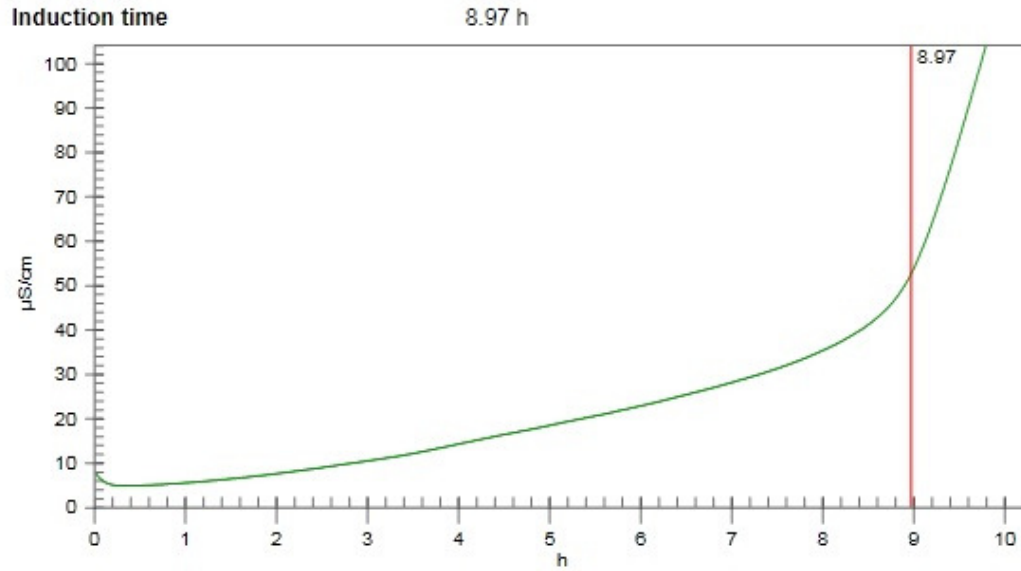


Figure 2.2. Example Rancimat curve determine induction period.

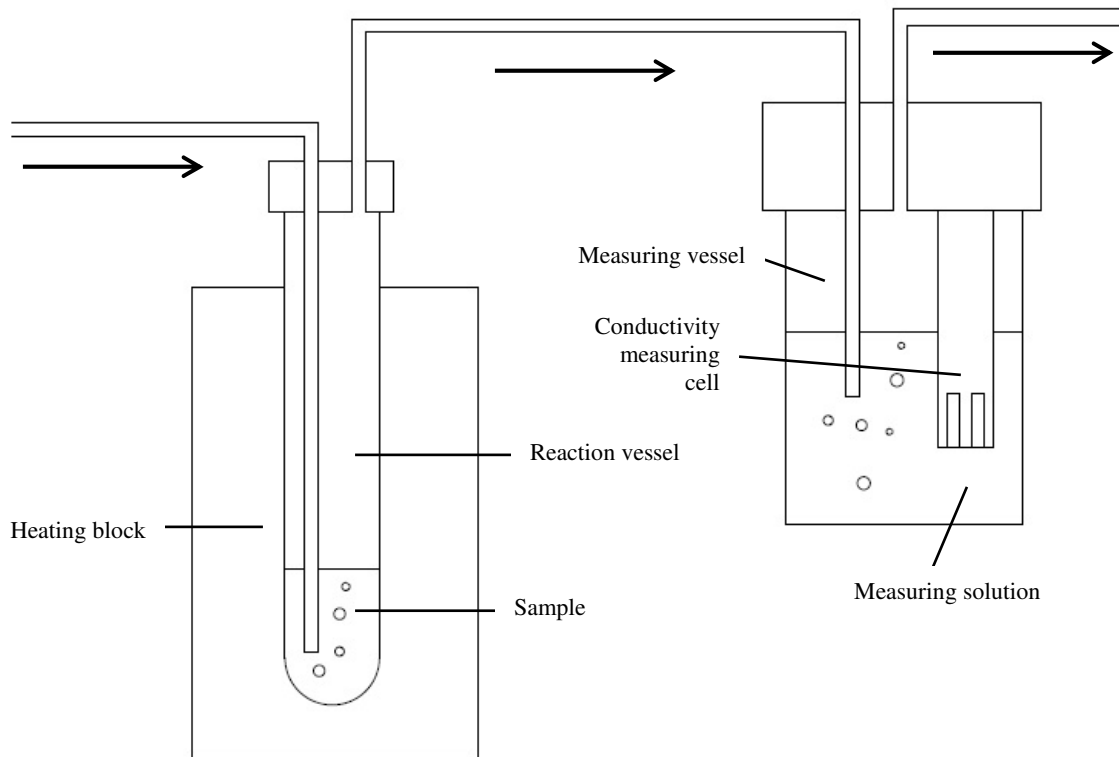


Figure 2.3. Rancimat schematic.

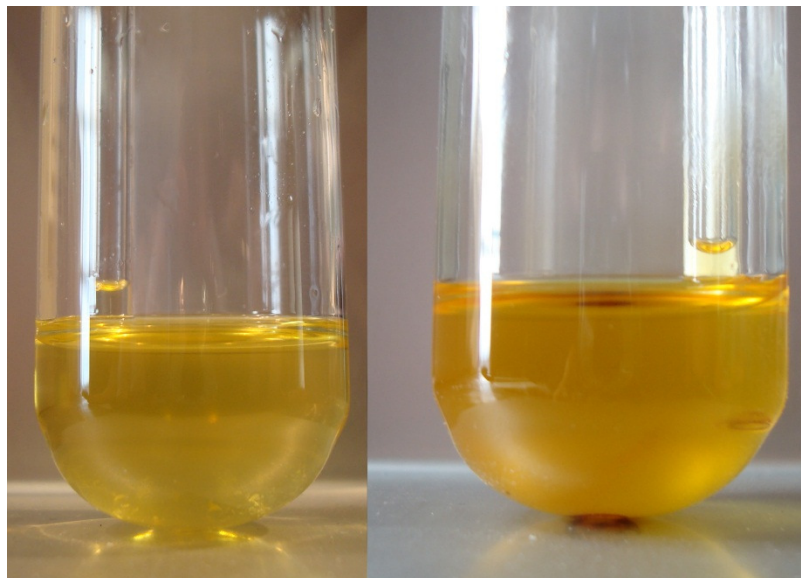


Figure 2.4. Biodiesel sample before (left) and after (right) Rancimat test.

The change in the appearance of a typical sample from the accelerated oxidation process during a Rancimat test is clearly seen in Figure 2.4.

The 743 Rancimat was calibrated for conductivity and temperature. The conductivity was calibrated using 0.01 M potassium chloride (KCl) conductivity solution from Sigma Aldrich (St. Louis, MO). The KCl was diluted to a 0.001 M solution resulting in 147 $\mu\text{S}/\text{cm}$ conductivity at 25°C. The temperature was calibrated using silicone oil from Sigma Aldrich (St. Louis, MO) resulting in a 0.7°C and 0.8°C temperature offset for heating block A and heating block B, respectively.

Polycarbonate measuring vessels were initially supplied and used in the Rancimat tests, but the volatile compounds caused the solution to gum and react with the walls of the measuring vessel (Figure 2.5). The measuring vessels were then replaced with reusable glass vessels and the conductivity measuring cells were recalibrated.



Figure 2.5. Measuring vessel before (left) and after (right) Rancimat test.

2.2 Waukesha FIT Description

The Cetane Number tests were conducted on a Waukesha Fuels Ignition Tester (FIT) (Figure 2.6), which determines a derived cetane number (DCN). The FIT is an approved instrument for biodiesel DCN determination by the ASTM D7170 method. The ASTM D6751 Standard requires a minimum cetane number of 47. Waukesha has developed the FIT for DCN as a substitute to the conventional CFR F5 Cetane Method Diesel Rating Unit for cetane number because the FIT method requires much less fuel and a smaller testing footprint. The FIT test parameters and specifications are shown in Table 2.2.



Figure 2.6. FIT pictured at EECL.

Table 2.2. Several of the Waukesha FIT DCN testing specifications

Instrument	Method	Standard	Specification	Test Parameters			
				# of Injections	Injection Period	Fuel Temperature	Coolant Temperature
Waukesha FIT	D7170	D6751	47 minimum	25 injections	5.00+/-0.25 ms	35+/-2°C	30+/-0.5°C

The FIT method of determining a DCN uses a constant volume combustion chamber. The constant volume combustion chamber is heated to a specified wall temperature and pressurized to 2.40+/-0.02 MPa. The FIT determines the DCN of a single sample from the average of a series of 25 injections. The average injection period must be 5.00+/-0.25 milliseconds with no single injection outside of 4.00 ms or 6.00 milliseconds.

Since the cetane number describes propensity of a fuel to autoignite, the ignition delay is measured and recorded by the FIT and then the DCN is calculated. The DCN is calculated from Equation 2.1 where ID is the ignition delay in milliseconds.

$$\text{Equation 2.1: } DCN = \frac{171}{ID}$$

The FIT connects to a PC, which displays and records the test results. To achieve the required ignition delay, the fuel injection pump rack is adjusted manually. To allow for priming and proper ignition delay adjustment, two test injections are performed immediately before the 25 recorded injections. The fuel injection system is pictured in Figure 2.7.



Figure 2.7. FIT fuel injection system.

The FIT uses a circulating bath with 50-50 antifreeze and coolant mixture of ethylene glycol and water adjustable between -20 and 100°C to one tenth of a degree using an integrated

PID controller and circulating pump. The high pressure combustion air is delivered from bottled high purity air containing 20.9 \pm 1.0 percent oxygen, less than 0.0003 percent hydrocarbons, and less than 0.025 percent water. The combustion air is provided to the FIT via a two stage regulator adjusted to 415 psi and a high pressure line with fittings. The low pressure air, which is used for the injection actuator, is provided from 120 psi shop air from the EECL's air compressor.

The FIT was calibrated by adjusting the combustion chamber wall temperature set point using n-heptane and methylcyclohexane (MCH) from Sigma Aldrich (St. Louis, MO). The wall temperature was adjusted until all the ignition parameters were met and the ignition delay for three consecutive n-heptane tests was 3.15 \pm 0.02 milliseconds. The FIT was then deemed calibrated when the measured ignition delay for MCH was 10.1 \pm 0.5 milliseconds for two consecutive tests. The FIT was checked for quality assurance before each operating period with n-heptane.

2.3 Anton Paar Stabinger SVM 3000 Description

The dynamic and kinematic viscosity measurements were conducted using the Anton Paar SVM 3000 Stabinger Viscometer instrument (Figure 2.8). The measurements followed the ASTM D7042 Standard Test Method for Dynamic Viscosity and Density of Liquids by Stabinger Viscometer (and the Calculation of Kinematic Viscosity), which is a built-in measurement setting for the SVM 3000.



Figure 2.8. SVM 3000 pictured at the EECL.

This setting takes three consecutive measurements of the sample at 40.00°C to determine the validity of the dynamic viscosity and density measurements. The kinematic viscosity is then calculated from:

$$\text{Equation 2.2: } \nu = \mu/\rho$$

Where ν is the kinematic viscosity, μ is the dynamic viscosity, and ρ is the density. The density was not reported for this study from the SVM 3000 because the Anton Paar DSA 5000 M measures density to six decimal places, while the SVM 3000 only measures to four decimal places.

The SVM 3000 measures the dynamic viscosity and density simultaneously by using a rotational coaxial cylinder measuring system and a U-shaped oscillating sample measuring tube. Both measuring cells are held at the same temperature by copper blocks surrounding the cells. A thermoelectric heating and cooling system ensures that the copper blocks are within $\pm 0.005^\circ\text{C}$.

Since dynamic viscosity describes the resistance of a fluid to flow or deform under external shear forces, the dynamic viscosity is measured with the rotational coaxial system. A motor drives the outer cylinder at a known rotational speed and the inner cylinder is held in position by the sample and a magnet soft iron ring. The inner low-density cylinder rotational speed is measured with an electronic Hall Effect sensor by counting the frequency of the rotating magnetic field when equilibrium of the driving torque, viscous forces, and eddy current torque are reached. The density is measured with the U-shaped oscillating sample tube by exciting the tube at its characteristic frequency electronically. This characteristic frequency changes depending on the density of the sample injected and the density is determined from a digital analyzer.

2.4 Anton Paar DSA 5000 M Description

The density and speed of sound measurements were conducted on the Anton Paar DSA 5000 M (Figure 2.9) at 40.00°C. The DSA 5000 M uses an oscillating U-tube method to simultaneously determine two physically independent properties from one sample injection. The sample is injected manually into a U-shaped borosilicate glass tube that is being excited at its characteristic frequency electronically. This characteristic frequency changes depending on the density of the sample injected.



Figure 2.9. DSA 5000 M pictured at the EECL.

Through determination of the characteristic frequency and a mathematical formula, the density of the sample is calculated. The formula the DSA 5000 M uses is:

$$\text{Equation 2.3: } \rho = KA \cdot Q^2 \cdot f_1 - KB \cdot f_2$$

Where KA and KB are instrument constants, Q is the quotient of the period of oscillation of the U-tube divided by the period of oscillation of the reference oscillator, and f_1 and f_2 are correction terms for temperature, viscosity, and nonlinearity.

The sound velocity is measured with an ultrasonic transmitter on one side of the measuring cell and a receiver on the other side. The transmitter sends sound waves of a known period through the sample and the sound velocity is determined by calculating the period of the received sound waves, shown in Equation 2.4.

$$\text{Equation 2.4: } v = \frac{\text{original length} (1+1.6e-5 \cdot \Delta\text{temp})}{\left(\frac{P_s}{\text{divisor}}\right) - \text{TAU} \cdot f_3}$$

In Equation 2.4 the original length is the path length of the sound waves, Δtemp is the temperature deviation to 20°C, P_s is the oscillation period of the received sound waves, divisor equals 512, TAU is the instrument constant, and f_3 is the correction term for temperature.

The DSA 5000 M was calibrated using pure water at 20°C. The oscillation period is measured by optical pickups and two integrated Pt 100 platinum thermometers with Peltier elements provide the precise thermostating of the sample. Since gas bubbles greatly affect the precision measurement, an automatic filling check detection warns of gas bubbles in the measuring cell and a built in camera allows the user to visually inspect the U-tube for gas bubbles on the integrated display and controller screen.

A summary of the measurements conducted, instrumentation used, methods followed, and specifications required for this thesis work is shown in Table 2.3.

Table 2.3. Summary of test parameters, instruments used, and methods followed.

Measurement	Instrumentation	Method Followed	Standard	Specification
Oxidative Stability	Metrohm 743Rancimat	EN 14112	D6751	3 hours minimum
			EN 14214	6 hours minimum
Cetane Number	Waukesha FIT	D7170	D6751	47 minimum
Dynamic Viscosity	Anton Paar Stabinger SVM 3000	D7042	None	None
Kinematic Viscosity	Anton Paar Stabinger SVM 3000	D7042	D6751	1.9 – 6.0 mm ² /s
Density	Anton Paar DSA 5000 M	None	None	None
Speed of Sound	Anton Paar DSA 5000 M	None	None	None

3 FUEL PRODUCTION AND ANALYSIS

The fuel used for testing was obtained and produced from a variety of sources. Unrefined algal lipids were provided by Eldorado Biofuels (Santa Fe, NM). An unrefined algal FAME product produced by a single step extraction and transesterification process was provided by Inventure Chemical, Inc. (Tuscaloosa, AL). A refined, distilled algal FAME, which was produced from the El Dorado algal lipids was provided by Catilin, Inc. (Ames, IA). These three samples were provided through the NAABB Consortium. The fatty acid profiles of these algae-derived samples are shown in Table 3.1. The Catilin and Eldorado samples' profiles were measured using Gas Chromatograph by Solix Biofuels, Inc. and the Inventure sample's profile was provided by New Mexico State University through the NAABB.

The algae FAME from Inventure contained 50 percent DHA, but was determined to be only 43 percent FAME, thereby disqualifying it from any direct comparisons to the other methyl ester formulations employed in this study. It did prove to perform consistently to the formulations in terms of oxidative stability, though. The Eldorado oil sample was the unrefined algal lipids that Catilin used to produce a clear, distilled FAME and hence the reason for the similar fatty acid profiles. The Catilin sample was shown to have been previously oxidized when subjected to Fourier Transform Ion Cyclotron Resonance (FT-ICR) mass spectrometry testing and was also therefore of limited value for comparisons against the other methyl esters (Schaub 2011). The Eldorado sample did not contain any EPA or DHA, but it did prove useful in validating results.

The algal lipids and algae FAME samples were in limited supply, so another methyl ester source was necessary for complete testing. In theory, it would be possible to purchase different pure fatty acid methyl esters from a chemical supply company, such as Sigma-Aldrich, to match

an exact algal profile. However, experience from past work (Fisher 2009) at the EECL suggested that this approach is cost prohibitive and algae FAME could be accurately simulated inexpensively using transesterified fish oil and vegetable oils. The model algal methyl ester formulations were synthesized to represent varying amounts of the removal of the LC-PUFAs EPA and DHA as discussed above in Chapter 1.6.1. The specific formulations and approach will be discussed in further detail later in Chapter 3.2. The additive used for testing was Bioproduct 350 from Vitablend (Wolvega, Netherlands), which contained 30 percent *tert*-Butylhydroquinone (TBHQ). All of the fuels used for the testing mixtures were stored in amber-colored glass bottles in a residential refrigerator at 14°C immediately after transesterification

Table 3.1. Aglae FAME samples' fatty acid profiles. *Algal oil converted to FAME for gas chromatography – mass spectrometry analysis.

	Catilin	Inventure	Eldorado*
C10:0		1.95	
12:0		5.16	
14:0		10.22	
16:0	7.07	13.82	6.73
18:0	2.48	1.62	2.46
16:1		0.92	
18:1	47.31	13.55	47.48
18:2	36.02	0.85	35.97
18:3	7.12		7.31
C22:6		50.70	
Total	100.00	98.79	99.94
Percent FAME	95.8	42.9	100.0

3.1 Model Algal Methyl Ester Compounds

As previously mentioned, the main difference between algal lipids and other vegetable oils currently used for biodiesel is the long-chain, highly unsaturated fatty acid content. Fish oil has similar LC-PUFA fatty acids to that of algal lipids produced by species such as

Nannochloropsis. The fatty acid composition of the fish oil is not, however, identical to that of the lipids produced by Nannochloropsis. The similarities between the fish oil and algal oil are a consequence of the aquatic species food chain that starts with algae. To produce the model algal methyl ester formulations, transesterified fish oil was mixed with other transesterified vegetable oils.

Pharmaceutical grade fish oil high in EPA and DHA was purchased from Jedwards International Inc. (Quincy, MA) and vegetable oils were purchased from a local supermarket. The vegetable oils used for formulation were Great Value pure corn oil, Great Value vegetable oil (100 percent soybean), and Wesson pure canola oil. A free sample of methyl laurate (C12:0; CE1295) from Procter & Gamble's chemical division (Cincinnati, OH) was also used as a formulation ingredient.

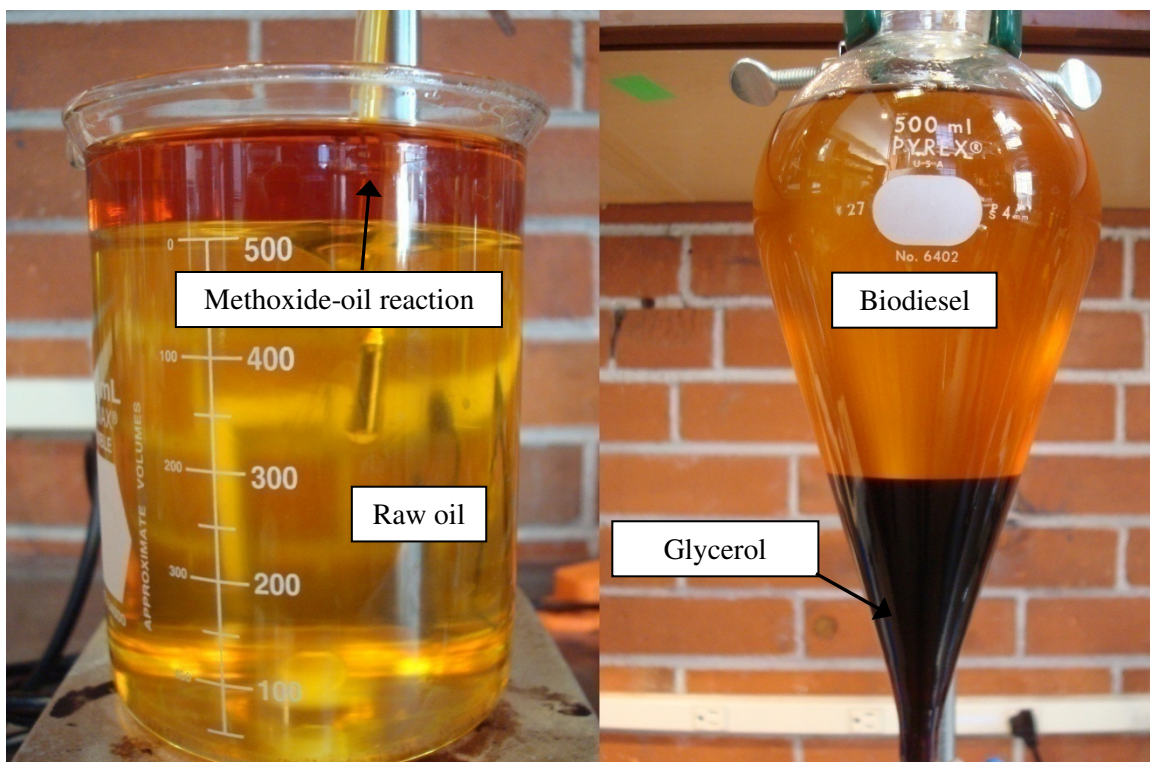


Figure 3.1. Bench-scale reactor at EECL. Left image: initial methoxide-oil reaction. Right image: glycerol-FAME separation.

The fish and vegetable oils were transesterified on the bench-scale as shown in Figure 3.1 in 500 mL batches using potassium hydroxide (KOH) tablets purchased from the Colorado State University Chemistry Stockroom and methanol purchased from Sigma-Aldrich USA (St. Louis, MO). The Eldorado algal lipid sample was transesterified in a similar fashion. The transesterified ingredient oils can be seen below in Figure 3.2 along with algae FAME samples.



Figure 3.2. Ingredient and algae FAMES. Left to right: methyl laurate, corn, canola, soy, fish, Inventure, Catilin.

3.2 Model Algal Methyl Ester Fuel Formulation

Model algal methyl ester compounds were formulated to obtain fatty acid profiles similar to the storage lipids produced by three different algae species that produce lipids that are high in LC-PUFA. The fatty acid composition from these algae species were obtained from the literature. The first alga chosen was *Nannochloropsis oculata* as profiled during a logarithmic growth stage (Roncarati, et al. 2004) because it is high in LC-PUFAs containing over 21 and three percent EPA and DHA, respectively. This alga is labeled *Nannochloropsis Oculata Growth* throughout the text. The second alga chosen was *Nannochloropsis Sp* (*Nanno Sp*) (Benamotz, Tornabene and Thomas 1985) because it was cited to contain 26.5 percent EPA. The last alga modeled was *Isochrysis Galbana* (*Iso Galbana*) (Hu, et al. 2008) because it contains 14 percent DHA and five percent EPA. The model algae fatty acid profiles are shown in Table 3.2.

Table 3.2. Modeled algae fatty acid profiles. 1 (Roncarati, et al. 2004) , 2 (Benamotz, Tornabene and Thomas 1985) , 3 (Hu, et al. 2008)

	<i>Nanno Oculata Growth</i> ¹	<i>Nanno Sp</i> ²	<i>Iso Galbana</i> ³
12:0		2.8	
14:0	2.39	3.2	23.1
15:0	0.65		1.1
16:0	14.53	9.2	14.0
18:0	1.83	2.1	1.1
20:0	1.96		
14:1	0.02	3.2	
16:1	15.67	19.8	3.0
17:1	4.12		
18:1	10.12	3.6	14.0
20:1	0.91		
22:1	0.68		
18:2	3.61	1.1	5.0
20:2	1.61	6.6	
22:2			1.0
18:3	2.52	9.1	7.0
20:3	0.53	2.5	
18:4			10.0
20:4	5.98		
20:5-EPA	21.48	26.5	5.0
22:6-DHA	3.23		14.0
Unknown	8.16	10.4	1.7
Total:	100	100	100

To accurately model methyl esters produced from lipids from these algae strains, the BAPE and APE of the model compounds were matched to those values that would be produced from the fatty acid compositions of the algal lipids in Table 3.2. The BAPE and APE were matched since the bis-allylic carbon site is the point of initial oxidation as previously discussed. Even though the allylic site is not known as a strong participator in initial oxidation reactions, both BAPE, APE, and BAPE + APE were matched to yield a more complete and accurate representation of the fatty acids' total double bond count and structure. For example, 20 percent of linolenic acid (C18:3) and 10 percent EPA (C20:5) both have a BAPE value of 40. However,

C18:3 has an APE of 40 while C20:5 has an APE of 20. The BAPE and APE of each species and each methyl ester were calculated using Equation 1.1 and Equation 1.2. The fatty acid profiles of each ingredient oil can be seen in Table 3.3.

Table 3.3. Ingredient fatty acid profiles. 1 (Berthiaume and Tremblay November 2006), 2 (Knothe 2002), 3 (Proctor & Gamble), 4 (Fisher 2009)

	Soy ¹	Canola ¹	Corn ²	CE1295 ³	Fish Oil ⁴
8:0				0.10	
10:0				0.30	
12:0				98.20	
14:0	0.10		0.15	1.14	6.46
15:0				0.10	0.46
16:0	10.60	4.20	12.55		15.09
17:0	0.00	0.10			1.96
18:0	4.10	1.90	2.15		3.20
20:0	0.20	0.70			0.80
22:0		0.40			
24:0		0.20			
14:1					0.63
16:1	0.10	0.20			9.24
17:1	0.10	0.20			0.46
18:1	24.20	60.70	31.10		13.09
20:1	0.20	1.50			2.19
22:1		0.30	0.05		1.09
24:1		0.20			0.61
18:2	52.50	19.30	50.95		1.06
20:2		0.20			
18:3	7.90	9.90	1.00		1.24
20:4					1.09
22:5					2.12
20:5-EPA					17.75
22:6-DHA					11.49
Unknown	0.00	0.00	2.05	0.16	9.96
Total:	100	100	100	100	100

To test the effects of fuel properties with respect to removal of varying levels of LC-PUFA, the removal of EPA and DHA were simulated in amounts of roughly 0, 25, 50, 75, and 100 percent. The BAPE and APE of the three algal methyl esters subjected to varying levels of LC-PUFA removal were calculated for each removal percentage and then model algal methyl ester compounds were formulated by matching the BAPE, APE, and BAPE + APE with the appropriate amounts of fish, soy, canola, corn, and CE1295 methyl esters. The overall formulation mixtures that were tested are shown in Table 3.4. A zero percent removal formulation was not accurately attained for *Nannochloropsis Sp* or *Isochrysis Galbana*. Table 3.5 shows the BAPE and APE comparisons for each model compound formulation along with that of the actual species. Since the algae species could not be modeled exactly due to the nature and limitations of the ingredient oils, an average actual removal percentage was calculated based on the formulated BAPE, APE, and BAPE + APE.

Table 3.4. Test fuel formulations.

Formulation	% EPA + DHA Removed	Ingredient Oil Percentage Amount					
		Fish Oil	Soy	Canola	Corn	CE1295	Total
Nanno Oculata Growth	100%	5	25	35	5	30	100
	75%	25	15	20	20	20	100
	50%	45	15	5	25	10	100
	25%	70	10	5	15	0	100
	0%	75	0	25	0	0	100
Nanno Sp	100%	10	10	50	0	30	100
	75%	40	0	45	0	15	100
	50%	60	5	30	0	5	100
	25%	75	0	25	0	0	100
Iso Galbana	100%	35	0	30	0	35	100
	75%	50	15	10	0	25	100
	50%	70	5	5	5	15	100
	25%	80	5	5	0	10	100

A visual comparison of the model methyl ester formulations to the real species based on BAPE, APE, and BAPE + APE can be seen in Figure 3.3, Figure 3.4, and Figure 3.5 for Nannochloropsis Oculata Growth, Nannochloropsis Sp, and Isochrysis Galbana, respectively. The real and formulated EPA and DHA removal comparisons can be easily seen in Figure 3.6, Figure 3.7, and Figure 3.8 for Nannochloropsis Oculata Growth, Nannochloropsis Sp, and Isochrysis Galbana, respectively. These figures show that the fuel formulations accurately describe the algae species complete double bond structure.

Table 3.5. BAPE and APE comparisons with actual removal rates.

	Desired % EPA + DHA Removed	BAPE	APE	BAPE + APE	Average Actual % EPA + DHA Removed	Standard Deviation	Actual % EPA + DHA Formulated
Nanno Oculata Growth – Model Compound Formulation	100%	40.66	121.77	162.43	98.82%	0.40%	1.46%
	75%	64.63	126.78	191.41	77.82%	0.48%	7.31%
	50%	90.13	132.16	222.29	51.97%	0.46%	13.16%
	25%	117.36	138.08	255.44	19.00%	0.16%	20.47%
	0%	117.63	139.36	256.99	15.61%	4.33%	21.93%
Nanno Oculata Growth	100%	38.86	121.58	160.45			
	75%	67.24	127.53	194.77			
	50%	91.61	132.64	224.25			
	25%	112.78	137.07	249.85			
	0%	131.33	140.96	272.29			
Nanno Sp – Model Compound Formulation	100%	40.85	121.91	162.77	104.54%	4.91%	2.92%
	75%	75.18	132.91	208.09	71.01%	4.38%	11.70%
	50%	101.45	138.48	239.93	44.32%	5.94%	17.55%
	25%	117.63	139.36	256.99	28.69%	3.99%	21.93%
Nanno Sp	100%	42.04	124.76	166.80			
	75%	71.64	130.98	202.62			
	50%	96.71	136.25	232.97			
	25%	118.23	140.78	259.01			
Iso Galbana-Model Compound Formulation	100%	62.10	98.95	161.05	99.40%	0.16%	10.24%
	75%	86.05	106.07	192.12	68.11%	2.09%	14.62%
	50%	108.65	112.96	221.61	30.99%	0.45%	20.47%
	25%	120.37	117.06	237.44	8.69%	2.42%	23.39%
Iso Galbana Species	100%	61.73	98.77	160.49			
	75%	84.55	104.37	188.92			
	50%	104.97	109.39	214.36			
	25%	123.36	113.91	237.27			

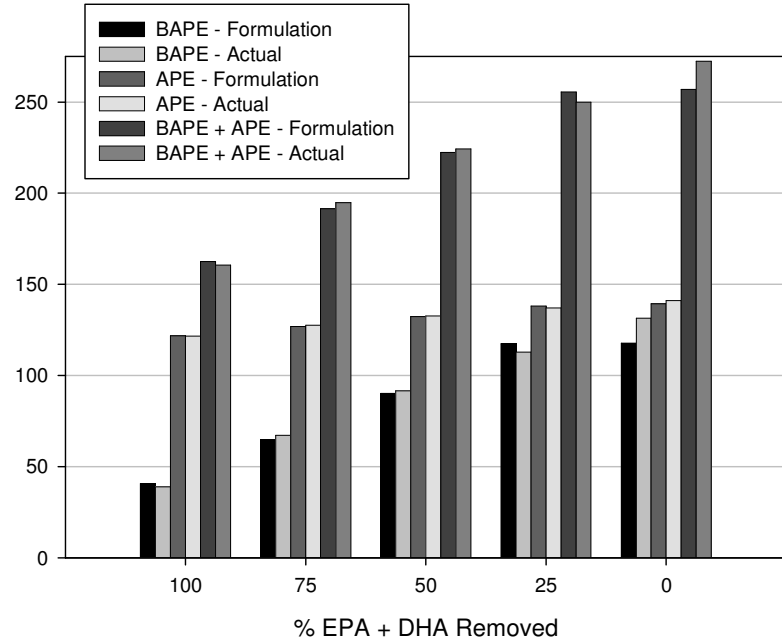


Figure 3.3. *Nannochloropsis Oculata* Growth Formulation BAPE, APE, and BAPE + APE comparison.

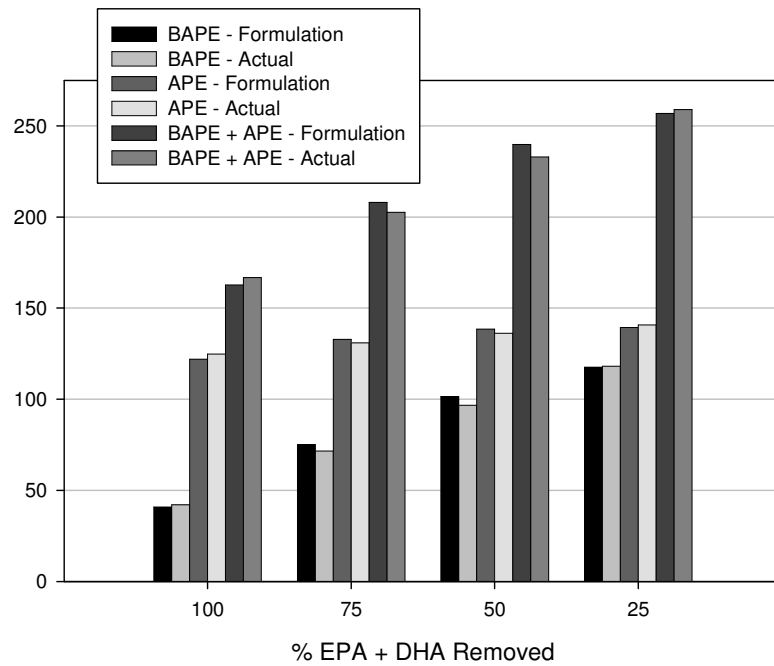


Figure 3.4. *Nannochloropsis Sp* - Formulation BAPE, APE, and BAPE + APE comparison.

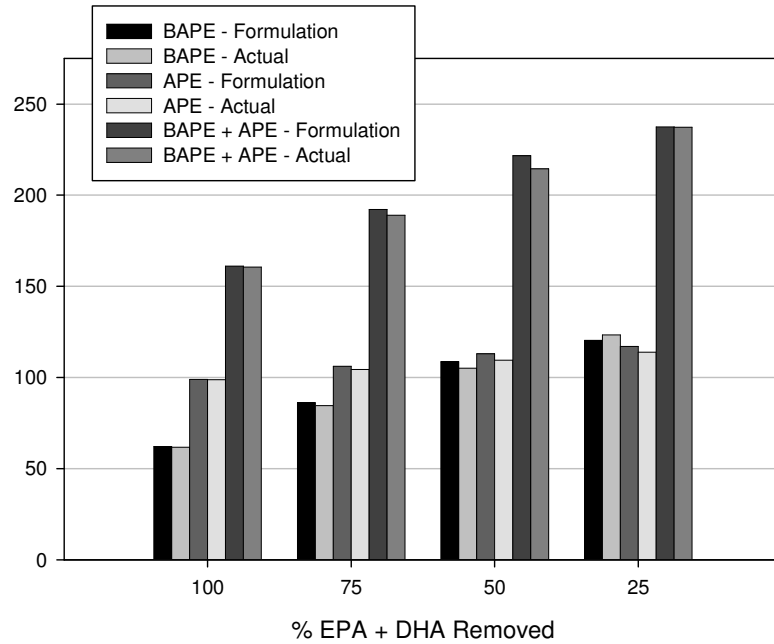


Figure 3.5. Isochrysis Galbana - Formulation BAPE, APE, and BAPE + APE comparison.

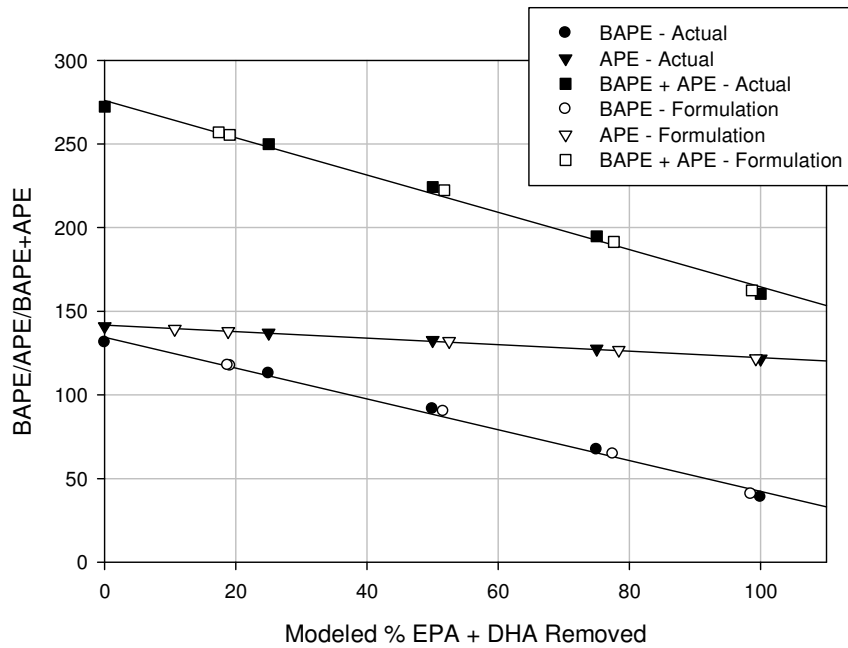


Figure 3.6. Nannochloropsis Oculata - Formulation and actual BAPE, APE, and BAPE + APE comparison.

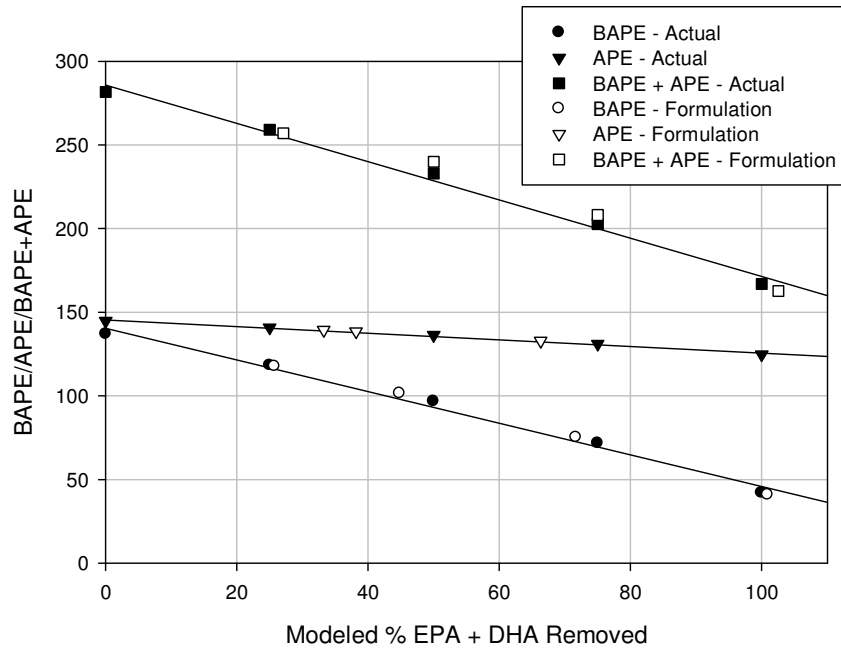


Figure 3.7. Nannochloropsis Sp - Formulation and actual BAPE, APE, and BAPE + APE comparison.

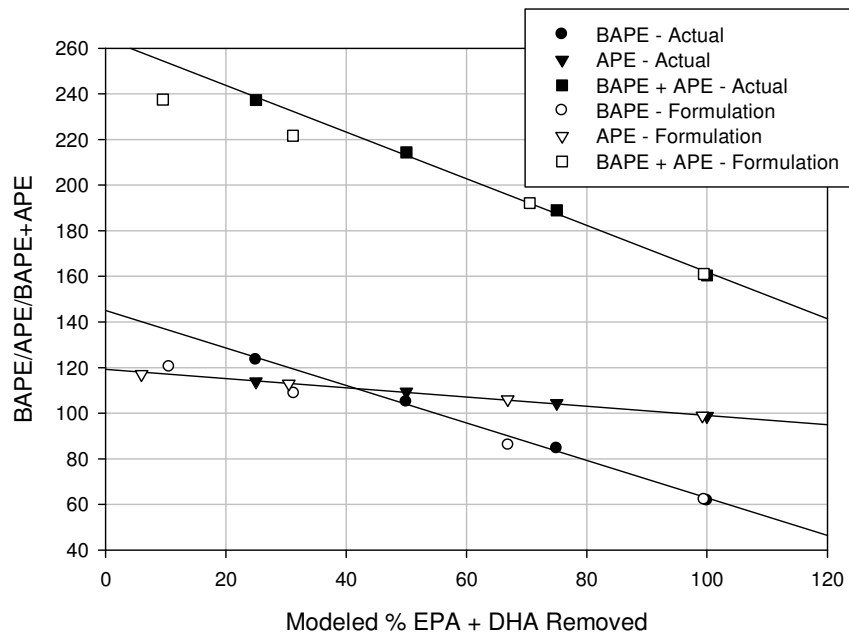


Figure 3.8. Isochrysis Galbana - Formulation and actual BAPE, APE, and BAPE + APE comparison.

4 EXPERIMENTAL PROCEDURE

4.1 Oxidative Stability

For the oxidative stability study, the Metrohm 743 Rancimat was operated following the ASTM D6751 B100 Standard Specification which calls for the EN 14112 test method. The EN 14112 requirements specify a three gram sample heated at 110 degrees Celsius subjected to an air flow rate of ten liters per hour. Each three gram sample was weighed to the nearest hundredth of a gram. The automatic induction period determination was used for all samples and each sample was subjected to two trials. In total, 42 samples were tested. Twenty-six different samples were tested without additives as shown in Table 4.1:

Table 4.1. Oxidative stability test matrix.

Methyl Esters	Algae Formulations	EPA + DHA Removal
Fish	Nanno Oculata	15.61%
Soy		19.00%
Canola		51.97%
Corn		77.82%
Flaxseed with DHA additive		98.82%
Methyl Laurate – Fish Methyl Ester Blends		
0% Fish	Nanno Sp	28.69%
25% Fish		44.32%
50% Fish		71.01%
75% Fish		104.54%
Algae Samples		
Inventure Algal FAME	Iso Galbana	8.69%
Catilin Algal FAME		30.99%
Eldorado Algal Oil		68.11%
Eldorado Algal FAME		99.40%

The methyl laurate – fish methyl ester blends were first tested to validate the BAPE theory of oxidation. Then the algae formulations and ingredient FAMEs were tested followed by the actual algae oil and FAMEs. Lastly, nutraceutical flaxseed oil with a DHA additive was purchased from a local health-foods store, transesterified, and tested to better determine the DHA effects on oxidation.

The Metrohm 743 Rancimat was then operated identically for FAME samples with the Bioproduct additive. The improver was added on a weight basis. Sixteen more samples were tested with four different additives shown in Table 4.2:

Table 4.2. Oxidative stability with additive test matrix.

Algae Formulations	EPA + DHA Removal	Additive Amount Tested			
Nanno Sp	28.69%	0.10%	0.15%	0.20%	0.33%
	44.32%	0.10%	0.15%	0.20%	0.33%
	71.01%	0.10%	0.15%	0.20%	0.33%
	104.54%	0.10%	0.15%	0.20%	0.33%

Each sample was weighed immediately before testing after the 743 Rancimat had stabilized at the testing temperature. Fifty milliliters of distilled water was measured using a graduated cylinder to the nearest one-half milliliter for each conductivity measuring vessel. The sample airflow was started simultaneously via the Metrohm software, and the samples were immediately placed in the heating block. Since the automatic induction period determination was used, several of the longer induction period tests were concluded overnight. After each test, the glassware was cleaned with a 1:1:1 mixture of acetone, toluene, and methanol, rinsed with distilled water, dried, and stored for future use. No glassware was used for more than one test except the glass measuring vessels. The plastic components were cleaned with isopropyl alcohol, rinsed with distilled water, dried, and stored for future use. No plastic components were used for more than one test except the conductometric measuring cell covers.

4.2 Derived Cetane Number

The Derived Cetane Number testing followed ASTM D7170 Standard Test Method for Determination of Derived Cetane Number (DCN) of Diesel Fuel Oils using the FIT. Each sample tested was subjected to two trials. Thirteen model algal methyl ester formulations were tested as shown in Table 4.3:

Table 4.3. Ignition quality test matrix.

Algae Formulations	EPA + DHA Removal
Nanno Oculata	15.61%
	19.00%
	51.97%
	77.82%
	98.82%
Nanno Sp	28.69%
	44.32%
	71.01%
	104.54%
Iso Galbana	8.69%
	30.99%
	68.11%
	99.40%

The El Dorado and Inventure algae FAME were not tested for DCN due to sample volume limitations.

During testing, the FIT and cooling system were operated for a period of at least 12 hours prior to testing to ensure thermal equilibrium. Diesel fuel and n-heptane were first run in a similar fashion to the calibration procedure described in the Waukesha FIT Description to ensure quality control. Both trials for each sample were tested consecutively. For each first sample trial, an initial 100 mL of the sample was poured into the fuel cup and flushed through the system.

Then the cup was refilled before starting the test. For each second trial, the cup was refilled and then the test was started. Each test was controlled and monitored by the FIT computer software. At the end of each testing day, any remaining sample was flushed through the FIT fuel system, the FIT was turned off, the combustion air was turned off, and the cooling system was turned off 30 minutes after the FIT.

4.3 Density, Speed of Sound, and Viscosity

The Anton Paar DSA 5000M was used to complete the density and speed of sound testing while the Anton Paar SVM 3000 – Stabinger Viscometer was used to complete the viscosity testing. Each test was performed at 40 degrees Celsius. Twenty-two samples were each tested for density, speed of sound, and viscosity shown in Table 4.4:

Table 4.4. Density, speed of sound, and viscosity test matrix.

Methyl Esters	Algae Formulations	EPA + DHA Removal
Fish	Nanno Oculata	15.61%
Soy		19.00%
Canola		51.97%
Corn		77.82%
Methyl Laurate		98.82%
Algae Samples	Nanno Sp	28.69%
Inventure Algal FAME		44.32%
Catilin Algal FAME		71.01%
Eldorado Algal Oil		104.54%
Eldorado Algal FAME		
	Iso Galbana	8.69%
		30.99%
		68.11%
		99.40%

To conduct the density and speed of sound measurements, a six milliliter syringe was filled with the sample and approximately three milliliters were injected into the instrument. The

instrument internal camera and display screen were used to ensure that no air bubbles were in the measuring cell. If air bubbles were observed in the measuring cell, then additional sample was injected until the air bubble was removed. The instrument graphical user interface was then used to start each automatic test. For each subsequent test, approximately three milliliters were used to flush out the previous sample before proceeding with the new test. To clean the DSA 5000M kerosene was injected to remove any large deposits and naphtha was injected to remove any residual residue, then the measuring cell was pumped dry with the internal fan.

To conduct the viscosity measurements, a six milliliter syringe was filled with the sample and approximately two milliliters were injected to prime the measuring cell. The remaining four milliliters were added in two separate injections during the automatic run cycle of the instrument. For each subsequent test, approximately two milliliters were first added to displace the previous sample. To clean the SVM 3000 – Stabinger Viscometer kerosene was injected to remove any large deposits and naphtha was injected to remove any residual residue, then the measuring cell was pumped dry with the internal fan.

5 RESULTS AND DISCUSSION

5.1 Oxidative Stability

The induction period test results provided great insight into to the role that double bonds and unsaturation plays with the oxidative stability of FAME. The methyl laurate/fish oil methyl ester blends confirmed that the BAPE index is an effective means of predicting oxidative stability and confirmed that the test approach employed herein was an effective means of elucidating the role of LC-PUFA on oxidative stability of algal methyl esters. Specifically, as the percentage of fish methyl ester increased in the mixture, the induction period decreased due to the addition of LC-PUFA. The results of the methyl laurate/fish oil methyl ester blends oxidative stability testing can be seen in Table 5.1. These results show that only the addition of 25 percent fish methyl ester to the pure saturated methyl laurate (C12:0) greatly decreases the induction period. The induction period decreases near linearly with the additions of 25, 50, and 75 percent fish methyl ester, but the pure methyl laurate induction period dramatically increased from the other mixtures. The 100 percent methyl laurate induction period was actually never determined as the experiment was terminated after 26 hours. Using the Rancimat software, the methyl laurate induction curve showed no signs of a rapid rise in measured conductivity measured. Since there was no visible oxidation, the methyl laurate data was plotted with an induction period of 26 hours for the corresponding results and graphs. Other studies have also found an induction period greater than 24 hours when testing synthesized esters with no double bonds in the alkyl chain (Sarin, et al. 2009).

Table 5.1. Methyl laurate - fish methyl ester oxidatve stability results.

Sample	Test	Induction Period (hr)	Average (hr)	Standard Deviation	BAPE	APE	BAPE+APE
100 % CE1295	1	> 26	> 26	0.00	0.00	0.00	0.00
	2	> 26					
75% CE1295 + 25% Fish ME	1	3.05	3.07	0.02	35.94	31.04	66.98
	2	3.08					
50% CE 1295 + 50% Fish ME	1	1.59	1.59	0.01	71.87	62.07	133.94
	2	1.58					
25% CE1295 + 75% Fish ME	1	1.23	1.22	0.01	107.81	93.11	200.92
	2	1.21					
Fish Oil Methyl Ester	1	1.22	1.16	0.09	143.74	124.14	267.88
	2	1.09					

The plot of induction period as a function of BAPE for the methyl laurate/ fish oil methyl ester blends (Figure 5.1) clearly shows a strong logarithmic correlation as does induction period as a function of BAPE + APE (Figure 5.2). A correlation of APE and induction period was not considered because the APE does not provide insightful information to the complete double bond structure of the methyl ester.

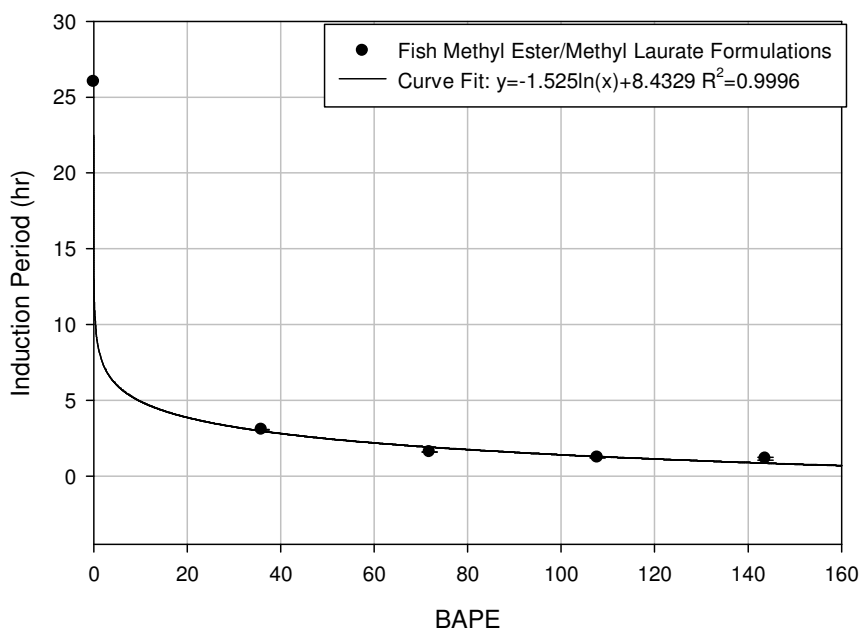


Figure 5.1. Induction period as a function of BAPE for the methyl laurate-fish methyl ester blends.

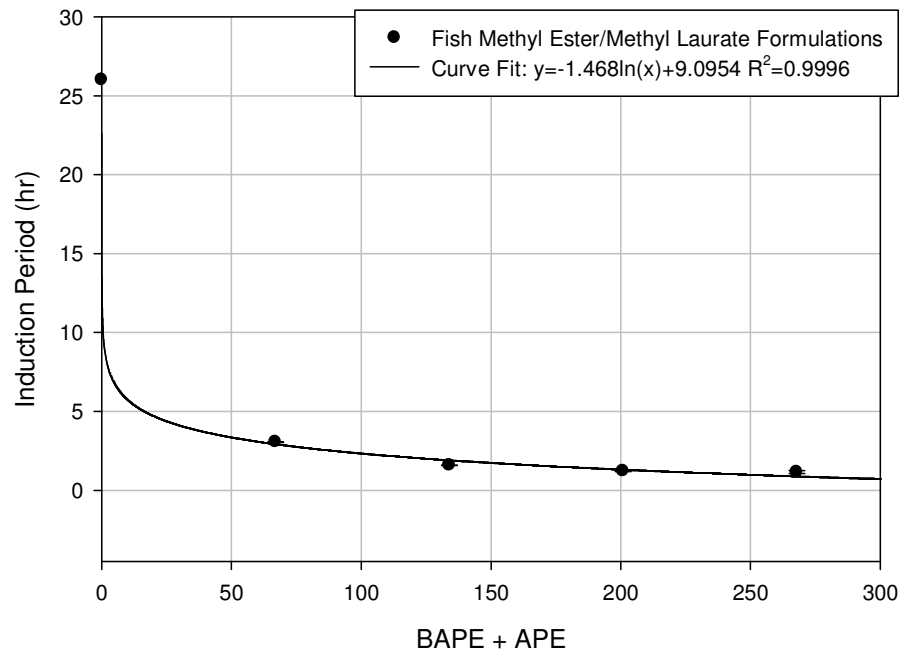


Figure 5.2. Induction period as a function of BAPE + APE for the methyl laurate-fish methyl ester blends.

The correlation of induction period to BAPE + APE for the methyl laurate/fish oil methyl esters was unsuspected since previous studies (Sanford, et al. 2009) showed no such correlation. However, the results of all the oxidative stability samples plotted on one graph confirmed that the BAPE correlation holds true, but not the BAPE + APE correlation. Figure 5.3 clearly shows that there is BAPE correlation with respect to oxidative stability, but Figure 5.4 shows that there is no BAPE + APE correlation when a wide range of data is considered. The induction period as a function of BAPE had an exponential curve fit with an R-squared value of 0.86. No curve was fitted to the induction period as a function of BAPE + APE plot because the plotted data clearly showed no correlation. The Catilin algal FAME was not included in these plots or correlations because tests showed that this was not a high quality FAME. The Eldorado algal oil was not

included because it is not a FAME. According to the curve fit a BAPE of 80.5 and a BAPE of 50.4 would be sufficient to pass the ASTM and EN oxidative stability specifications, respectively.

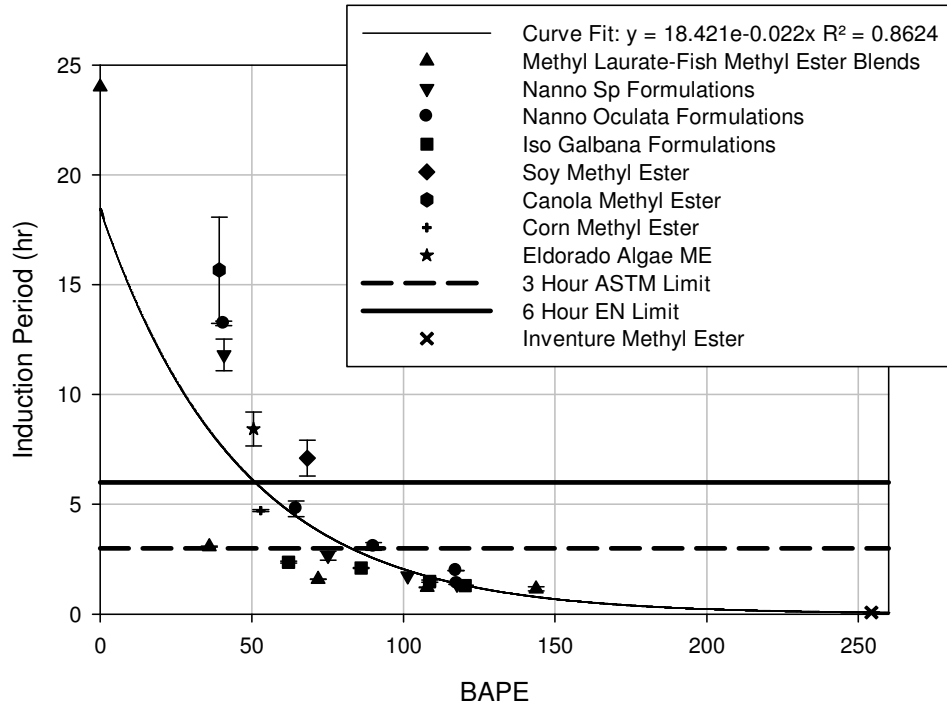


Figure 5.3. Induction period as a function of BAPE for all tested methyl esters.

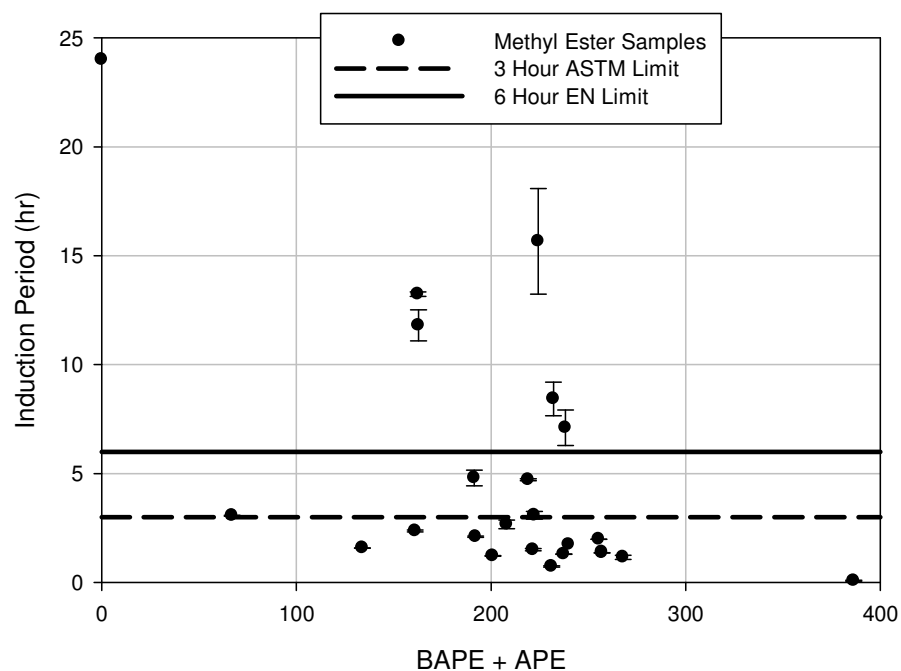


Figure 5.4. Induction period as a function of BAPE + APE for all tested methyl esters.

The individual results for each algae formulation also showed an exponential correlation of induction period as a function of BAPE. The correlation between induction period and BAPE + APE was not determined since this correlation was shown to be not valid.

The *Nannochloropsis Oculata* Growth formulation oxidative stability results are shown in Table 5.2. The highest simulated LC-PUFA removal rates of 98.82 and 77.82 percent EPA and DHA removal passed the ASTM three hour induction period limit. Only when 98.82 percent of the EPA and DHA were removed from the *Nannochloropsis Oculata* Growth formulation did the EN six hour induction period limit passed. The induction period as a function of BAPE for the *Nannochloropsis Oculata* Growth formulations is plotted in Figure 5.5 and has an exponential correlation with an R-squared value of 0.95. From the plot, a BAPE of approximately 95 and 65 would be sufficient to pass the ASTM and EN oxidative stability specifications, respectively.

Table 5.2. Nanno Oculata Growth formulation oxidative stability results.

Nanno Oculata Growth Formulations							
Modeled % EPA + DHA Removed	Standard Deviation	Actual % EPA + DHA Formulated	Test	Induction Period (hr)	Average (hr)	Standard Deviation	BAPE
98.82%	0.40%	1.46%	1	13.16	13.24	0.11	40.66
			2	13.31			
77.82%	0.48%	7.31%	1	4.54	4.80	0.36	64.63
			2	5.05			
51.97%	0.46%	13.16%	1	3.21	3.09	0.18	90.13
			2	2.96			
19.00%	0.16%	20.47%	1	1.98	1.99	0.01	117.36
			2	1.99			
15.61%	4.33%	21.93%	1	1.40	1.40	0.00	117.63
			2	1.40			

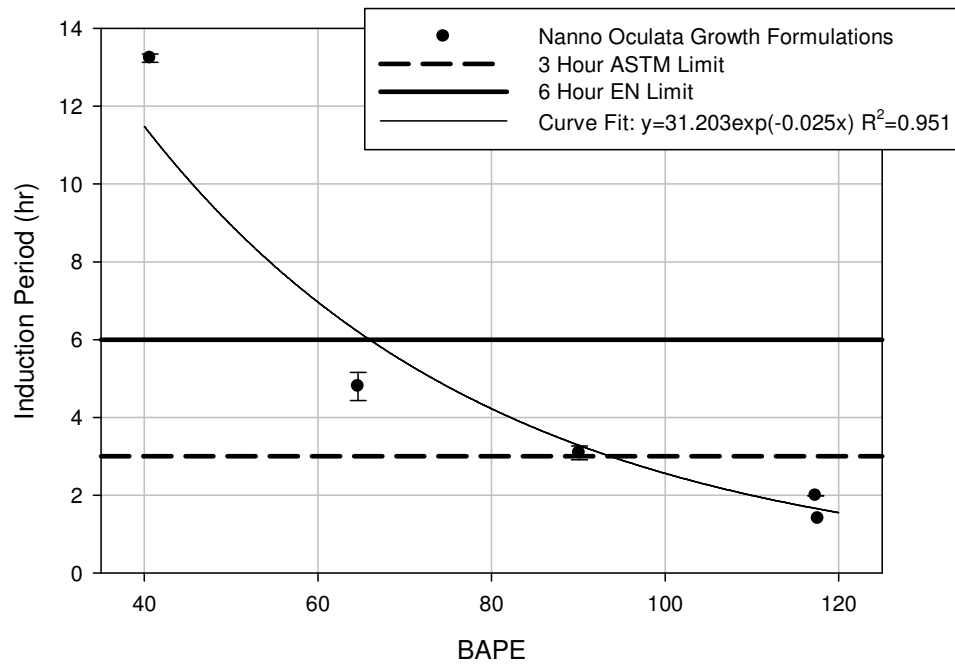


Figure 5.5. Induction period as a function of BAPE for the Nanno Oculata Growth formulations.

As shown in Figure 5.6, when the induction period is plotted as a function of the percentage of EPA and DHA removed for the Nannochloropsis Oculata Growth formulations, an

exponential correlation with an R-squared value of 0.93 is observed. Based on the experimental results and the associated curve fit, removal of approximately 45 percent of the EPA and DHA from Nannochloropsis Oculata Growth FAME would be required to pass the three hour ASTM oxidative stability limit, To pass the six hour EN oxidative stability limit, removal of approximately 75 percent of the EPA and DHA from Nannochloropsis Oculata Growth FAME would be required.

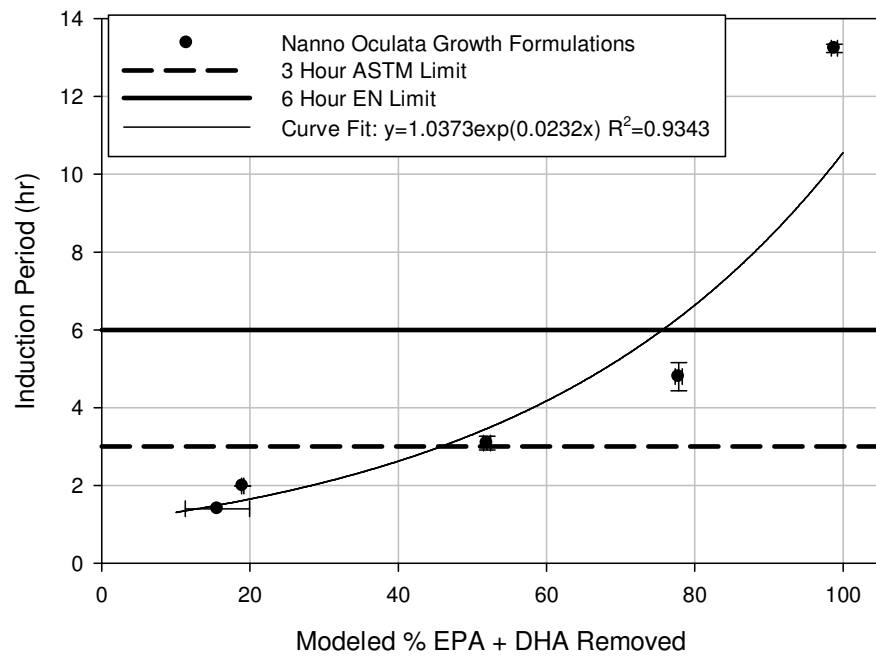


Figure 5.6. Induction period as a function of modeled percent EPA and DHA removed for the Nanno Oculata Growth formulations.

The induction period as a function of percent EPA and DHA formulated is plotted (Figure 5.7) for the Nannochloropsis Oculata Growth formulations and it has an exponential correlation with an R-squared value of 0.95. According to the data and curve fit, a Nannochloropsis Oculata Growth formulation with a total of greater than 14 percent of EPA and DHA would fail the three hour ASTM oxidative stability limit. A Nannochloropsis Growth

formulation with greater than seven percent of EPA and DHA would fail the six hour EN oxidative stability limit.

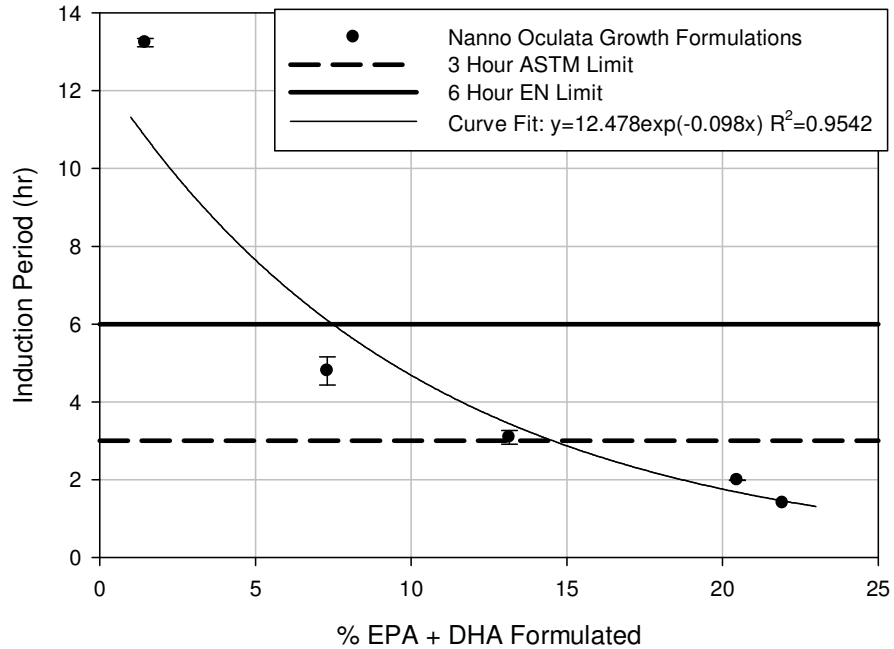


Figure 5.7. Induction period as a function of percent EPA and DHA formulated for the Nanno Oculata Growth formulations.

The Nannochloropsis Sp formulation oxidative stability results are shown in Table 5.3. Only the maximum removal rate of 100 percent EPA and DHA passed the ASTM three hour induction period limit and it was the only Nannochloropsis Sp formulation to pass the EN six hour induction period limit. The induction period as a function of BAPE for the Nannochloropsis Sp formulations is plotted in Figure 5.8. Figure 5.8 and has an exponential correlation with an R-squared value of 0.94. From the plot, a BAPE of approximately 85 and 6 would be sufficient to pass the ASTM and EN oxidative stability specifications, respectively.

Table 5.3. Nanno Sp formulation oxidative stability results.

Nanno Sp Formulations							
Modeled % EPA + DHA Removed	Standard Deviation	Actual % EPA + DHA Formulated	Test	Induction Period (hr)	Average (hr)	Standard Deviation	BAPE
104.54%	4.91%	2.92%	1	11.29	11.80	0.72	40.85
			2	12.31			
71.01%	4.38%	11.70%	1	2.52	2.66	0.20	75.18
			2	2.80			
44.32%	5.94%	17.55%	1	1.74	1.74	0.00	101.45
			2	1.74			
28.69%	3.99%	21.93%	1	1.36	1.36	0.01	117.63
			2	1.35			

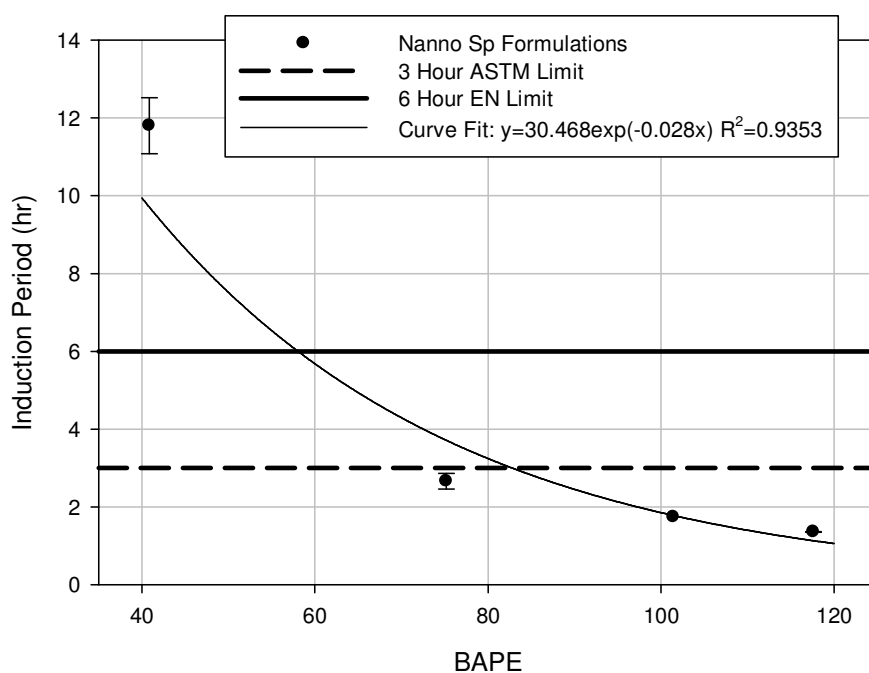


Figure 5.8. Induction period as a function of BAPE for Nanno Sp formulations.

When the induction period is plotted as a function of percent EPA and DHA removal (Figure 5.9) for the Nannochloropsis Sp formulations, an exponential correlation with an R-squared value of 0.93 is observed. According to the data and associated curve fit, removal of

approximately 65 percent of EPA and DHA from Nannochloropsis Sp FAME would be required to pass the three hour ASTM oxidative stability limit. To pass the six hour EN oxidative stability limit, removal of approximately 85 percent of the EPA and DHA from Nannochloropsis Sp FAME would be required.

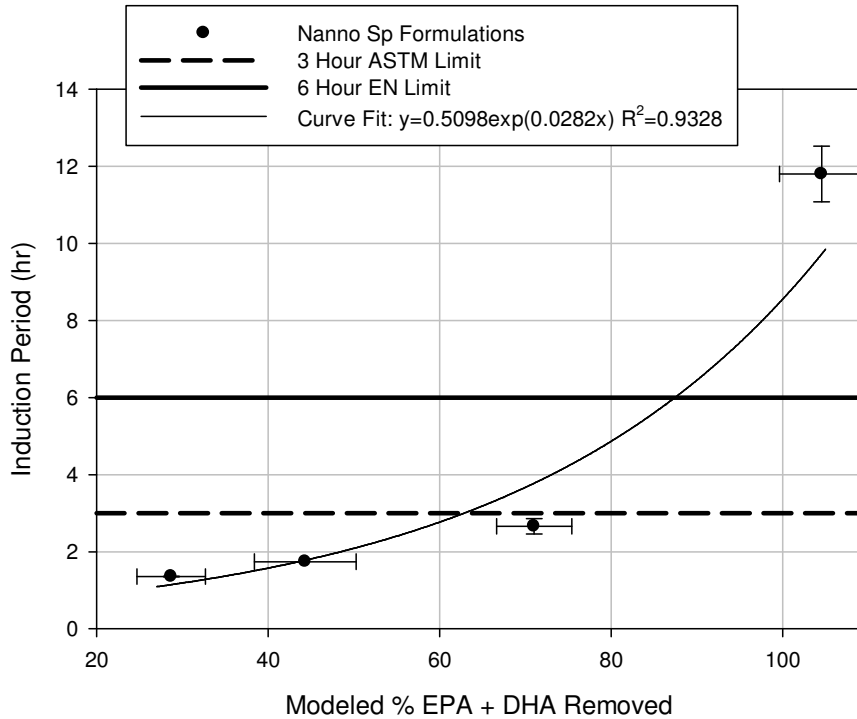


Figure 5.9. Induction period as a function of modeled percent EPA and DHA removed for Nanno Sp formulations.

The induction period as a function of percent EPA and DHA formulated is plotted (Figure 5.10) for the Nannochloropsis Sp formulations and an exponential correlation with an R-squared value of 0.94. According to the curve 13 percent of EPA and DHA formulated in Nannochloropsis Sp will result in failing the three hour ASTM oxidative stability limit. According to the plot, formulation of only seven percent of the EPA and DHA from Nannochloropsis Sp will result in failing the six hour EN oxidative stability limit. The only

sample to pass both limits was the 2.92 percent EPA and DHA formulation with an induction period of 11.80+/-0.72 hours.

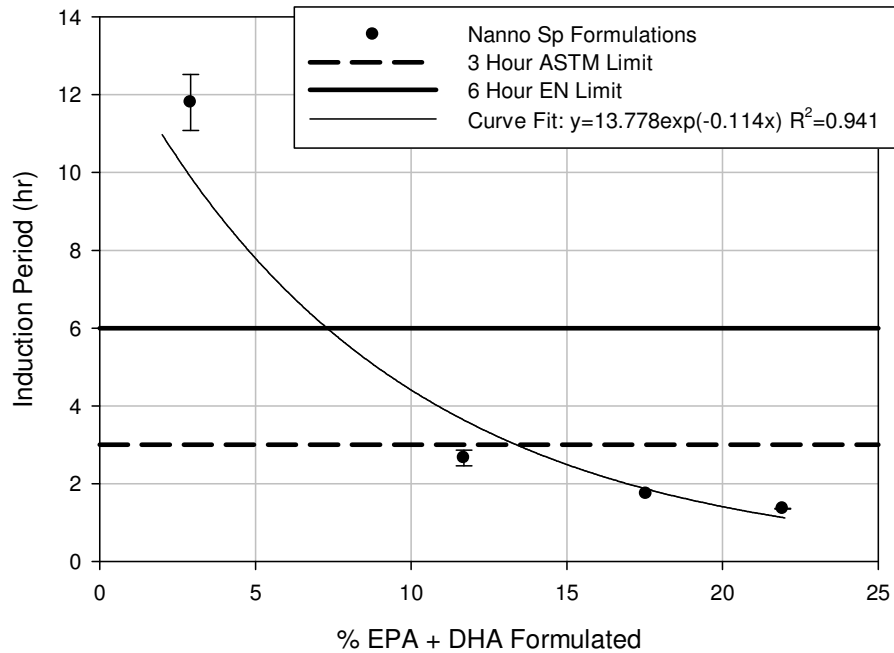


Figure 5.10. Induction period as a function of percent EPA and DHA formulated for Nanno Sp formulations.

The oxidative stability results for the Isochrysis Galbana formulations are shown in Table 5.4. For these formulations, none of the simulated EPA and DHA removal rates passed either the ASTM or EN specification. The induction period as a function of BAPE for the Isochrysis Galbana formulations is plotted in Figure 5.11 and has an exponential correlation with an R-squared value of 0.95. According to the curve fit, a BAPE of approximately 42 would be sufficient to pass the ASTM oxidative stability specifications, but no BAPE would ever correlate to a six hour EN oxidative stability specification for Isochrysis Galbana.

Table 5.4. Iso Galbana formulaton oxidative stability results.

Iso Galbana Formulations							
Modeled % EPA + DHA Removed	Standard Deviation	Actual % EPA + DHA Formulated	Test	Induction Period (hr)	Average (hr)	Standard Deviation	BAPE
99.40%	0.16%	10.24%	1	2.39	2.36	0.04	62.10
			2	2.33			
68.11%	2.09%	14.62%	1	2.12	2.10	0.03	86.05
			2	2.08			
30.99%	0.45%	20.47%	1	1.46	1.50	0.06	108.65
			2	1.54			
8.69%	2.42%	23.39%	1	1.29	1.30	0.01	120.37
			2	1.31			

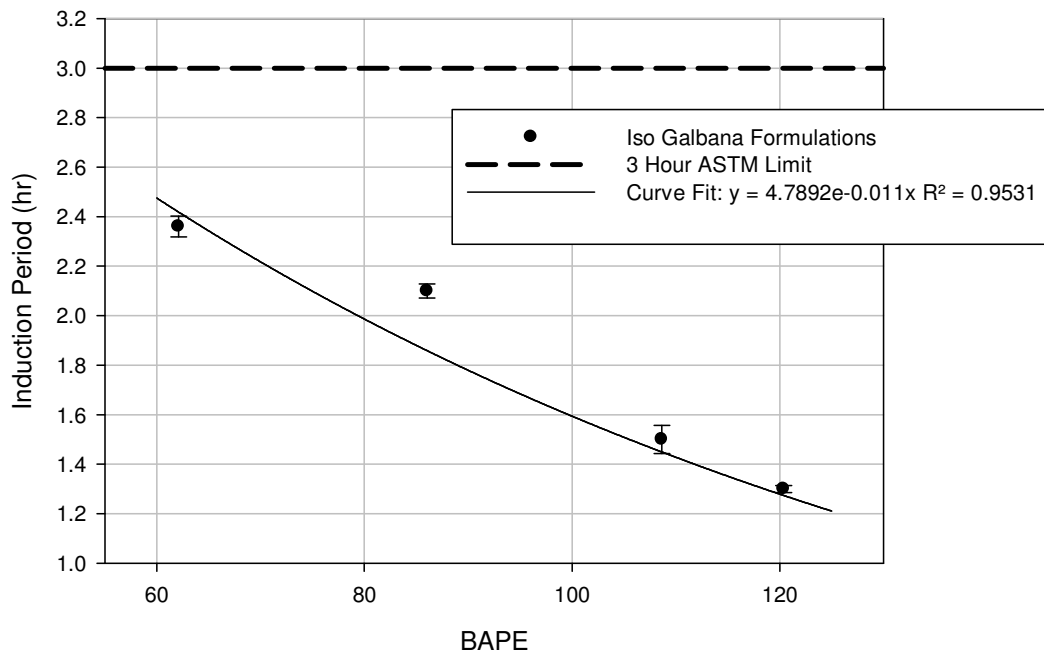


Figure 5.11. Induction period as a function of BAPE for Iso Galbana formulations.

When the induction period as a function of modeled percent EPA and DHA removed is plotted (Figure 5.12) for the Isochrysis Galbana formulations, an exponential correlation with an R-squared value of 0.98 is observed. According to the curve no realistic removal of EPA and

DHA would result in a passing induction period for oxidative stability for either ASTM or EN Standard. If all of the EPA and DHA were removed, an induction period of 2.46 hours would be reached according to the curve fit. The best observed induction period was 2.36+/-0.04 hours for 99.40 percent removal of EPA and DHA.

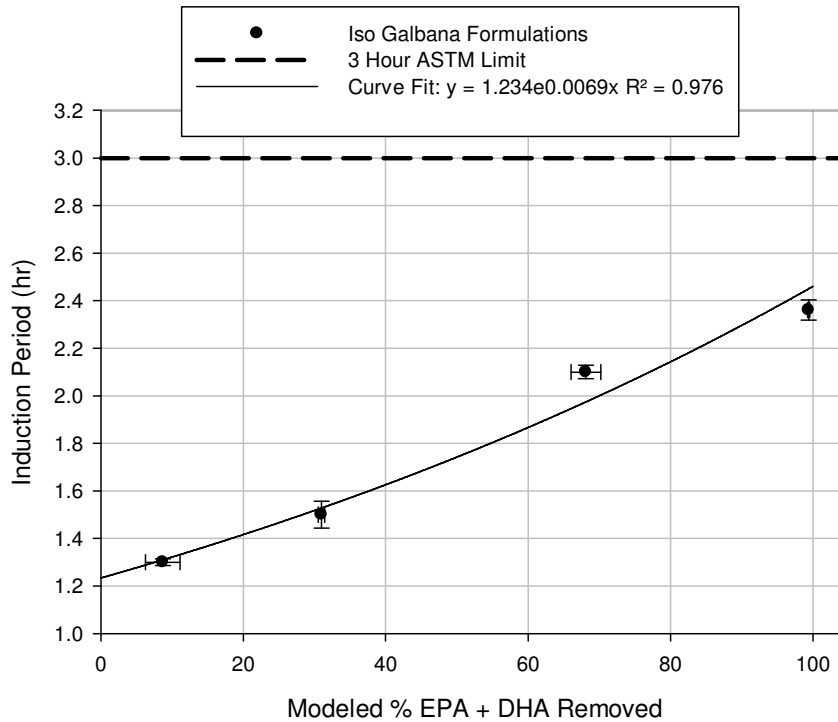


Figure 5.12. Induction period as a function of modeled percent EPA and DHA removed for Iso Galbana formulations.

The induction period as a function of percent EPA and DHA formulated is plotted (Figure 5.13) for the Isochrysis Galbana formulations and an exponential correlation with an R-squared value of 0.98. According to the curve fit six percent of EPA and DHA formulated in Isochrysis Galbana will result in failing the three hour ASTM oxidative stability limit. The formulation with 10.24 percent EPA and DHA was closest to passing the ASTM Standard with and induction period of 2.36+/-0.04 hours. The EN Standard will never be reached formulating Isochrysis Galbana, according to the curve fit.

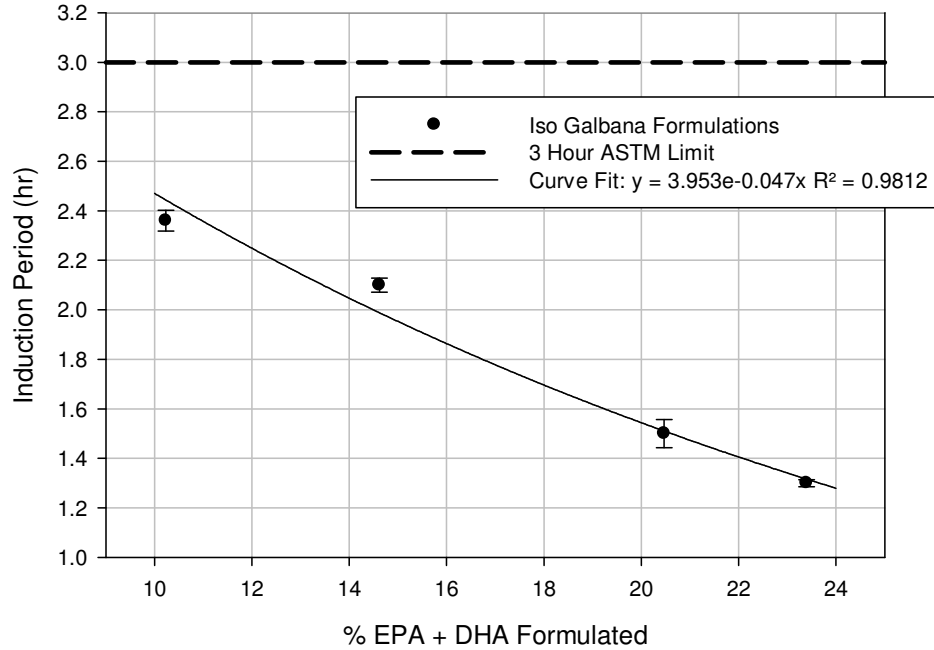


Figure 5.13. Induction period as a function of percent EPA and DHA formulated for Iso Galbana formulations.

The oxidative stability results for the real algal lipids and methyl esters are shown in Table 5.5. The clear distilled Catilin sample had a poor induction period, about 45 minutes. This could be caused by the distilling process. To bring the methyl ester to a clear liquid natural antioxidants could have been removed (as discussed previously in Chapter 1.5.1 Oxidative Stability) or it could be possible that the distillation process itself caused oxidation. The exact reason for this result is beyond this scope of work. Similar oxidative stability results would have been expected for the Catilin and Eldorado methyl esters since they were produced from the same lipid feedstock. The Eldorado algal methyl ester passed both the ASTM and EN oxidative stability standards with an induction period of 8.43 \pm 0.77 hours. The Eldorado algal oil had a lower induction period than its counterpart at 3.76 \pm 0.03 hours, which passes only the methyl ester ASTM limit. The Inventure algal FAME was extremely poor in regards to oxidative

stability with an induction period of less than five minutes. This was expected due to the fact that it is 50 percent DHA leading to the highest BAPE of all samples tested at 254.

Table 5.5. Algae oxidative stability results.

Sample	Test	Induction Period (hr)	Average (hr)	Standard Deviation	BAPE
Catilin Distilled Algae ME	1	0.71	0.73	0.03	57.08
	2	0.75			
Eldorado Algal Oil	1	3.78	3.76	0.03	50.58
	2	3.74			
Eldorado Algal ME	1	8.97	8.43	0.77	50.58
	2	7.88			
Invnture Algal ME	1	0.06	0.08	0.02	254.33
	2	0.09			

When all the algal methyl esters are included in the plot of induction period as a function of BAPE (Figure 5.14), it is clear that all of the algal methyl esters did not behave similarly. The Eldorado and Catilin algae methyl esters are of the same feedstock and have extremely similar fatty acid profiles, as previously mentioned. Since the BAPE are equivalent, but the induction periods are quite different, something other than the algae's fatty acid composition must be affecting the oxidative stability. The Eldorado methyl ester, which was transesterified at the EECL, and the Invnture methyl ester do fit on the BAPE curve, though.

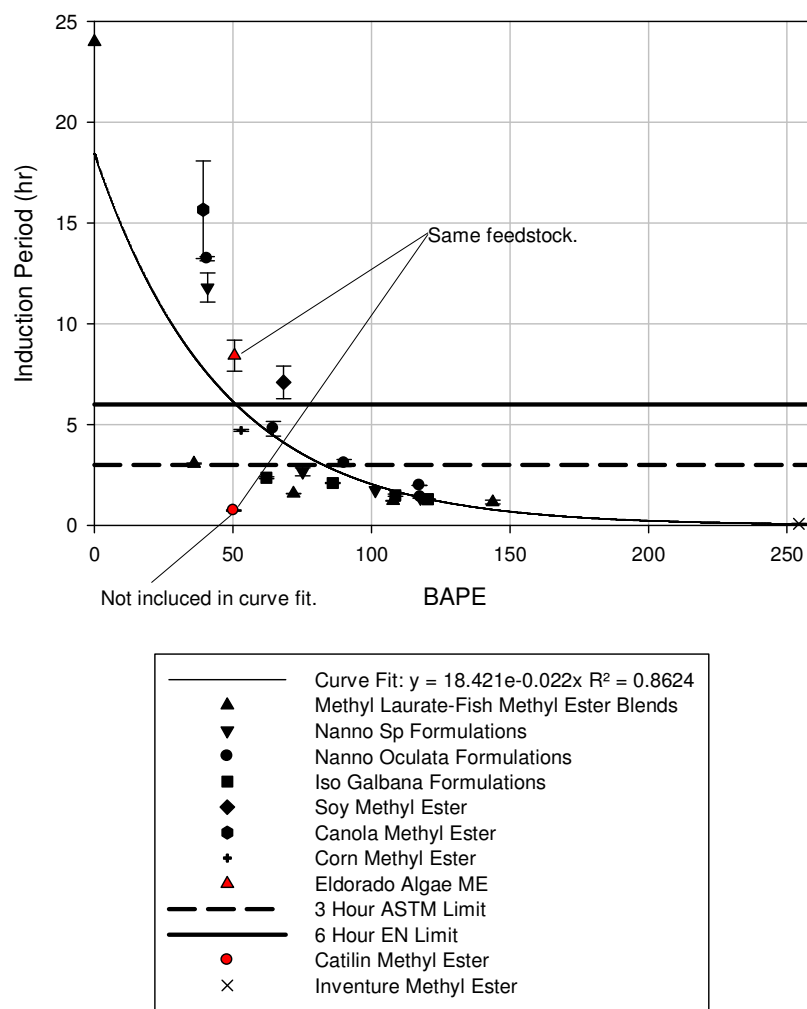


Figure 5.14. Induction period as a function of BAPE including algae methyl esters.

Table 5.6. Additional oxidative stability results.

Sample	Test	Induction Period (hr)	Average (hr)	Standard Deviation	BAPE
Soy Methyl Ester	1	7.67	7.10	0.81	68.30
	2	6.52			
Canola Methyl Ester	1	17.37	15.66	2.42	39.30
	2	13.95			
Corn Methyl Ester	1	4.68	4.71	0.04	52.95
	2	4.74			

The flaxseed oil with DHA additive, purchased from a local health-foods store, oxidative stability results were not comparable to the flaxseed methyl ester oxidative stability results found in literature. These results were from the same study (Sanford, et al. 2009) as discussed previously in Chapter 1.5.1 Oxidative Stability. According to the label 0.93 percent DHA was added and 0.03 percent EPA. These LC-PUFA additive percentages are comparable to the oxidative stability additive percentages discussed in the next section, 5.1.1 Additive Effects, but the flaxseed methyl ester induction period appears to be unaltered by the DHA and EPA. In fact the DHA additive sample performed better than the reported sample (Table 5.7). This could be due to the fact that the flaxseed oil with DHA was processed for human consumption or unreported antioxidants could have been added.

Table 5.7. Flaxseed methyl ester comparison with DHA additive. * Data from (Sanford, et al. 2009).

Sample	Test	Induction Time (hr)	Average (hr)	Standard Deviation	BAPE
Flaxseed Methyl Ester with DHA additive	1	4.08	4.85	1.09	126.97
	2	5.62			
Flaxseed Methyl Ester*	-	0.20	0.20	-	125.10

5.1.1 Effect of Oxidative Stability Additives

To determine the effectiveness of oxidative stability additives on the oxidative stability of algal methyl esters, the *Nannochloropsis Sp* formulations were retested for oxidative stability with the addition of Vitablend Bioproduct 350, which contains 30 percent of the active ingredient TBHQ. The *Nannochloropsis Sp* formulations were chosen for testing the additive effects because it yielded both passing and failing oxidative stability results, and it contained only four formulations allowing for simpler and faster Rancimat tests. The first additive amount tested, 0.1 percent or 0.03 percent TBHQ, yielded promising results. Next 0.33 percent additive or 0.1

percent TBHQ was tested and all formulations passed both the ASTM and EN Standards. To have a more complete understanding of how much additive is needed to increase induction period, two other additive amounts were tested at 0.15 and 0.20 percent additive or 0.0045 and 0.06 percent TBHQ, respectively. The no-additive oxidative stability results are repeated again in Table 5.8 and the additive results are shown in Table 5.9, Table 5.10, Table 5.11, and Table 5.12 for 0.1, 0.15, 0.20, and 0.33 percent additive, respectively. Each table also shows the percent increase in induction period the additive has with respect to the no-additive formulation and the percent increase needed to attain the ASTM and EN specifications.

Table 5.8. Nanno Sp formulations oxidative stability results with no additive.

Nanno Sp Formulations								
Modeled % EPA + DHA Removed	BAPE	Test	Induction Period (hr)	Average (hr)	Standard Deviation	Percent Increase	Percent Increase Needed	
							ASTM	EN
No Additive								
104.54%	40.8542	1	11.29	11.80	0.7212	-	None	None
		2	12.31					
71.01%	75.1818	1	2.52	2.66	0.1980	-	12.78%	125.56%
		2	2.80					
44.32%	101.4502	1	1.74	1.74	0.0000	-	72.41%	244.83%
		2	1.74					
28.69%	117.6314	1	1.36	1.36	0.0071	-	121.40%	342.80%
		2	1.35					

The Nannohloropsis Sp formulation without any additive passed the ASTM and EN oxidative stability standards when all of the EPA and DHA were removed with an induction period of 13.52+/-0.20 hours, but no other formulations pass either standard. The greatest increase needed is a 342.80 percent induction period increase for the Nannohloropsis Sp formulation with only 28.69 percent EPA and DHA removed to meet the EN six hour specification. The Nannohloropsis Sp formulation with 71.01 percent EPA and DHA removed needs only a 12.78 percent induction period increase to pass the ASTM three hour specification.

When only 0.1 percent of the Bioproduct 350 (0.03 percent TBHQ) is added to the Nannohloropsis Sp formulations all of the blends meet the ASTM Standard. A 14.50 percent increase in induction period is still needed for the 71.01 percent EPA and DHA removal formulation to reach the EN Standard, and an 87.79 percent increase in induction period is needed to attain the EN Standard for the 28.69 percent EPA and DHA removal formulation.

Table 5.9. Nanno Sp formulations oxidative stability results with 0.1 percent additive.

Nanno Sp Formulations								
Modeled % EPA + DHA Removed	BAPE	Test	Induction Period (hr)	Average (hr)	Standard Deviation	Percent Increase	Percent Increase Needed	
							ASTM	EN
0.1 % Additive = 0.03% TBHQ								
104.54%	40.8542	1	13.38	13.52	0.20	14.58%	None	None
		2	13.66					
71.01%	75.1818	1	5.20	5.24	0.06	96.99%	None	14.50%
		2	5.28					
44.32%	101.4502	1	3.29	3.30	0.01	89.37%	None	82.09%
		2	3.30					
28.69%	117.6314	1	3.17	3.20	0.04	135.79%	None	87.79%
		2	3.22					

When 0.15 percent of the Bioproduct 350 (0.045 percent TBHQ) is added to the Nannohloropsis Sp formulations all of the blends except the 28.69 percent EPA and DHA removal now meet the EN Standard. A 23.33 percent increase in induction period is still needed for the 28.69 percent EPA and DHA removal formulation to reach the EN Standard.

Table 5.10. Nanno Sp formulations oxidative stability results with 0.15 percent additive.

Nanno Sp Formulations								
Modeled % EPA + DHA Removed	BAPE	Test	Induction Period (hr)	Average (hr)	Standard Deviation	Percent Increase	Percent Increase Needed	
							ASTM	EN
0.15% Additive = 0.045% TBHQ								
104.54%	40.8542	1	16.28	17.07	1.11	44.62%	None	None
		2	17.85					
71.01%	75.1818	1	8.44	8.40	0.06	215.60%	None	None
		2	8.35					
44.32%	101.4502	1	6.59	6.57	0.03	277.59%	None	None
		2	6.55					
28.69%	117.6314	1	4.87	4.87	0.01	259.04%	None	23.33%
		2	4.86					

When 0.2 percent of the Bioproduct 350 (0.06 percent TBHQ) is added to the Nannohloropsis Sp formulations all of the blends meet both standards. All of the mixtures also meet the specifications when 0.33 percent, or 0.1 percent TBHQ, additive is added to the Nannohloropsis Sp formulations. By comparing all of the results, the additive appears most affective on the Nannohloropsis Sp oxidative stability when more of the EPA and DHA are left in the compounds.

Table 5.11. Nanno Sp formulations oxidative stability results with 0.2 percent additive.

Nanno Sp Formulations								
Modeled % EPA + DHA Removed	BAPE	Test	Induction Period (hr)	Average (hr)	Standard Deviation	Percent Increase	Percent Increase Needed	
							ASTM	EN
0.2% Additive = 0.06% TBHQ								
104.54%	40.8542	1	20.26	21.47	1.71	81.95%	None	None
		2	22.68					
71.01%	75.1818	1	8.95	8.99	0.06	237.97%	None	None
		2	9.03					
44.32%	101.4502	1	8.48	8.59	0.16	393.68%	None	None
		2	8.70					
28.69%	117.6314	1	6.39	6.26	0.19	361.62%	None	None
		2	6.12					

Table 5.12. Nanno Sp formulations oxidative stability results with 0.33 percent additive.

Nanno Sp Formulations								
Modeled % EPA + DHA Removed	BAPE	Test	Induction Period (hr)	Average (hr)	Standard Deviation	Percent Increase	Percent Increase Needed	
							ASTM	EN
0.33% Additive = 0.1% TBHQ								
104.54%	40.8542	1	20.82	22.63	2.56	91.78%	None	None
		2	24.44					
71.01%	75.1818	1	13.58	13.35	0.33	401.88%	None	None
		2	13.12					
44.32%	101.4502	1	8.93	8.92	0.01	412.64%	None	None
		2	8.91					
28.69%	117.6314	1	7.58	7.63	0.070	463.10%	None	None
		2	7.68					

Figure 5.15 and Figure 5.16 continue to show that there is an exponential correlation between induction period and BAPE or removal of EPA and DHA. Figure 5.16 clearly shows that for Nannohloropsis Sp any negative effect of EPA and DHA can be offset with fuel additives, specifically TBHQ.

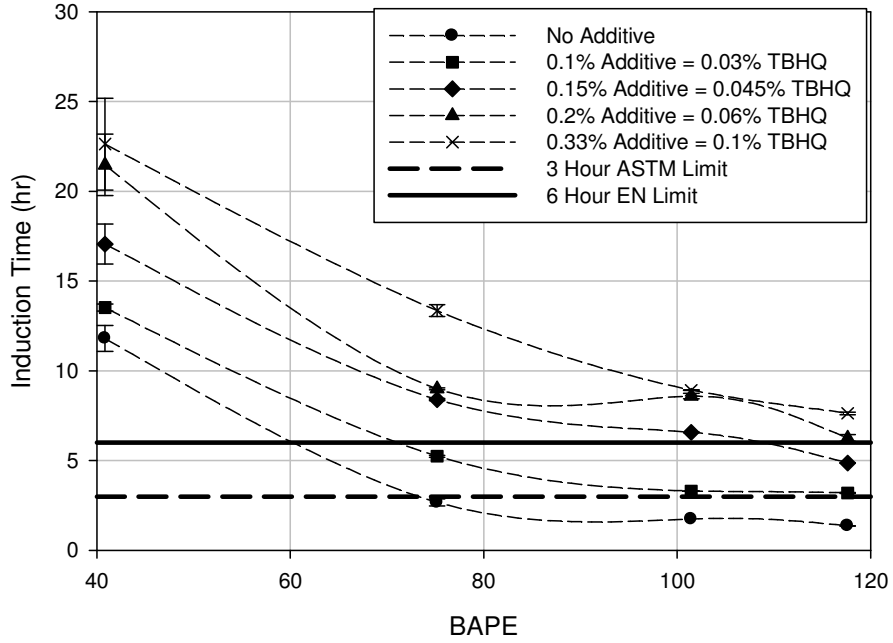


Figure 5.15. Induction period as a function of BAPE for Nanno Sp formulations with additive.

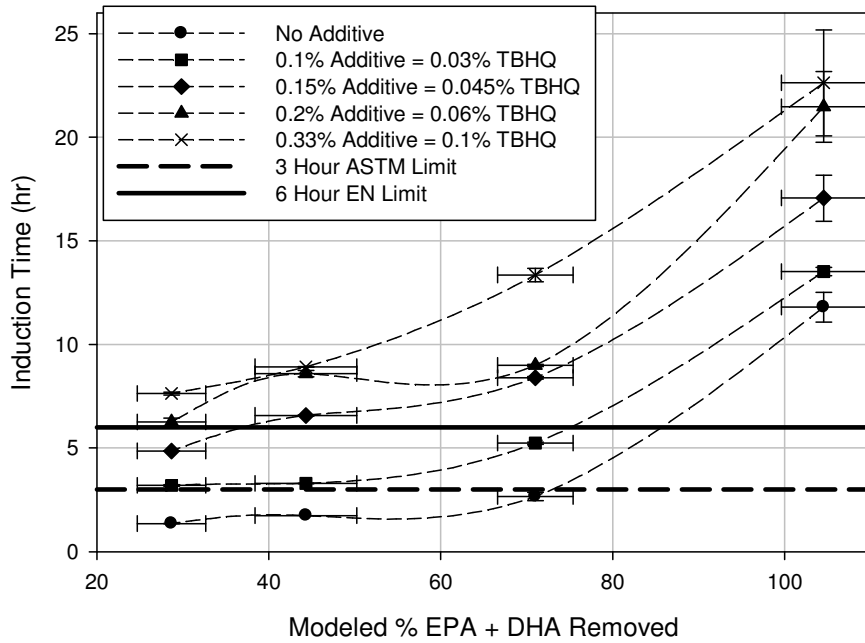


Figure 5.16. Induction Period as a function of modeled percent EPA and DHA removed for Nanno Sp formulations with additive.

Figure 5.15 through Figure 5.20 indicate that there is a linear increase in induction period with respect to additive increase over a constant formulation. These figures also clearly show that the TBHQ is most affective when the LC-PUFAs, EPA and DHA, remain in the Nannohloropsis Sp by comparing the slope of the linear correlations.

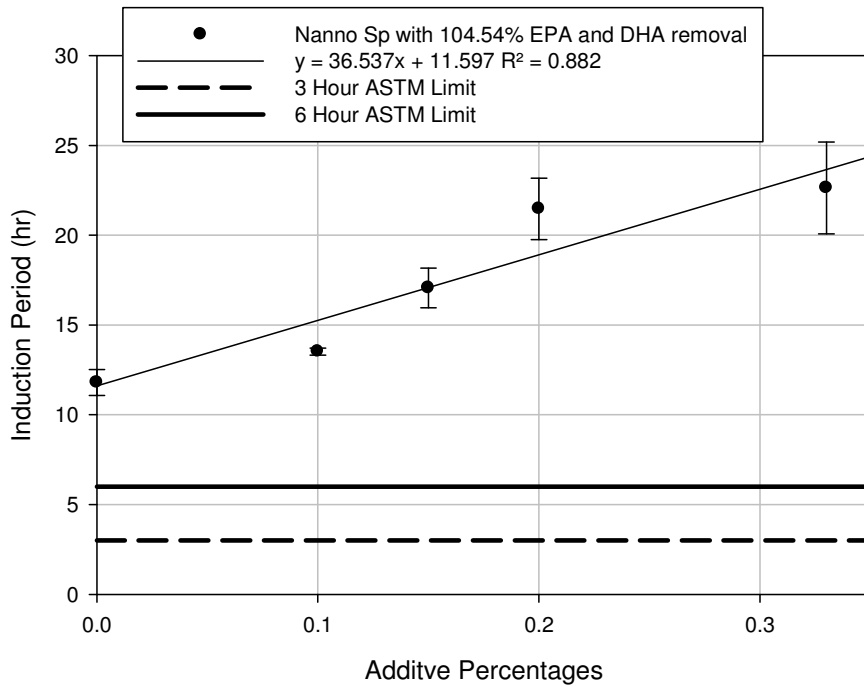


Figure 5.17. Induction period as a function of additive percentage for Nanno Sp formulation of 104.54 percent EPA and DHA removal.

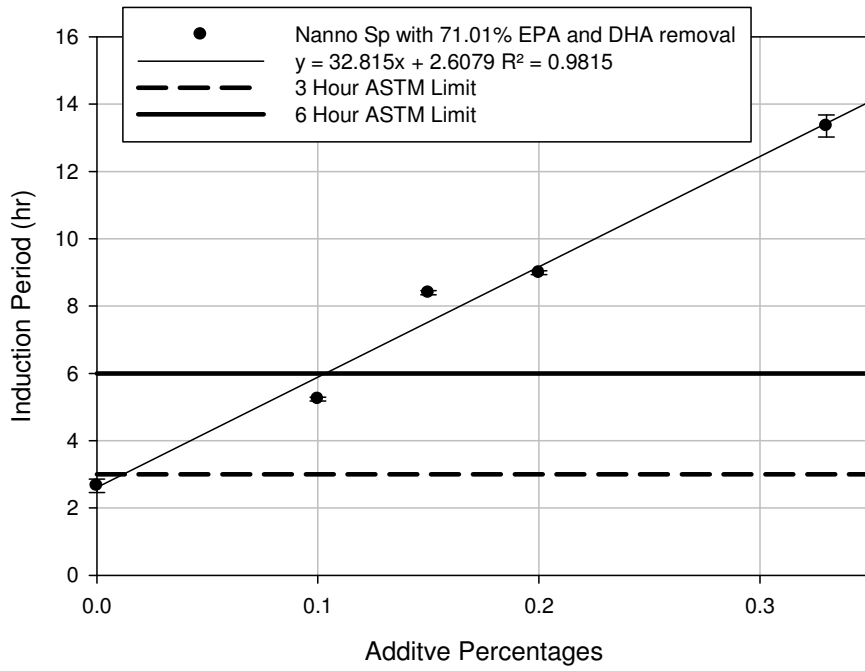


Figure 5.18. Induction period as a function of additive percentage for Nanno Sp formulation of 71.01 percent EPA and DHA removal.

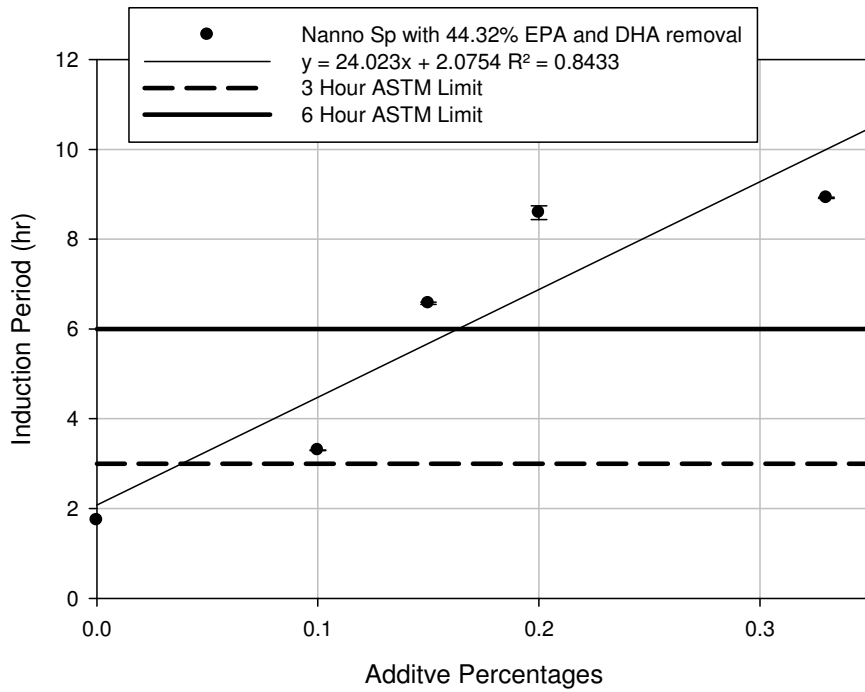


Figure 5.19. Induction period as a function of additive percentage for Nanno Sp formulation of 44.32 percent EPA and DHA removal.

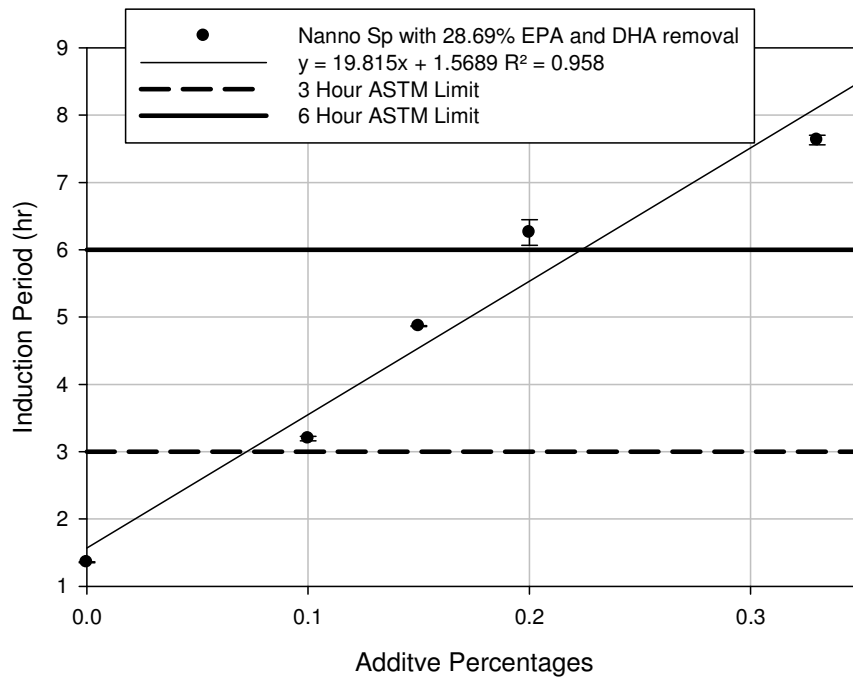


Figure 5.20. Induction period as a function of additive percentage for Nanno Sp formulation of 28.69 percent EPA and DHA removal.

5.2 Derived Cetane Number

The Derived Cetane Number (DCN) was determined using the FIT for the algal methyl ester formulation samples. Since DCN is a direct function of ignition delay, results for both ignition delay and DCN have been tabulated and plotted. The DCN are reported to the nearest tenth and the ignition delays are reported to the nearest hundredth of a millisecond as required by the ASTM D7107 Standard. Many of the formulation tests were not adequately repeated due to testing issues and hence, not every test result has a standard deviation. The results were invalid due to inconsistent ignition delay beyond the specified standards. The sporadic ignition delays were believed to be caused by plugging of the fuel injection system during an irregularly cold period of test days, which is a biodiesel problem previously discussed in Chapter 1.5.3 Cold Temperature Properties. The *Nannohloropsis* Sp 26.89 percent removal of EPA and DHA formulation and the *Nannohloropsis* *Oculata* Growth 15.61 percent removal formulation are the same mixture and only one data point was tested due to the limited amount of fish methyl ester available for completing testing.

The results for ignition delay for the algal methyl ester formulations are shown in Table 5.13. The algae methyl ester formulations exhibited a linear relationship to ignition delay. All three plots (Figure 5.21, Figure 5.22, and Figure 5.23) for ignition delay as a function of BAPE, modeled percent EPA and DHA removal, and percent EPA and DHA formulated, respectively, show that there is a linear relationship with R-square values of 0.86 for modeled percent EPA and DHA removal and 0.92 for the other two plots. This linear relationship shows that as the level of saturation increases in the algal methyl ester formulations, the ignition delay increases. Overall, the ignition delays range from 3.54 ms for 104.54 percent EPA and DHA removal in the *Nannohloropsis* Sp formulation to 4.63 ms for 8.69 percent EPA and DHA removal in the *Isochrysis* *Galbana* formulation. The only inconsistent result within a single formulation species was a decrease in ignition delay from 19.00 percent EPA and DHA removal in the

Nannohloropsis Oculata Growth formulation to the 15.61 percent removal, but multiple valid test results were not available for comparison.

Table 5.13. Ignition delay results for algae methyl ester formulations. (* Invalid results)

Modeled % EPA + DHA Removed	Standard Deviation	Actual % EPA + DHA Formulated	BAPE	Test	Average Air Temp (°C)	Ignition Delay (ms)	Average (ms)	Standard Deviation
Nanno Sp Formulations								
104.54%	4.91%	2.92%	40.85	1	461.2	3.54	3.54	0.01
				2	460.9	3.53		
71.01%	4.38%	11.70%	75.18	1	459.3	3.98	3.98	-
				2	*	*		
44.32%	5.94%	17.55%	101.45	1	*	*	4.22	-
				2	463.8	4.22		
28.69%	3.99%	21.93%	117.63	1	*	*	4.37	-
				2	464.3	4.37		

Nanno Oculata Growth Formulations

98.82%	0.40%	1.46%	40.66	1	*	*	3.68	-
				2	460.3	3.68		
77.82%	0.48%	7.31%	64.63	1	*	*	4.03	-
				2	463.8	4.03		
51.97%	0.46%	13.16%	90.13	1	*	*	4.18	-
				2	465.8	4.18		
19.00%	0.16%	20.47%	117.36	1	466.3	4.44	4.44	-
				2	*	*		
15.61%	4.33%	21.93%	117.63	1	*	*	4.37	-
				2	464.3	4.37		

Iso Galbana Formulations

99.40%	0.16%	10.24%	62.10	1	462.3	4.01	4.03	0.0212
				2	463	4.04		
68.11%	2.09%	14.62%	86.05	1	463.9	4.27	4.31	0.0495
				2	464.2	4.34		
30.99%	0.45%	20.47%	108.65	1	464.7	4.49	4.45	0.0636
				2	464.8	4.40		
8.69%	2.42%	23.39%	120.37	1	464.8	4.69	4.63	0.0849
				2	466.6	4.57		

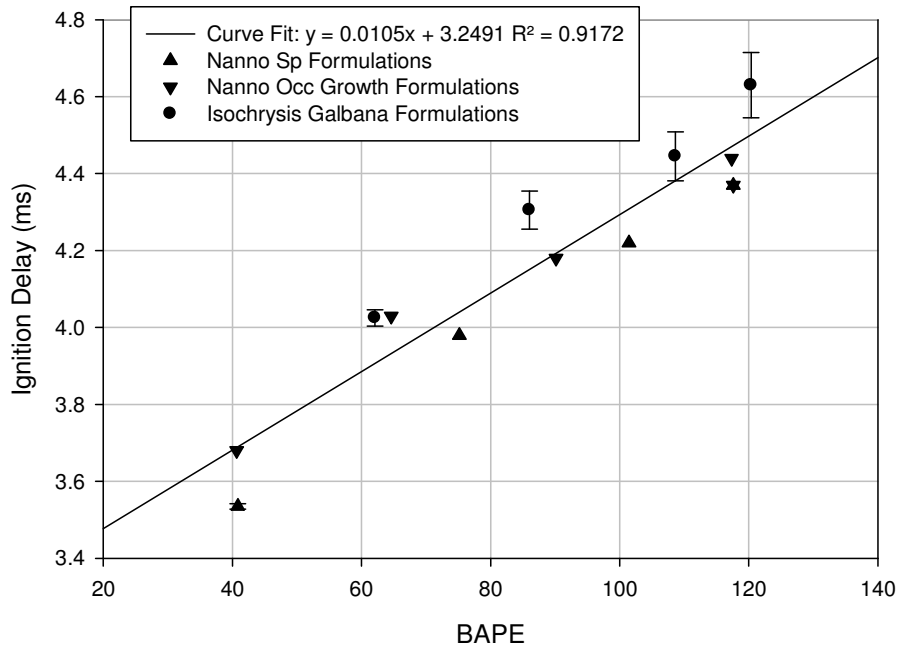


Figure 5.21. Ignition delay as a function of BAPE for algae methyl ester formulations.

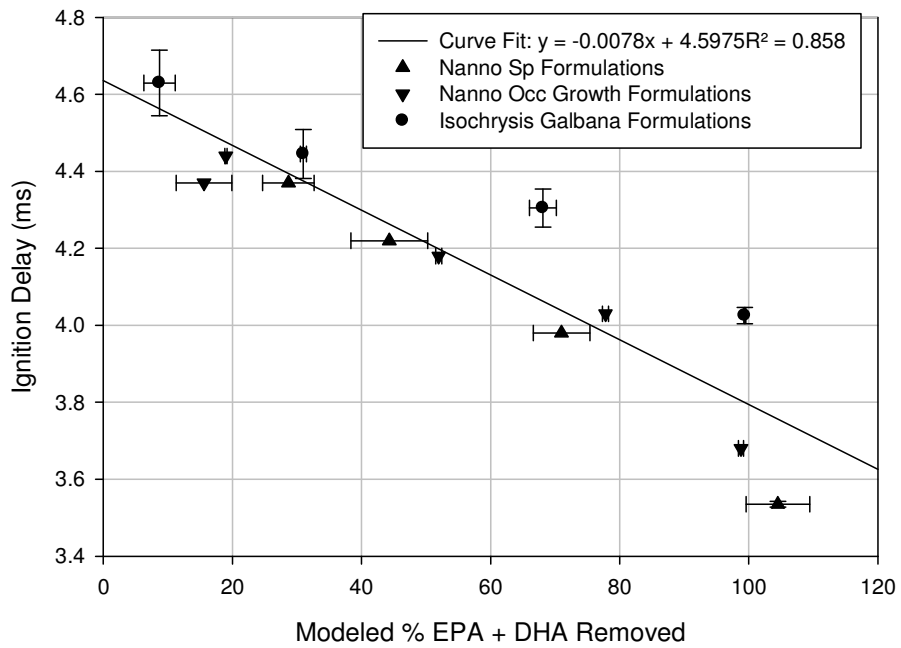


Figure 5.22. Ignition delay as a function of modeled percent EPA and DHA removed from the algae methyl ester formulations.

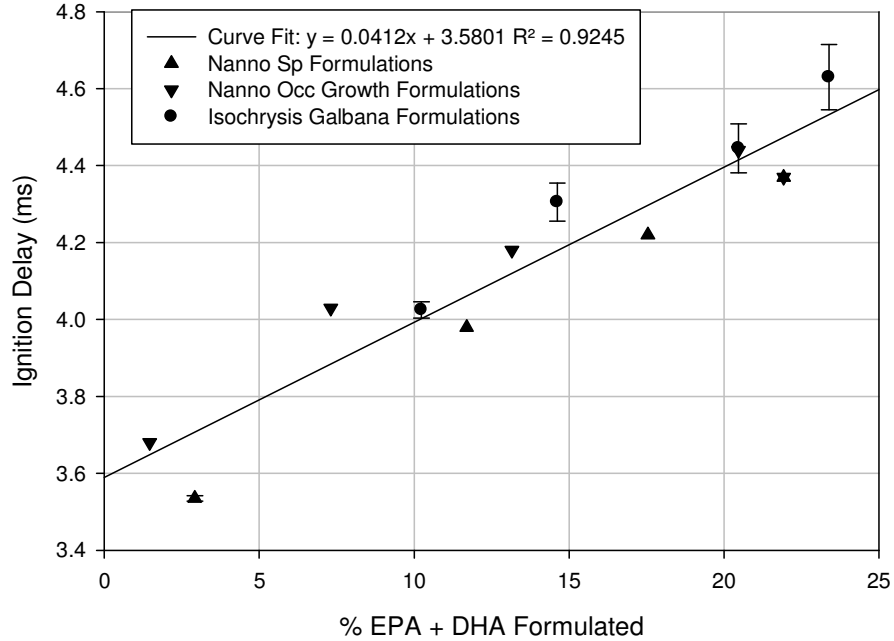


Figure 5.23. Ignition delay as a function of percent EPA and DHA formulated for algae methyl ester formulations.

The algal methyl ester formulations DCN results are reported in Table 5.14. The algal methyl ester formulations exhibited a linear relationship to DCN as was expected from the ignition delay correlations. All three plots (Figure 5.24, Figure 5.25, and Figure 5.26) for DCN as a function of BAPE, modeled percent EPA and DHA removal, and percent EPA and DHA formulated, respectively, show that there is a linear relationship with an R-square values ranging from 0.81 for modeled percent EPA and DHA removal to 0.91 for percent EPA and DHA formulated. This linear relationship shows that as the level of saturation increases in the algae methyl ester formulations the DCN decreases. Overall, the DCN ranges from 48.4 for 104.54 percent EPA and DHA removal in the Nannohloropsis Sp formulation to 37.0 for 8.69 percent EPA and DHA removal in the Isochrysis Galbana formulation. The only inconsistent result within a single formulation species was a decrease in ignition delay from 19.00 percent EPA and

DHA removal in the Nannohloropsis Oculata Growth formulation to the 15.61 percent removal, but multiple valid test results were not available for comparison.

Table 5.14. Derived cetane number results for algae methyl ester formulations.

Modeled % EPA + DHA Removed	Standard Deviation	Actual % EPA + DHA Formulated	BAPE	Test	Average Air Temp (°C)	DCN	Average	Standard Deviation
Nanno Sp Formulations								
104.54%	4.91%	2.92%	40.85	1	461.2	48.30	48.4	0.1131
				2	460.9	48.46		
71.01%	4.38%	11.70%	75.18	1	459.3	43.00	43.0	-
				2	*	*		
44.32%	5.94%	17.55%	101.45	1	*	*	40.6	-
				2	463.8	40.57		
28.69%	3.99%	21.93%	117.63	1	*	*	39.1	-
				2	464.3	39.14		

Nanno Oculata Growth Formulations

98.82%	0.40%	1.46%	40.66	1	*	*	46.5	-
				2	460.3	46.47		
77.82%	0.48%	7.31%	64.63	1	*	*	42.4	-
				2	463.8	42.43		
51.97%	0.46%	13.16%	90.13	1	*	*	41.0	-
				2	465.8	40.95		
19.00%	0.16%	20.47%	117.36	1	466.3	38.85	38.9	-
				2	*	*		
15.61%	4.33%	21.93%	117.63	1	*	*	39.1	-
				2	464.3	39.14		

Iso Galbana Formulations

99.40%	0.16%	10.24%	62.10	1	462.3	42.70	42.5	0.2828
				2	463	42.30		
68.11%	2.09%	14.62%	86.05	1	463.9	40.10	39.8	0.4950
				2	464.2	39.40		
30.99%	0.45%	20.47%	108.65	1	464.7	38.10	38.5	0.4950
				2	464.8	38.80		
8.69%	2.42%	23.39%	120.37	1	464.8	36.50	37.0	0.6364
				2	466.6	37.40		

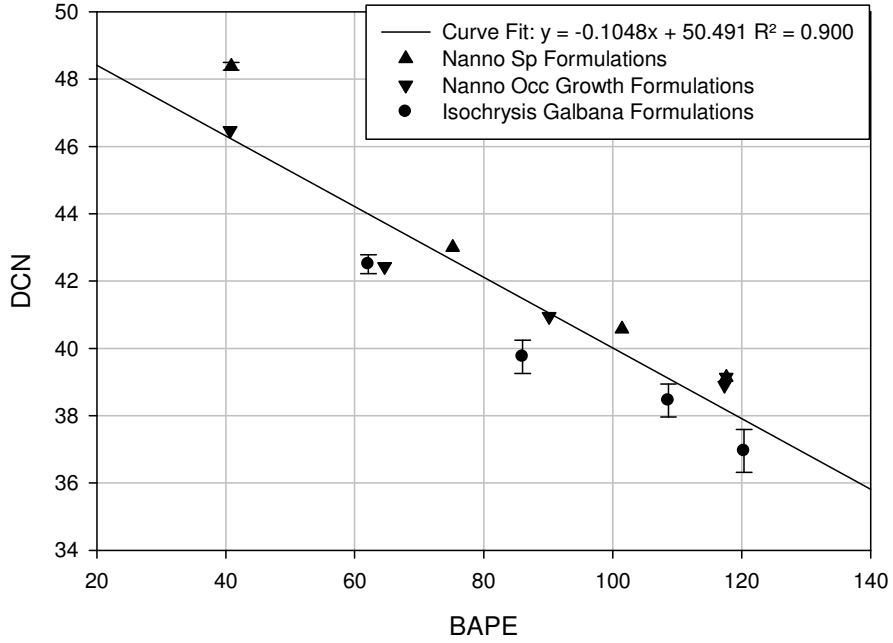


Figure 5.24. Derived cetane number as a function of BAPE for algae methyl ester formulations.

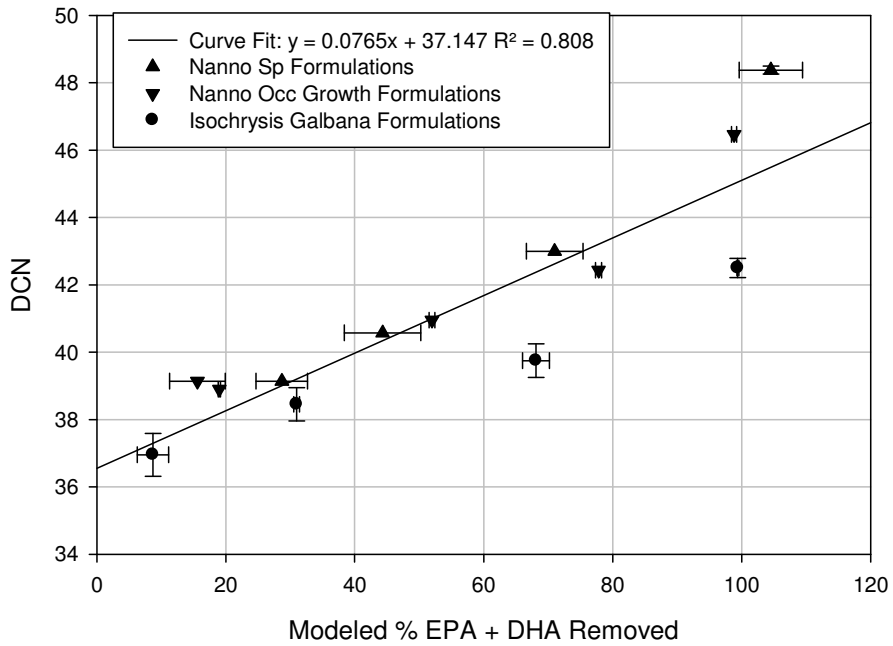


Figure 5.25. Derived cetane number as a function of modeled percent EPA and DHA removed from the algae methyl ester formulations.

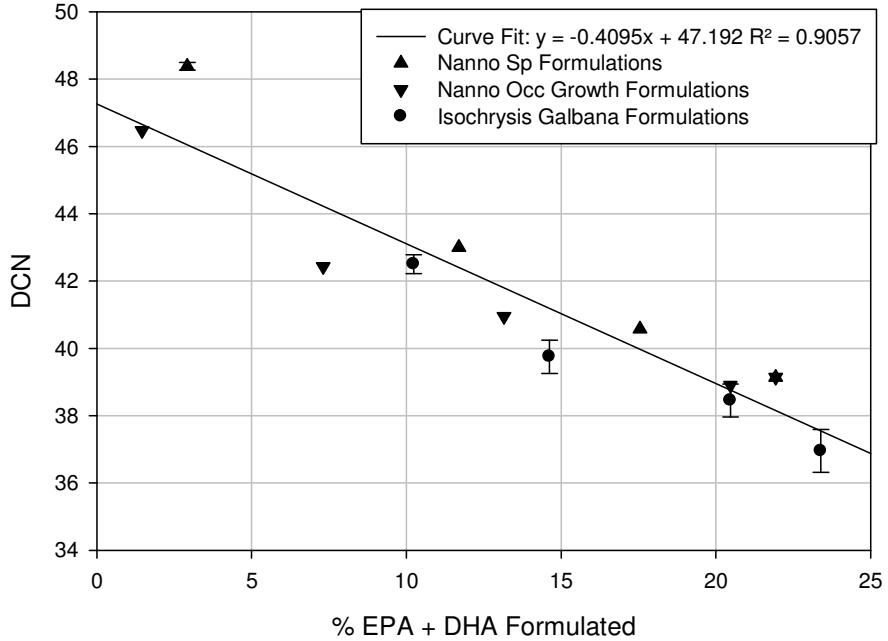


Figure 5.26. Derived cetane number as a function of percent EPA and DHA formulated for algae methyl ester formulations.

The minimum cetane number required to meet the B100 ASTM D6751 Standard is 47. None of the Isochrysis Galbana formulations met this standard and only when all of the EPA and DHA are removed from the Nannohloropsis Sp and Nannohloropsis Oculata Growth formulations is this minimum value met, indicating that the PUFA in the EPA and DHA has a stronger effect on CN than the long chain length.

5.3 Density, Viscosity, Speed of Sound

The density, viscosity, both dynamic and kinematic, and speed of sound were measured for the algal methyl ester formulations and the formulation ingredient methyl esters along with Catilin, Eldorado, and Inventure algae methyl esters and the Eldorado algal oil. These results are shown along with the calculated bulk modulus in Table 5.15.

Table 5.15. Density, viscosity, and speed of sound results for tested methyl esters and oil.

Sample Name	BAPE	Viscosity		Density, ρ (g/cm ³)	Speed of Sound (m/s)	Bulk Modulus (MPa)
		Dynamic, μ (mPa*s)	Kinematic, ν (mm ² /s)			
Fish Methyl Ester	143.74	3.9455	4.4779	0.882526	1356.31	1623.47
Soy Methyl Ester	68.3	3.7777	4.3528	0.870547	1344.94	1574.70
Canola Methyl Ester	185	4.0154	4.6419	0.885595	1371.49	1665.79
Corn Methyl Ester	166.2	3.7218	4.2948	0.867803	1341.92	1562.70
CE-1295	0.00	2.0662	2.4238	0.853668	1278.27	1394.87
Nanno Oculata Growth Formulation	40.66	3.9428	4.5275	0.871879	1325.29	1531.36
	64.63	3.1407	3.6182	0.869237	1326.87	1530.36
	90.13	3.4748	3.9837	0.873553	1339.27	1566.84
	117.36	3.8962	4.4427	0.877347	1351.78	1603.18
	117.63	4.5215	5.1401	0.881121	1356.37	1621.03
Nanno Sp Formulations	40.85	2.8537	3.3035	0.865276	1315.13	1496.55
	75.18	3.2272	3.7144	0.869521	1331.66	1541.94
	101.45	3.8824	4.4384	0.875459	1346.17	1586.48
	117.63	4.5046	5.1229	0.880255	1355.95	1618.44
Iso Galbana Formulations	62.1	2.7536	3.1742	0.869079	1314.15	1500.89
	86.05	3.0343	3.4820	0.872080	1325.80	1532.89
	108.65	3.3618	3.8402	0.876369	1337.92	1568.73
	120.37	3.2706	3.7373	0.876506	1340.84	1575.83
Catalin Algal ME	57.08	3.5990	4.1656	0.864443	1340.14	1552.52
Inventure Algal ME	0	4.0225	4.5404	0.886083	1352.24	1620.25
Eldorado Algal Oil	50.58	30.3000	33.5150	0.902443	1403.48	1777.59
Eldorado Algal ME	50.58	3.9825	4.5945	0.868249	1344.03	1568.42

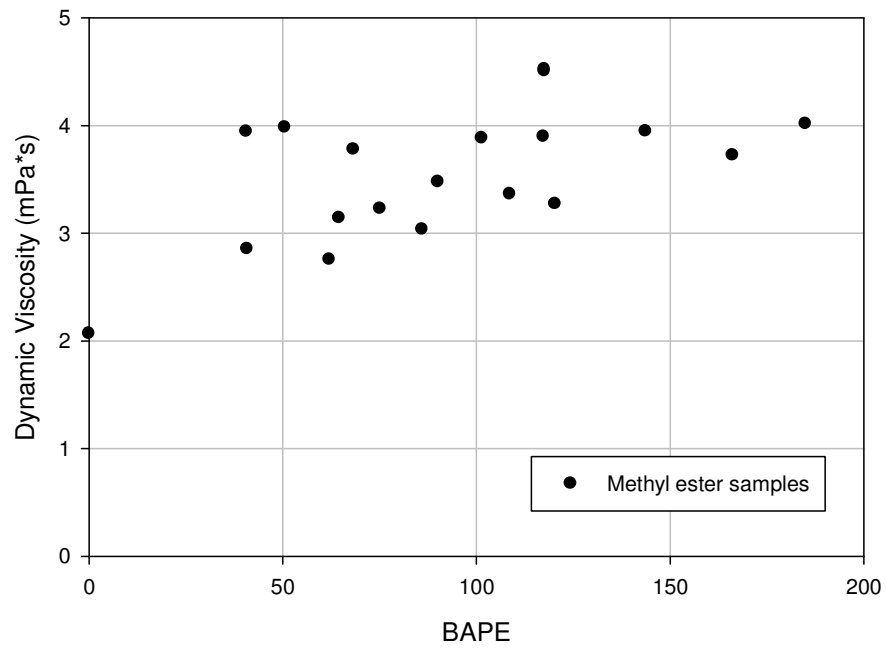


Figure 5.27. Dynamic viscosity for tested methyl esters.

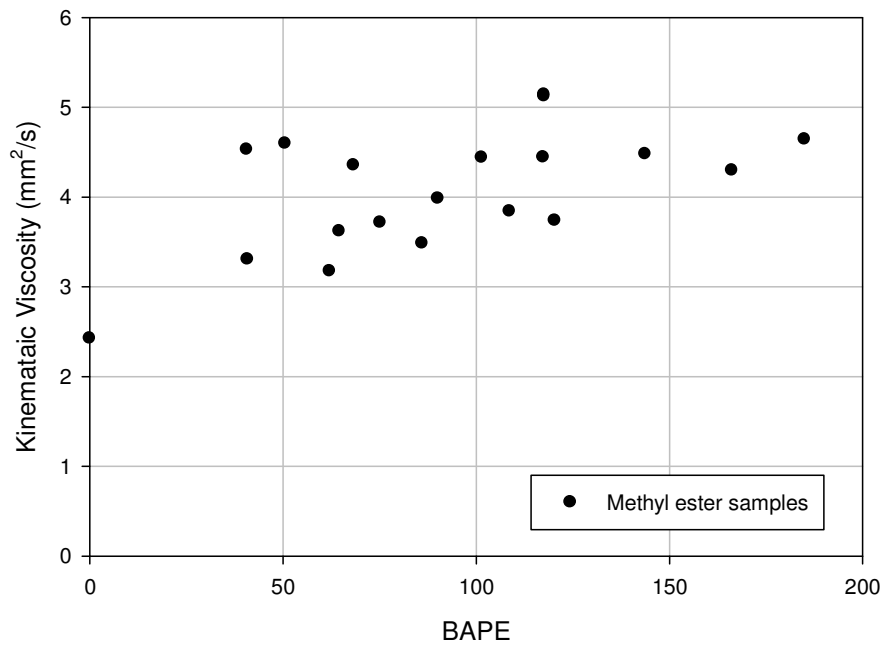


Figure 5.28. Kinematic viscosity for tested methyl esters.

The dynamic and kinematic viscosity plotted as a function of BAPE is shown in Figure 5.27 and Figure 5.28, respectively. All of the methyl ester ingredients and algae methyl ester formulations meet the ASTM B100 Standard of 1.9 – 6.0 mm²/s for kinematic viscosity. When the viscosities are plotted as a function of BAPE there appears to be no correlation, but most of the samples have dynamic viscosity from 3 – 4 mPa*s and a kinematic viscosity from 3 – 5 mm²/s.

The density of the methyl ester ingredients and algae methyl ester formulations appears to correlate to a linear function of BAPE (Figure 5.29) with an R-square value of 0.62, with obvious outliers.

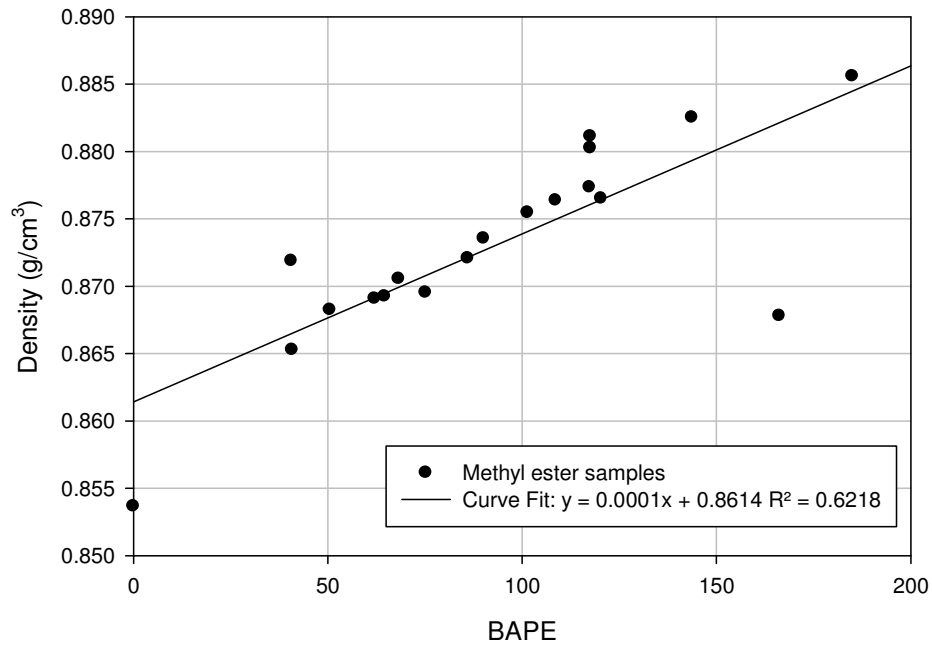


Figure 5.29. Density for tested methyl esters.

The speed of sound of the methyl ester ingredients and algae methyl ester formulations appears to correlate to a linear function of BAPE (Figure 5.30) with an R-square value of 0.67, also with obvious outliers.

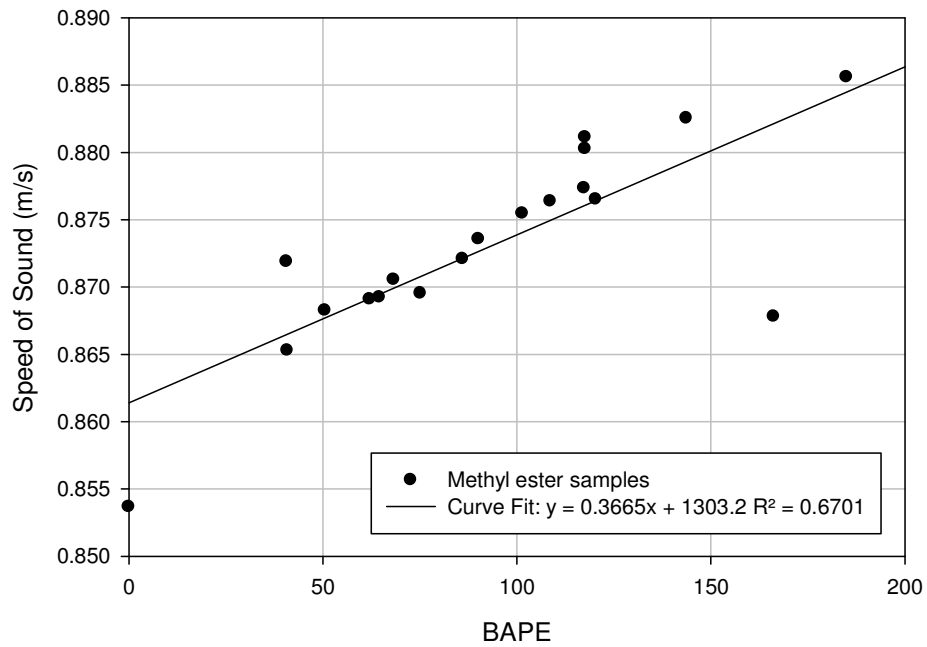


Figure 5.30. Speed of sound for tested methyl esters.

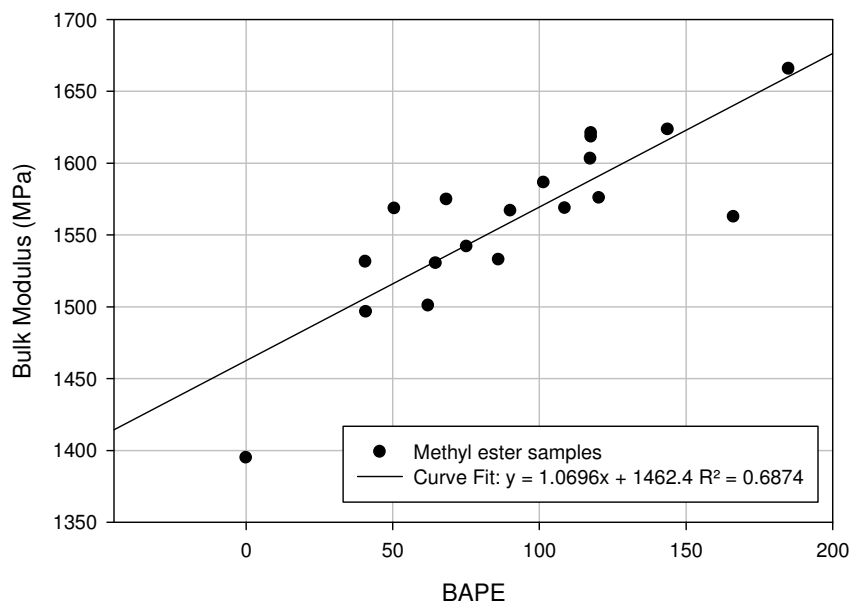


Figure 5.31. Bulk modulus as a function of BAPE.

The bulk modulus, calculated from Equation 5.1, is plotted in Figure 5.31. The bulk modulus also varies linearly with BAPE with an R-squared value of 0.69, again with outliers.

$$\text{Equation 5.1} \quad \beta = c^2 \cdot \rho \quad (\text{Tat and Van Gerpen 2003})$$

The algae methyl esters also meet the kinematic specification. The Eldorado oil has a greater viscosity, density, and speed of sound than the Eldorado methyl ester which is why oils are transesterified as previously discussed in Chapter 1.4 Algae Biodiesel. The viscosity of the Eldorado algae is reduced by over seven times when it is transesterified; the density is reduced by about four percent and the speed of sound is reduced by about five percent. These properties have been shown to have a great affect on injection timing, which can cause exhaust emissions and performance to be compromised (Tat and Van Gerpen 2003). The increase in bulk modulus has shown to have an increase in advancing the injection timing which leads to an increase in nitrous oxide emissions (Boehman, Morris and Szybist 2004).

6 CONCLUSIONS

This work was intended to evaluate the effects of unsaturation on oxidative stability and Cetane Number of algae-based biodiesel. The viscosity, density, and speed of sound of the fuels were also measured. The study was accomplished by using specific instruments to assess the properties of model algal methyl ester compounds along with some algal methyl esters derived from algal lipids from several different sources. The model algal methyl compounds were formulated based on fatty acid compositions of specific algae species from the literature. The model compounds were then reformulated to represent varying amounts of LC-PUFA removal of EPA and DHA.

Based on earlier research, the highly unsaturated EPA and DHA were expected to cause poor oxidative stability. The final outcome was to determine the amount of EPA and DHA removal from algal methyl esters that would be required to meet the ASTM and EN Standards for oxidative stability. It was found that the oxidative stability induction period correlates strongly to the calculated BAPE value of the algal methyl esters. The results of this study suggest that approximately 45 to 65 percent of the EPA and DHA would need to be removed from the *Nannochloropsis* species to meet the three hour ASTM oxidative stability specification and 75 to 85 percent would need to be removed to meet the EN six hour specification. For *Isochrysis Galbana*, removal of 100 percent of the EPA and DHA was insufficient for passing either the ASTM or EN oxidative stability requirements.

When additives were tested with the same algae methyl ester formulations, it was found that addition of only 0.03 percent of TBHQ is sufficient for *Nannochloropsis* Sp methyl esters to pass the ASTM specification even if no EPA or DHA were removed. To pass the EN

specification, 0.06 percent of TBHQ would need to be added to Nannochloropsis Sp methyl ester if no EPA or DHA were removed. Two of the real algal methyl esters proved to perform consistently with the algae methyl ester formulation results. One of the real algal methyl esters contained nearly all FAMEs and passed both the ASTM and EN Standards at an 8.43 hour induction period. The other sample was a raw algal methyl ester that was produced from algal biomass via a supercritical methanol extraction and transesterification technique. This unrefined sample contained less than 50 percent total FAME, which consisted of nearly 50 percent DHA. As expected, this sample had a very low oxidative stability induction period.

The Cetane Number was determined to vary linearly with BAPE for all of the algal methyl ester formulations. The algal methyl ester formulations passed the ASTM biodiesel Cetane Number specification of 47 only if virtually 100 percent of the EPA and DHA were removed from the Nannochloropsis formulations. Conversely, the Isochrysis Galbana formulations were unable to meet the biodiesel Cetane Number specifications even with removal of 100 percent of the EPA and DHA. The speed of sound and density also varied linearly increasing with BAPE for all of the algal methyl ester formulations. The viscosity measurements did not appear to correlate with BAPE, but all of the methyl esters fell within the ASTM kinematic viscosity requirements for biodiesel.

6.1 Recommendations for Future Work

In the short time between the planning stages of this project and the completion of this thesis, the production and development (and availability) of algal lipids and refined biofuels through the NAABB consortium continues to increase. For example, the Advanced Biofuel Combustion and Characterization Laboratory has recently received samples of algal lipids derived from Nannochloropsis Salina and synthetic paraffinic aviation fuels from North Carolina State University and UOP. As more pure samples of algal lipids and biofuels become available,

the oxidative stability and Cetane Number testing should be repeated. Most of the algal methyl esters received to date were either not purified enough (e.g. the Inventure sample) to provide adequate oxidative stability testing or were not available in large enough quantities to perform Cetane Number testing.

Also, since inception of this work additional fuel characterization instruments have been acquired and installed in the Advanced Biofuel Combustion and Characterization Laboratory at the EECL. These instruments include a cold properties test apparatus (cloud point and cold filter plugging point), inductively couple plasma instrument (ICP) for measuring metal contaminants in fuels, KF coulometer for measurement of acid number, an instrument for measuring iodine number, and a calorimeter for measuring heating value. Cold temperature properties such as cloud point and cold filter plugging point should definitely be tested for the algal methyl ester formulations since these properties are also known to vary with unsaturation for biodiesel. The ICP and contaminants testing would be beneficial for testing the real algal methyl esters since, as observed with this study, algae biodiesel does not always contain pure FAMES. A follow up study with Cetane Number enhancers would also be beneficial to determine the optimum ratio of cetane enhancer, oxidative stability additive, and LC-PUFA removal required to meet B100 requirements for algal methyl esters produced from various sources.

7 REFERENCES

- Anton Paar. "Instruction Manual DSA 5000 M." 2010.
- . "Instruction Manual SVM 3000/G2 Stabinger Viscometer." 2010.
- Appenzeller, Tim. "The End of Cheap Oil." *National Geographic*, 2004.
- Arisoy, K. "Oxidative and Thermal Instability of Biodiesel." *Energy Sources, Part A: Recovery, Utilization, and Environmental Effects*, 2008: 1516-1522.
- ASTM D6751: Standard Specification for Biodiesel Fuel Blend Stock (B100) for Middle Distillate Fuels*. ASTM International, 2009.
- ASTM D7042: Standard Test Method for Dynamic Viscosity and Density of Liquids by Stabinger Viscometer (and the Calculation of Kinematic Viscosity)*. ASTM International, 2010.
- ASTM D7170: Standard Test Method for Determination of Derived Cetane Number (DCN) of Diesel Fuel Oils - Fixed Range Injection Period, Constant Volume Combustion Chamber Method*. ASTM International, 2009.
- Benamotz, A., T. Tornabene, and W. Thomas. "Chemical Profile of Selected Species of Microalgae with Emphasis on Lipids." *Journal of Phycology* 21.1 (1985): 72-81.
- Berthiaume, D., and A. Tremblay. *Study of Ranicmat Test Method in Measuring the Oxidation Stability of Biodiesel Ester and Blends*. Oleotek, Inc., November 2006.
- Berthiaume, D., and A. Tremblay. *Study of Ranicmat Test Method in Measuring the Oxidation Stability of Biodiesel Ester and Blends*. Oleotek, Inc., 2006.
- Boddiger, D. "Boosting Biofuel Crops Could Threaten Food Security." *Lancet*, 370: 923-924.
- Boehman, A, D Morris, and J Szybist. "The Impact of the Bulk Modulus of Diesel Fuels on Fuel Injection Timing." *Energy & Fuels*, 2004.
- Campbell, C., and J. Laherrere. "Preventing the Next Oil Crunch - The End of Cheap Oil." *Scientific American*, 1998: 77-83.
- Canes, M. "US Fuels-1: Study Forecasts US Fuel Demand for Next Decade." *Oil & Gas Journal*, 2007: 66.
- Carolan, M. S. "Environmental Review: The Cost and Benefits of Biofuels: A Review of Recent Peer-Reviewed Research and a Sociological Look Ahead." *Environmental Practice*, 2009: 17-24.

- Carraretto, C., A. Macor, A. Mirandola, A. Stoppato, and S. Tonon. "Biodiesel as Alternative Fuel: Experimental Analysis and Energetic Evaluations." *Energy*, 2004: 2195-2211.
- Chapman, L. "Transport and Climate Change: A Review." *Journal of Transport Geography*, 2007: 354-367.
- Chisti, Y. "Biodiesel from Microalgae." *Biotechnology Advances*, 2007: 294-306.
- Chisti, Y. "Biodiesel from Microalgae Beats Bioethanol." *Trends in Biotechnology*, 2008: 126-131.
- Congress, 110th United States. "Energy Independence and Security Act of 2007." House Bill H.R.6, 2007.
- Demirbas, A. "Importance of Biodiesel as Transportation Fuel." *Energy Policy*, 2007: 4661-4670.
- Demirbas, A. "Production of Biodiesel from Algae Oils." *Energy Sources Part A: Recovery, Utilization, and Environmental Effects*, 2009: 163-168.
- Dunahay, T., E. Jarvis, S. Dais, and P. Roessler. "Manipulation of Microalgal Lipid Production Using Genetic Engineering." *Applied Biochemistry and Biotechnology*, 1996: 223-231.
- Durrett, T., C. Benning, and J. Ohlrogge. "Plant Triacylglycerols as Feedstocks for the Production of Biofuels." *The Plant Journal*, 2008: 593-607.
- EN 14112 Determination of Oxidation Stability (Accelerated Oxidation Test)*. European Standard, 2003.
- EPA. *A Comprehensive Analysis of Biodiesel Impacts on Exhaust Emissions*. EPA 420-P-02-001, 2002.
- Fisher, Bethany. "Characterization of Gaseous and Particulate Matter Emissions from Combustion of Algae Based Methyl Ester Biodiesel." Master's Thesis, 2009.
- Foroohar, K. "Exxon \$600 Million Algae Investment Makes Khosla See Pipe Dream." *Bloomberg*, 2010.
- Frankel, E. N. *Lipid Oxidation*. Dundee, Scotland: The Oily Press Ltd, 1998.
- Gouveia, L., and A. Oliveira. "Microalgae as a Raw Material for Biofuels Production." *Journal of Industrial Microbiology & Biotechnology*, 2009: 269-274.
- Gouveia, L., and A. Oliveira. "Microalgae as a Raw Material for Biofuels Production." *Journal of Industrial Microbiology & Biotechnology*, 2009: 269-274.
- Graboski, M., and R. McCormick. "Combustion of Fat and Vegetable Oil Derived Fuels in Diesel Engines." *Progress in Energy and Combustion Science*, 1998: 125-164.
- Greenwell, H., L. Laurens, R. Shields, R. Lovitt, and K. Flynn. "Placing Microalgae on the Biofuels Priority List: A Review of the Technological Challenges." *Journal of the Royal Society Interface*, 2010: 703-726.

- Grundwald, M. "The Clean Energy Scam." *Time Magazine*, March 27, 2008.
- Guschina, I., and J. Harwood. "Algal lipids and the Effect of the Environment on Their Biochemistry." *Lipids in Aquatic Ecosystems*, 2009: 1-24.
- Hu, Q., et al. "Microalgal Triacylglycerols as Feedstocks for Biofuel Production: Perspectives and Advances." *The Plant Journal*, 2008: 621-639.
- IPCC. *Climate Change 2007*. Fourth Assessment Report, United Nations, 2007.
- Jain, S., and M. Sharma. "Stability of Biodiesel and Its Blends: A Review." *Renewable & Sustainable Energy Reviews*, 2010: 667-678.
- Karavalakis, G., and S Stournas. "Impact of Antioxidant Additives on the Oxidation Stability of Diesel/Biodiesel Blends." *Energy and Fuels*, 2010.
- Karavalakis, G., D. Karonis, and S. Stournas. *Evaluation of the Oxidation Stability of Diesel/Biodiesel Blends Using the Modified Rancimat Method*. 2009-01-1828, SAE, 2009.
- Knothe, G. "Analyzing Biodiesel: Standards and Other Methods." *Journal of the American Oil Chemists' Society*, 2006: 823-833.
- Knothe, G. "Biodiesel: Current Trends and Properties." *Topics in Catalysis*, 2010: 714-720.
- Knothe, G. "Dependence of Biodiesel Fuel Properties on the Structure of Fatty Acid Alkyl Esters." *Fuel Processing Technology*, 2005: 1059-1070.
- Knothe, G. "Some Aspects of Biodiesel Oxidative Stability." *Fuel Processing Technology*, 2007: 669-667.
- Knothe, G. "Structure Indices in FA Chemistry: How Relevant is the Iodine Value?" *Journal of the American Oil Chemists' Society*, 2002: 847-854.
- Knothe, G., A. Matheaus, and T. Ryan. "Cetane Numbers of Branched and Straight-Chain Fatty Esters Determined in an Ignition Quality Tester." *Fuel*, 2003: 971-975.
- Knothe, G., and R. Dunn. "Dependence of Oil Stability Index of Fatty Compounds on Their Structure and Concentration and Presence of Metals." *Journal of the American Oil Chemists' Society*, 2003: 1021-1026.
- Knothe, G., R. Dunn, and M. Bagby. "Biodiesel: The Use of Vegetable Oils and Their Derivatives as Alternative Diesel Fuels." *Fuels and Chemicals From Biomass*, 1997: 172-208.
- Loury, M. "Possible Mechanisms of Autoxidated Rancidity." *Lipids*, 1972: 671.
- Maeda, K., M. Owada, N. Kimura, K. Omata, and I. Karube. "CO₂ Fixation from the Flue-Gas on Coal-Fired Thermal Power-Plant by Microalgae." *Energy Conversion and Management*, 1995: 717-720.
- Martek Biosciences Corporation. 2009. <http://www.lifesdha.com/Finding-lifesDHA-/Partner-Products/tabid/129/Default.aspx> (accessed 2009).

- Mata, T., A. Martins, and N. Caetano. "Microalgae for Biodiesel Production and Other Applications." *Renewable & Sustainable Energy Reviews*, 2010: 217-232.
- McCormick, R., and S. Westbrook. "Storage Stability of Biodiesel and Biodiesel Blends." *Energy & Fuels*, 2010: 690-698.
- McCormick, R., M. Graboski, T. Alleman, A. Herring, and K.S. Tyson. "Impact of Biodiesel Source Material and Chemical Structure on Emissions of Criteria Pollutants from a Heavy-Duty Engine." *Environmental Science and Technology*, 2001: 1742-1747.
- McCormick, R., M. Ratcliff, L. Moens, and R. Lawrence. "Several Factors Affecting the Stability of Biodiesel in Standard Accelerated Tests." *Fuel Processing Technology*, 2007: 651-657.
- Meher, L., D. Sagar, and S. Naik. "Technical Aspects of Biodiesel Production by Transesterification - A Review." *Renewable & Sustainable Energy Reviews*, 2006: 248-268.
- Metrohm Ion Analysis. "743 Rancimat Manual." 2009.
- Monyem, A., and J. Van Gerpen. "The Effect of Biodiesel Oxidation on Engine Performance and Emissions." *Biomass & Bioenergy*, 2001: 317-325.
- Monyem, A., J. Van Gerpen, and M. Canakci. "The Effect of Timing and Oxidation on Emissions from Biodiesel-Fueled Engines." *Transactions of the ASAE*, 2001: 35-42.
- Moser, B.R. "Influence of Blending Canola, Palm, Soybean, and Sunflower oil Methyl Esters on Fuel Properties of Biodiesel." *Energy & Fuels*, 2008: 4301-4306.
- Nagle, N., and P. Lemke. "Production of Methyl-Ester Fuel From Microalgae." *Applied Biochemistry and Biotechnology*, 1990: 355-361.
- National Biodiesel Board. *U.S. Biodiesel Production Capacity*. U.S. Biodiesel Board, 2009.
- Pahgova, J., L. Jorikova, and J. Cvengros. "Study of FAME Stability." *Energy & Fuels*, 2008: 1991-1996.
- Qiang, H., et al. "Microalgal Triacylglycerols as Feedstocks for Biofuel Production: Perspectives and Advances." *The Plant Journal*, 2008: 621-639.
- Ramos, M., C. Fernandez, A. Casas, L. Rodriguez, and A. Perez. "Influence of Fatty Acid Composition of Raw Materials on Biodiesel Properties." *Bioresource Technology*, 2009: 261-268.
- Ratledge, C., and Z. Cohen. "Microbial and Algal Oils: Do They Have a Future for Biodiesel or as Commodity Oils?" *Lipid Technology*, 2008: 15-160.
- Rodolfi, L., et al. "Microalgae for Oil: Strain Selection, Induction of Lipid Synthesis and Outdoor Mass Cultivation in a Low-Cost Photobioreactor." *Biotechnology and Bioengineering*, 2009: 100-112.
- Roncarati, A., A. Meluzzi, S. Acciarri, N Tallarico, and P. Melotti. "Fatty Acid Composition of Different Microalgae Strains (*Nannochloropsis* sp., *Nannochloropsis oculata* (Droop) Hibberd, *Nannochloris atomus* Butcher and *Isochrysis* sp.) According to the Culture Phase and the Carbon Dioxide Concentration." *Journal of the World Aquaculture Society*, 2004: 401-411.

- Runge, C., and B. Senauer. "How Biofuels Could Starve the Poor." *Foreign Affairs*, 2007: 41.
- Sanford, S., J. White, P. Shah, C. Wee, M. Valverde, and G. Meier. *Feedstock and Biodiesel Characteristics Report*. Renewable Energy Group, 2009.
- Sarin, R., et al. "Biodiesel Surrogates: Achieving Performance Demands." *Bioresource Technology*, 2009: 3022-3028.
- Sawayama, S., S. Inoue, Y. Dote, and S. Yokoyama. "CO₂ Fixation and Oil Production Through Microalga." *Energy Conversion and Management*, 1995: 729-731.
- Schaub, Tanner, interview by Anthony Marchese. *Fatty Acid Profile for El Dorado Water White FAME* (January 18, 2011).
- Schenk, P., et al. "Second Generation Biofuels: High-Efficiency Microalgae for Biodiesel Production." *Bioenergy Research*, 2008: 20-43.
- Sheehan, J., T. Dunahay, J. Benemann, and P. Roessler. *A Look Back at the US Department of Energy's Aquatic Species Report: Biodiesel from Algae*. NREL/TP-580-24190, NREL, 1998.
- Tat, M., and J. Van Gerpen. *Measurement of Biodiesel Speed of Sound and Its Impact on Injection Timing*. NREL/SR-510-31462, National Renewable Energy Laboratory, 2003.
- Tiwari, A.K., A. Kumar, and H. Raheman. "Biodiesel Production from Jatropha Oil (Jatropha curcas) with High Free Fatty Acids: An Optimized Process." *Biomass & Bioenergy*, 2007: 569-575.
- Tsokounogiou, M., G. Ayerides, and E. Tritopoulou. "The End of Cheap Oil: Current Status and Prospects." *Energy Policy*, 2008: 3797-3806.
- U.S. Department of Energy. *National Algal Biofuels Technology Roadmap*. DOE Biomass Program, 2010.
- U.S. Energy Information Administration. "Annual Energy Outlook 2010." DOE/EIA-0383, 2010.
- Van Gerpen, J. H., R. Pruszko, D. Clemets, B. Shanks, and G. Knothe. *Building a Successful Biodiesel Business: Technology Considerations, Developing the Business, Analytical Methodologies*. United States: Biodiesel Basics, 2006.
- Van Gerpen, J., E. Hammond, L. Yu, and A. Monyem. *Determining the Influence of Contaminants on Biodiesel Properties*. SAE Paper No. 971685, Warrendale, PA: SAE, 1997.
- Wang, Z., N. Ullrich, S. Joo, S. Waffenschmidt, and U. Goodenough. "Algal Lipid Bodies: Stress Induction, Purification, and Biochemical Characterization in Wild-Type and Starchless *Chlamydomonas Reinhardtii*." *Eukaryotic Cell*, 2009: 1856-1868.
- Waukesha Engine Dresser, Inc. "Fuel Ignition Tester User Manual." 2006.
- Waynick, J. A. *Characterization of Biodiesel Oxidation and Oxidation Products: CRC Project No. AVFL-2b*. NREL/TP-540-39096, NREL, 2005.

Weyer, K., D. Bush, A. Darzins, and B. Willson. "Theoretical Maximum Algal Oil Production." *Bioenergy Research*, 2010: 204-213.

Williard, D., T. Kaduce, S. Harmon, and A. Spector. "Conversion of Eicosapentaenoic Acid to Chain-Shortened Omega-3 Fatty Acid Metabolites by Peroxisomal Oxidation." *Journal of Lipid Research*, 1998: 978-986.

Yuan, W., A.C. Hansen, and Q. Zhang. "Predicting the Temperature Dependent Viscosity of Biodiesel Fuels." *Fuel*, 2009: 1120-1126.

Zeiler, K., D. Heacox, S. Toon, K. Kadam, and L. Brown. "The Use of Microalgae for Assimilation and Utilization of Carbon-Dioxide from Fossil Fuel-Fired Power-Plant Flue-Gas." *Energy Conversion and Management*, 1995: 707-712.